

**Fakultät für Medizin**

**Forschungszentrum für krebskranke Kinder**

**Klinik und Poliklinik für Kinder- und Jugendmedizin**

# **Generation of transgenic, antigen-specific, allogeneic, HLA-A\*02:01-restricted, cytotoxic T cells directed against Ewing Sarcoma specific target antigen STEAP1**

**David Schirmer**

Vollständiger Abdruck der von der Fakultät für Medizin der Technischen Universität München zur Erlangung des akademischen Grades eines

**Doctor of Philosophy (Ph.D.)**

genehmigten Dissertation.

**Vorsitzende/r:** Univ.-Prof. Dr. Dr. Stefan Engelhardt

**Betreuer/in:** Priv.-Doz. Dr. Günther H. S. Richter

**Prüfer der Dissertation:**

1. Univ.-Prof. Dr. Stefan Burdach

2. Univ.-Prof. Dr. Angela Krackhardt

Die Dissertation wurde am 15.12.2015 bei der Fakultät für Medizin der Technischen Universität München eingereicht und durch die Fakultät für Medizin am 06.04.2016 angenommen.

*For Julia and my parents*

# Table of contents

<b>1</b>	<b>Introduction</b>	<b>6</b>
1.1	Ewing Sarcoma	6
1.2	STEAP1	8
1.3	Adoptive T cell therapy	11
1.4	Aim of this study	16
<b>2</b>	<b>Material</b>	<b>17</b>
2.1	List of manufacturers	17
2.2	List of consumables	19
2.3	List of instruments and equipment	20
2.4	List of chemical and biological reagents	22
2.5	List of commercial reagent kits	24
2.6	Antibodies	25
2.6.1	List of antibodies for ELISpot assays	25
2.6.2	List of antibodies for flow cytometry	25
2.6.3	Antibodies for MHC-I blockade	26
2.7	Buffer, Media and Solutions	26
2.7.1	List of cell culture media and universal solutions	26
2.7.2	List of buffer and gel for DNA electrophoresis	27
2.8	Oligonucleotides	27
2.8.1	List of primers for polymerase chain reaction (PCR)	27
2.8.2	TaqMan Gene Expression Assays	30
2.9	List of human cancer cell lines	31
2.10	Bacterial strain for plasmid multiplication	33
2.11	Vectors	33
2.12	Mouse model	36
<b>3</b>	<b>Methods</b>	<b>38</b>
3.1	Cultivation of adherent and suspension tumor cell lines	38
3.2	Freezing and thawing	39
3.3	<i>In silico</i> prediction of HLA-A*02:01 peptide binding properties	39
3.4	HLA-A*02:01 binding assay	39

3.5	Isolation of peripheral blood mononuclear cells from buffy coats .....	40
3.6	Generation of monocyte derived dendritic cells (moDCs).....	40
3.7	Isolation of T cell subpopulations .....	41
3.8	Expansion of allo-restricted, peptide specific, cytotoxic T cells (CTL) .....	41
3.9	Sorting and expansion of STEAP1 <sup>130</sup> multimer positive CTLs .....	42
3.10	Generation of stem cell memory like T cells (T <sub>SCM</sub> ) .....	42
3.11	Transduction of PBMCs and T <sub>SCM</sub> with STEAP1 specific TCRs .....	43
3.12	Flow cytometry.....	44
3.13	ELISpot .....	45
3.14	xCelligence assay .....	45
3.15	RNA isolation .....	46
3.16	Reverse transcription .....	46
3.17	Quantitative Real Time PCR (qRT-PCR) .....	47
3.18	Identification of TCR $\alpha$ - and $\beta$ -repertoire .....	48
3.19	Design of retroviral TCR construct .....	51
3.20	Agarose gelelectrophoresis.....	51
3.21	Mini and maxi plasmid preparation.....	51
3.22	<i>In vivo</i> experiments .....	52
3.23	Bioluminescent measurements .....	53
3.24	Immunohistochemistry .....	54
3.25	Statistics .....	54
4	Results .....	55
4.1	Identification of STEAP1 <sup>130</sup> as suitable target for adoptive T cell therapy in Ewing Sarcomas .....	55
4.2	STEAP1 <sup>130</sup> specific T cell clone P2A5 specifically recognizes target cells.	58
4.3	T cell clone STEAP1 <sup>P2A5</sup> inhibits growth of target structures.....	63
4.4	Identification of V $\alpha$ - and V $\beta$ -chains of T cell clone STEAP1 <sup>P2A5</sup> .....	64
4.5	Generation of STEAP1 <sup>P2A5</sup> transgenic cytotoxic T <sub>SCM</sub> .....	65
4.6	Functionality of STEAP1 <sup>P2A5</sup> TCR transgenic T cells .....	68
4.7	Potential cross reactivity of STEAP1 <sup>P2A5</sup> TCR transgenic T cells .....	70
4.8	<i>In vivo</i> reactivity of STEAP1 <sup>P2A5</sup> TCR transgenic T cells in Rag2 <sup>-/-</sup> $\gamma$ c <sup>-/-</sup> mice	71

<b>5</b>	<b>Discussion.....</b>	<b>75</b>
<b>6</b>	<b>Conclusion and future perspectives.....</b>	<b>82</b>
<b>7</b>	<b>Summary.....</b>	<b>84</b>
<b>8</b>	<b>References.....</b>	<b>85</b>
<b>9</b>	<b>Appendix.....</b>	<b>102</b>
<b>9.1</b>	<b>Supplemental Figures .....</b>	<b>102</b>
<b>9.2</b>	<b>Supplemental Table .....</b>	<b>106</b>
<b>9.3</b>	<b>List of figures .....</b>	<b>109</b>
<b>9.4</b>	<b>List of tables.....</b>	<b>111</b>
<b>9.5</b>	<b>List of abbreviations.....</b>	<b>112</b>
<b>9.6</b>	<b>Publications derived from this Ph.D thesis.....</b>	<b>116</b>
	<b>Acknowledgements.....</b>	<b>118</b>

# 1 Introduction

## 1.1 Ewing Sarcoma

Ewing Sarcomas (ES), first described in 1921 by the American pathologist James Ewing, belong together with peripheral primitive neuroectodermal tumors (PNET) and Askin tumors to the Ewing Sarcoma family tumors (ESFT). They are characterized by an undifferentiated small blue round cell appearance (1) and are mainly localized in bone and soft tissue, but can also be found almost everywhere within the body. The most common sites are pelvis, femur and chest wall bones (26%, 20% and 16%) (2). It emerges with an incidence of 3.3 cases in  $1 \times 10^6$  under the age of 15 (3), making it the second most common malignant bone cancer after osteosarcoma, with the second decade of life being the most common age at diagnosis (2). There are somewhat more males affected than females (1.2:1 ratio of male: female) (2), but more interestingly the Caucasian population seems to be much more susceptible to the disease than other populations (2, 4, 5).

The initial symptom of patients is mainly localized pain and is often mistaken for signs of growth or injury (6). In about 25% of patients there is evidence of metastases, which correlates with a very bad prognosis (7). Modern therapeutic modalities have raised the overall survival (OS) of patients with localized, standard risk disease up to 75% (8). However, there still remains a poor prognosis for patients with initial metastatic disease (<30 %), especially when bone and bone marrow are involved, whereas patients with localized pulmonary metastasis have a better prognosis (30% - 40%) (7, 9-12). Even worse than metastatic disease is the outcome for patients with local or distant relapse, which occurs in 30% - 40% of treated patients and where the probability of long-term survival is under 20% - 25% (13, 14).

Current treatment modalities include surgery, chemotherapy, radiation therapy and allogeneic stem cell transplantation (9, 12, 15). Whenever possible, tumors are removed surgically and development of modern prosthetic devices has helped to include almost every affected bone in the body. Nevertheless, especially in growing children bone replacement is still a challenge. As ES are known for their radiosensitivity (1), post-operative radiation is suggested if not the whole tumor mass could be removed or a

poor histologic response is observed (16, 17). In patients where radiation therapy could reduce the tumor mass to allow function preserving surgery, even pre-operative radiation is used (17). Nonetheless, especially in children there is always the risk of secondary malignancies after radiation including disorders of bone growth (2). As most of the patients died as a result of metastasis in earlier decades, nowadays chemotherapy is included in the treatment of the disease. Depending on the area of living, either a combination of vincristine, ifosfamide, doxorubicin and etoposide (VIDE) is recommended in Europe (18) or a combination of ifosfamide and etoposide together with vincristine, doxorubicin and cyclophosphamide (VDC-IE) in North America (19, 20). An ongoing phase III clinical trial is comparing both regimens and tries to find a universally applicable treatment option (Euro-Ewing 2012, CRUK/11/050). However, despite the increasing success of current treatments there is still research going on to further improve outcome of patients, especially in advanced disease.

ES are characterized by EWS-ETS (Ewing sarcoma break point region 1 - E-twenty-six) fusion proteins. The most commonly occurring one is the chimeric transcription factor EWS-FLI1 (Ewing sarcoma breakpoint region 1 / friend leukemia virus integration 1) (21), a consequence of t(11;22)(q24;q12) translocations (22). Where EWS is known to have a RNA binding as well as a transcriptional activation domain, FLI1 has its function as a DNA binding domain. This leads to altered binding characteristics to many downstream targets, which are either activated or suppressed (23, 24). Some of the proteins up-regulated by EWS-FLI1 are enhancer of zeste homolog 2 (EZH2), G protein-coupled receptor 64 (GPR64), six-transmembrane epithelial antigen of prostate (STEAP1) and insulin like growth factor 1 (IGF1) promoting an oncogenic phenotype and improving proliferation, survival and invasiveness (25-28). There are over 1000 genes regulated by EWS-FLI1, with most of them (80%) being down-regulated (29). Those genes are mainly involved in processes like apoptosis and cell cycle arrest (30, 31).

EWS-FLI1 cannot be expressed in most human primary cell lines as it leads to growth arrest or cell death (32). The only human cell lines allowing the expression of the fusion protein are mesenchymal stem cells, but the transformation from MSCs to ES cells by inducing EWS-FLI1 expression is not complete (33, 34). So the cell of origin is still under

debate. Another problem in identifying the right cell type is that ES appear as an undifferentiated tumor as stated by James Ewing (1). So there is only little lineage specific differentiation, proving evidence for the cell of origin. Apart from MSCs, neural crest cells are the most promising candidates. There is evidence that some surface markers typical for neuroectodermal differentiation are also expressed in ES (35, 36). Previously Staeger *et al.* (37) found in a DNA microarray analysis genes expressed in ES that can also be found during neural differentiation and in neural tissues. But furthermore, the study also showed that EWS-FLI1 expression in bone marrow cells leads to the up-regulation of neural genes. This might imply that EWS-FLI1 is the reason for the neural phenotype of Ewing Sarcoma and not that neural crest cells are the reason for this phenotype. This hypothesis gets support from other studies where EWS-FLI1 was ectopically expressed in rhabdomyosarcoma and neuroblastoma leading to the up-regulation of genes responsible for neural crest cell phenotype (38, 39). The second possible cell type responsible for the development of ES, are mesenchymal stem cells. These cells are, in contrast to other human cells, in the position to proliferate after ectopic expression of EWS-FLI1 and develop an expression profile comparable to ES (40). Furthermore, if EWS-FLI1 is silenced via RNA interference (RNAi), ES cells show the same lineage connected developmental ability as mesenchymal stem cells (41). But it might be that those two cell types do not exclude each other, so that the cell of origin in ES is either a neural-derived mesenchymal stem cell or a neural crest stem cell that holds mesenchymal features (29).

## 1.2 STEAP1

*Six transmembrane epithelial antigen of prostate 1* (STEAP1) encoding for the STEAP1 protein, belongs to a set of highly up-regulated genes identified previously by Staeger *et al.* (37). Together with STEAP2, also known as 6-transmembrane protein of the prostate 1 (STAMP1), STEAP3, also known as tumor-suppressor activated pathway-6 (TSAP6) and STEAP4, also known as 6-transmembrane protein of prostate 2 (STAMP2), it belongs to the STEAP family of proteins. They are characterized by a 6-transmembrane domain with cytosolic C-terminal and N-terminal domains, together with 2 intracellular and 3 extracellular loops (Fig 1). In contrast to the other STEAP

proteins, STEAP1 lacks the  $F_{420}H_2:NADP^+$  oxidoreductase (FNO)-like domain, as well as the Rossman fold, two structural properties allowing the other family members to act as metallo-reductase (42).

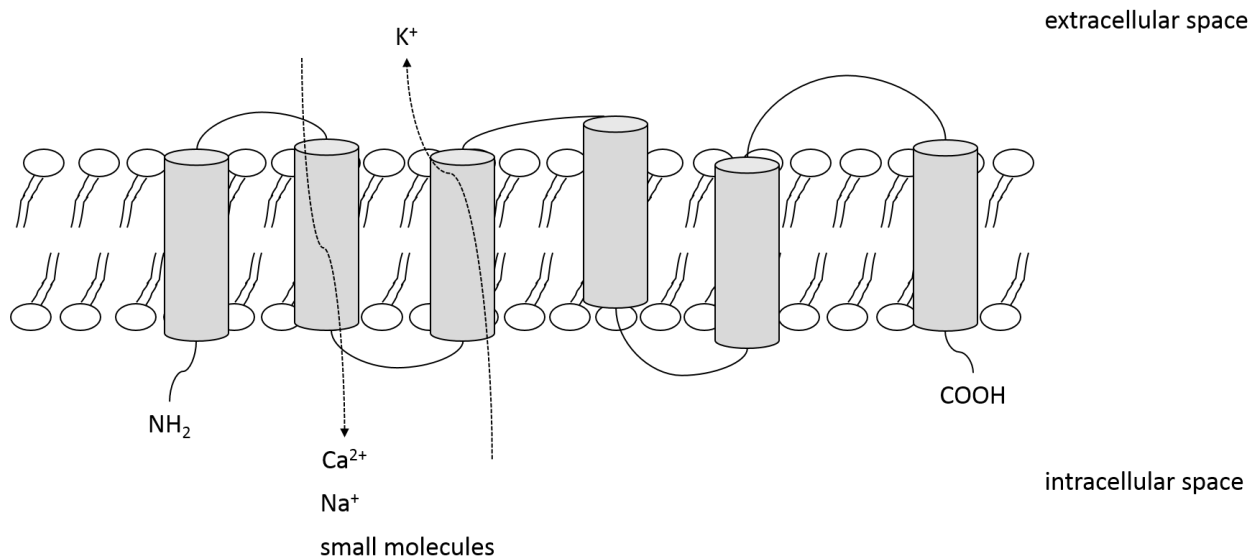


**Figure 1: Scheme of STEAP1 protein localization within the membrane.** 6 transmembrane domains pervade the membrane resulting in 3 extracellular and 2 intracellular loops. NH<sub>2</sub>- and COOH-domains are located in the intracellular space. STEAP1 might play a role in intracellular communication via active transport of Na<sup>+</sup>, Ca<sup>2+</sup> and small molecules.

*STEAP1* is transcribed into two different mRNAs (1.4 kb and 4 kb), whereas only the smaller one is further processed into a fully functional protein (43). This STEAP1 protein mainly localizes at cell-cell junctions in the plasma membrane of epithelial cells (44). Localization and structure suggest that it has functions as an ion channel or molecular transporter and therefore, to play a role in intracellular communication (45), presumably through the alterations of Na<sup>+</sup>, K<sup>+</sup>, Ca<sup>2+</sup> or small molecule levels (43).

Next to ES, STEAP1 is overexpressed in a variety of other human cancer cell lines and cancer tissues like bladder, breast, colon, cervix, testis, pancreas and prostate cancer. However, in normal tissue it is expressed in prostate and is described to show low-intensity histological staining in pancreas, colon, breast, pituitary, uterus, ureter and stomach (43).

Due to its expression in various cancers, STEAP1 is considered as a biomarker for diagnosis and treatment success in patients. Cheung *et al.* found STEAP proteins

(1 and 2) to be a suitable marker for the detection of bone marrow metastases in ES and their presence was related to worse outcome for the patient (46). Furthermore, STEAP1 has been discovered as first-class marker for the identification of MSCs (47), a cell type that is suspected to be the most likely cell of origin in ES (see above). In ES patients, high STEAP1 expression is associated with a superior outcome, presumably due to elevated intracellular reactive oxygen species (ROS) levels, making cells more sensitive for radiochemotherapy (48). Unfortunately it is only expressed in about 62% of Ewing Sarcoma patients (48), compared to almost 100% of prostate cancers (49). But STEAP1 may not only be used as a histological marker in tissues, since circulating *STEAP1* mRNA has been found in the serum of cancer patients, bearing solid tumors, with high sensitivity and specificity (50).

The role of STEAP1 in ES has recently been described in detail by Grunewald *et al.*. They showed that it is induced by EWS-FLI1 via 2 conserved ETS-binding sites of the STEAP1 promoter upstream of the transcriptional start site, which proved to be enriched for FLI1 in chromatin immunoprecipitation. Furthermore, ectopically expression of the fusion protein lead to a 6-fold increase of detectable *STEAP1* mRNA and vice versa silencing of EWS-FLI1 via RNAi led to a reduction of *STEAP1* expression in the ES cell lines SK-N-MC and A673. Additionally, proliferation, invasion and metastasis of ES cell lines were repressed, features that belong to the hallmarks of cancer (51). At least proliferation and invasiveness seem to be promoted by elevated levels of ROS, leading to an oxidative stress phenotype in ES, presumably to some extent via up-regulation of matrix metalloproteinase 1 (MMP1), adiponectin receptor 1 (ADIPOR1) and deltex 3 like, E3 ubiquitin ligase (DTX3L). Silencing of STEAP1 itself leads to decreased levels of ROS and some of its downstream targets (27).

The important role of STEAP1 in ES, its wide spread expression in a variety of cancers and the almost absent expression in vital organs make it a promising immunotherapeutic target. Indeed, there have some STEAP1 epitopes been addressed for immunotherapy in prostate, renal and bladder cancers. First of all, a group in the US used a naturally processed STEAP1 peptide (MIAVFLPIV) and its modified form (MLAVFLPIV) to induce a primary immune response against a couple of STEAP1 expressing tumors. They were able to generate cytotoxic T lymphocytes that recognized peptide-loaded cells and also

STEAP1 expressing tumor cells in a HLA\*02:01 restricted manner (52). Another group found two additional epitopes (STEAP1<sup>86-94</sup> and STEAP1<sup>262-270</sup>) capable of recognizing STEAP1<sup>+</sup> lung cancer cells *in vitro* but also in a HLA-A2 transgenic HHD mouse model. Furthermore, the same group found *ex vivo* reactive T cells of one of their specific lines (STEAP1<sup>86-94</sup>) in PBMCs of lung and prostate cancer patients indicating their possible use for immunotherapy (53).

### 1.3 Adoptive T cell therapy

The term adoptive cell therapy was first used by Billingham *et al.* in 1954, describing the transfer of cells to gain an effector function (54). In 1957 Barnes and Loutit had the idea that immune cells might be capable of eradicating tumor cells (55). Now 60 years later, the field of cellular immunotherapy has spread enormously with its peak of public acceptance in 2013, when cancer immunotherapy was named the “Science breakthrough of the year” (56). Today there are two main fields in adoptive T cell therapy (ACT). The infusion of tumor infiltrating lymphocytes (TIL) and the use of genetically engineered T cells. One of the first clinical trials showing the effective therapy of solid cancers with TILs was conducted by Rosenberg *et al.* in the late 80’s. They used autologous TILs from tumor samples, expanded them *ex vivo* with IL-2 and re-administered them to the patients. 60% of patients (9 of 15) without prior treatment with IL-2 and 40% of patients where prior IL-2 treatment had failed, showed objective tumor regression (57). With growing knowledge about treatment modalities, increased response rates of 50% - 70% (58) and even total tumor regression in 22% of melanoma patients (59) was obtained. To further improve the success of lymphocyte infusions, the idea was to use antigen-specific T cells as transplants. Initially developed to avoid infections after allogeneic hematopoietic stem cell transplantation (allo-HSCT), early success has been achieved for the transfer of Cytomegalovirus (CMV) and Epstein-Barr virus (EBV) specific T cells in clinical studies (60, 61). To translate the clinical success with antigen specific T cells from virus therapy to cancer treatment, the National Cancer Institute (NCI) published a list of antigens that seem to be optimal targets for adoptive immunotherapy (62). Nonetheless, therapeutic efficacy in solid cancers has so far been largely limited to melanomas (63). This might be because of the low frequency of high

avidity TILs in tumor tissues. As a result of self-protection, T cells with high affinity to self-antigens are depleted within the thymus (64). As a lot of tumor antigens are highly overexpressed self-antigens, with little expression in normal tissues and no tumor restricted antigens, only low affinity T cells can be isolated from the tumor mass and expanded *ex vivo*, which limits the therapeutic abilities of those cells.

To overcome this problem an approach was designed to transfer receptors into patient derived T cells, overcoming the negative selection in the thymus during their development. At the moment there are two major receptor constructs heavily under investigation. The introduction of  $\alpha/\beta$  T cell receptors (TCR) or chimeric antigen receptors (CAR). The later consist of an antigen recognizing single chain variable fragment (scFv) obtained from an antibody, coupled to an intracellular T cell signaling domain (usually CD3 $\zeta$ ) (65). Those first generation CARs consisting of just a scFv and a CD3 $\zeta$  signaling domain, only delivered disappointing results in tumor therapy. There was no clear anti-tumor activity of those CAR T cells, accompanied by low proliferative capacity and persistence (66). To avoid these problems of anergy, additional co-stimulatory domains were incorporated into the CARs, leading to the development of second (one co-stimulatory domain) and third (two co-stimulatory domains) generation CARs. Those CARs usually carry CD28 or 4-1BB and for third generation CARs additionally for example ICOS or OX40 (67). The major advantage of those CARs is the major histocompatibility complex (MHC) independent recognition of their antigen, making the treatment of malignancies available to a broader spectrum of patients, as they can be treated irrespective of their human leukocyte antigen (HLA) status (68). Furthermore, those CAR T cells combine the high affinity binding of an antibody with the lytic potential of a T cell. During the last years there have been most impressive results published for patients treated with CAR engineered T cells, mainly against hematologic malignancies (67, 68). In 2011 June *et al.* injected a second generation CAR containing T cells (4-1BB as co-stimulatory molecule), directed against CD19, into patients with refractory chronic lymphoid leukemia (CLL). 2 of 3 patients achieved complete remission and the CAR engineered T cells persisted for months as memory CAR T cells with sustained effector function (69, 70). These findings could be confirmed in an acute lymphoid leukemia (ALL) setting with 2 of 2 complete remissions (71). Furthermore, they

treated 14 patients with relapsed and refractory CLL. 8 of the 14 patients responded to the treatment with 4 complete remissions (CR), from which no one suffered relapse so far. In two of the patients with CR, CAR engineered T cells persisted for over 4 years with retained effector function (72). In a clinical trial including mostly children (25 of 30 < 22 years old) which were treated with T cells bearing an anti-CD19 second generation CAR to treat ALL, 90% of the patients were in a morphological CR one month after administration of the cells. There was an event free survival rate of 67% and an overall survival (OS) rate of 78% after 6 months (73). In another phase I study Lee *et al.*, obtained a 67% CR rate and an OS of 56% with a median follow up of 10 months after administration of a second generation CAR to treat ALL in children and young adults (74). However, success with CAR T cells is so far mainly limited to hematological malignancies. Even though some achievements have been obtained in treating solid cancers, those effects were mostly short termed and research translating the success in hematological malignancies into solid cancers is ongoing (63). But next to the limited tumor entities that can be treated so far, there are several other drawbacks in CAR T cell therapy. A side effect emerging very frequently is the cytokine release syndrome (CRS) and macrophage activation syndrome (67), as a result of extremely fast tumor destruction. Furthermore, as the recognition of antigen is based on binding of an antibody without involvement of MHC, only surface antigens can be targeted. This leads to a restricted amount of possible target structures. Moreover, as most tumor antigens are overexpressed self-antigens, questions about the safety of targeting those arise (68).

To avoid those problems another method of engineering receptor expressing T cells is available. The introduction of high affinity tumor antigen specific  $\alpha/\beta$  heterodimeric TCRs into donor T cells. With this approach the limitation of extracellular antigens can be circumvented, since recognition of the antigen occurs in a MHC dependent manner. The first achievements of transferring TCRs into human T cells were obtained by Clay *et al.* 1999 (75), who successfully transferred a melanoma antigen recognized by T cells 1 (MART-1) specific TCR into human lymphocytes, with the help of retroviruses. The first clinical trial with TCR transduced autologous T cells conducted in 2006, showed safety and practicality of this approach together with persistence of injected T cells up to one

year, however response rates did not reach the success of TIL therapy (76). So far over 60 patients with different types of cancer have been medicated with TCR transgenic T cells and response rates range from 19% - 67% (68, 77, 78). The most promising results were obtained from a clinical trial treating metastatic synovial cell carcinoma and melanoma patients with cancer/testis antigen NY-ESO-1 directed transgenic T cells. 4 of 6 patients with synovial cell carcinoma and 5 of 11 patients with NY-ESO-1 positive melanomas showed objective clinical response. This study was the first to show an effective treatment of a tumor other than melanoma with TCR transduced T cells (78). Until now there has been no toxicity observed due to the retroviral transfer of an exogenous TCR. To further improve efficacy of TCR transgenic T cells and overcome the problem of depletion of high affinity TCRs within the thymus during development, different methods of enhancing the affinity between TCR and peptide/MHC complex have been investigated. One option is the enhancement of the TCR affinity by so called affinity maturation, where single amino acids especially in the complementarity determining region 3 (CDR3) are exchanged (79). However, severe cases of off-target toxicity with death of two patients, due to the recognition of titin in cardiomyocytes by an affinity enhanced TCR, have been reported (80). Another possibility is the use of allogeneic TCRs. Allo-reactivity of T cells is defined by the recognition of peptide in the context of foreign MHC, which avoids negative selection of high affinity TCRs within the thymus. Thus, allo-reactive TCRs can bind their target peptide/MHC complex with higher affinity than TCRs recognizing peptides on self-MHC (81). Allogeneic stem cell transplantation (allo-SCT) is a proven therapeutic treatment option for leukemia and is also studied as a treatment option for other hematologic and non-hematologic malignancies (82), but success in solid cancers seems to be limited (68). In ES allo-SCT is a therapy option for some patients (12, 83), but is accompanied by extraordinary toxicity (84). There are several studies showing the existence of highly peptide specific allo-reactive T cells (81), which might circumvent the problem of unwanted off-tumor reactivity of the graft. To direct those T cells against distinct tumor associated antigens (TAA) in the context of a specific MHC, receptors can be isolated and transferred into donor lymphocytes. Therefore, antigen presenting cells (APC) with surface expression of the desired HLA molecules can be loaded with the respective antigenic peptide. With use of multimers, reflecting a natural TCR/peptide-MHC binding, allo-restricted T cells

can be isolated, allowing the enrichment of small populations within the T cell pool (85, 86). Methods for the isolation and characterization of their allo-restricted TCRs are now an established procedure (87, 88).

Recent success in the field of adoptive T cell therapy has drawn interest of the pharmaceutical industry and various established as well as start-up companies are investing money for ACT research and the possibility of commercialization (89), hopefully accelerating the gain of knowledge in this important field of cancer therapy.

### 1.4 Aim of this study

Based on the recent success in ACT, the aim of this study was to generate transgenic, antigen-specific, HLA-A\*02:01 restricted, cytotoxic T cells directed against ES associated antigen STEAP1. Therefore, suitable target peptides need to be evaluated and T cells recognizing the antigen in a HLA-A\*02:01 restricted manner to be generated. After *in vitro* characterization of those T cell lines, TCRs have to be identified and retroviral vectors for the infection of different human T cell subtypes be designed, to allow an off the shelf production of STEAP1 targeting cells for cancer treatment. The transgenic T cells need to be tested again for their target recognition and lytic capacity *in vitro* as well as for their anti-tumor effect in an immunodeficient mouse model. Furthermore, as there are increasing concerns about the safety and specificity of transgenic T cells, a cross-reactivity monitoring is recommended. An overview of the procedure to generate transgenic T cells for the therapy of patients is shown in Fig. 2.

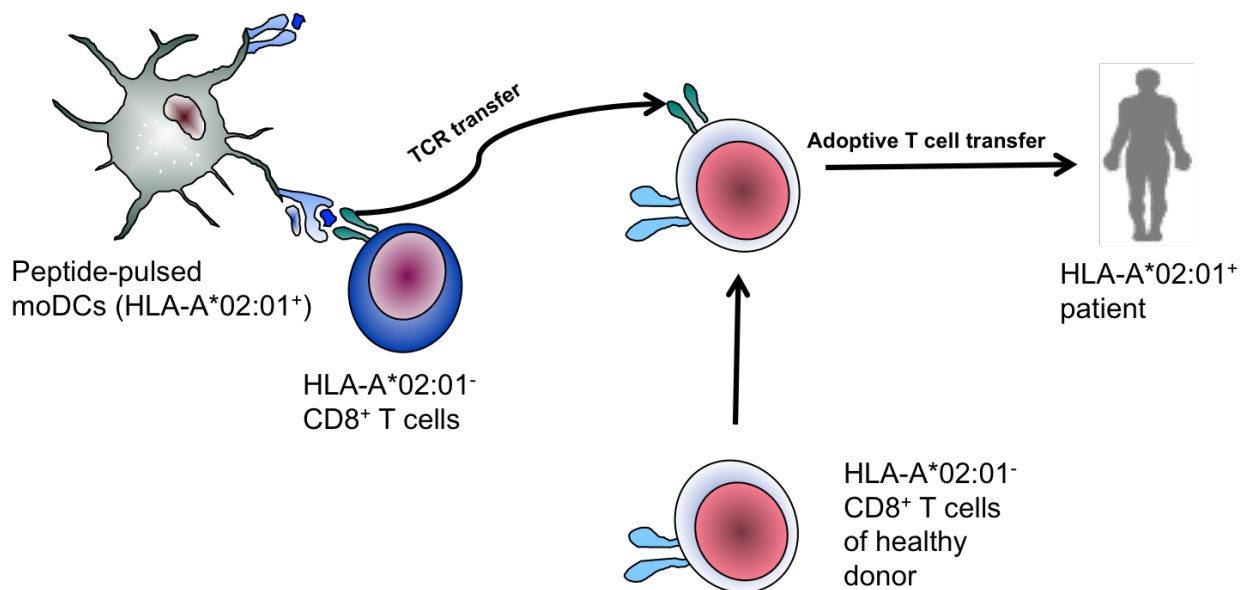


**Figure 2: Scheme of transgenic T cell development.** HLA-A\*02:01<sup>-</sup> CD8<sup>+</sup> T cells were primed with peptide pulsed HLA-A\*02:01<sup>+</sup> moDCs of a healthy donor. Specific TCRs were identified and transferred into CD8<sup>+</sup> T cells of a HLA-A\*02:01<sup>-</sup> donor. Those T cells are generated to treat HLA-A\*02:01<sup>+</sup> patients with STEAP1 expressing tumors.

## 2 Material

### 2.1 List of manufacturers

Manufacturer	Location
Abcam	Cambridge, UK
Abott	Wiesbaden, Germany
ACEA	San Diego, California, USA
Ambion	Austin, Texas, USA
Applied Biosystems	Darmstadt, Germany
ATCC	Rockyville, Maryland, USA
Autoimmun Diagnostika	Strassberg, Germany
B. Braun Biotech Int.	Melsungen, Germany
BD Bioscience Europe	Heidelberg, Germany
Beckman Coulter	Palo Alto, California, USA
Beckton Dickinson	Heidelberg, Germany
Berthold detection systems	Pforzheim, Germany
Biochrom	Berlin, Germany
BioRad	Richmond, California, USA
Biozym	Hessisch Oldendorf, Germany
Brand	Wertheim, Germany
Dako	Hamburg, Germany
DCS	Hamburg, Germany
Elma	Singen, Germany
Eppendorf	Hamburg, Germany
Falcon	Oxnard, California, USA
Fermentas	St. Leon-Rot, Germany
Cayman Chemical Company	Ann Arbor, Michigan, USA
GE Healthcare	Little Chalfont, UK
GeneArt	Regensburg, Germany
Genomed	St- Louis, Missouri, USA

---

**Material & Methods**

---

Genscript	New Jersey, USA
Genzyme	Neu-Isenburg, Germany
GFL GmbH	Segnitz, Germany
GLW	Würzburg, Germany
Greiner Bio-One GmbH	Frickenhausen, Germany
Heraeus	Hanau, Germany
ImmunoTools	Friesoythe, Germany
Implen GmbH	München, Germany
Leica	Wetzlar, Germany
LGC Standards GmbH	Wesel, Germany
Life Technologies	Carlsbad, California, USA
Lonza	Basel, Switzerland
Mabtech	Hamburg, Germany
Machery & Nagel	Düren, Germany
Merck Millipore	Darmstadt, Germany
Metabion	Planegg, Germany
Miltenyi	Bergisch Gladbach, Germany
Mirus	Madison, Wisconsin, USA
Molecular BioProducts	San Diego, California, USA
Nalgene	Rochester, New York, USA
Origene	Rockville, Maryland, USA
PAA	Cölbe, Germany
Peptidech	Rocky Hill, New Jersey, USA
Perkin Elmer	Akron, Ohio, USA
R&D Systems	Minneapolis, Minnesota, USA
Roche	Penzberg, Germany
Roth	Karlsruhe, Germany
Sarstedt	Nümbrecht, Germany
Sartorius	Göttingen, Germany
Scientific Industries	Bohemia, New York, USA

---

## Material & Methods

---

Scotsman	Milan, Italy
Sequiserve	Vaterstetten, Germany
Sempermed	Wien, Austria
Sigma Aldrich	St. Louis, Missouri, USA
Stratagene	Cedar Creek, Texas, USA
Syngene	Cambridge, UK
Systemc	Wettenberg, Germany
TaKaRa Bio Europe	Paris, France
Taylor-Wharton	Husum, Germany
Thermo Fisher Scientific	Ulm, Germany
Thermo Scientific	Braunschweig, Germany
TKA GmbH	Niederelbert, Germany
TPP	Trasadingen, Switzerland
VWR	Darmstadt, Germany

### 2.2 List of consumables

Material	Manufacturer
6 well tissue culture plate	Falcon
24 well non-tissue culture plate	Falcon
96 well cell culture plate (round and flat bottom)	TPP
96 well cell culture plate (v bottom)	Greiner Bio-One
Cell culture flasks (25, 75 and 175 cm <sup>2</sup> )	Greiner Bio-One
Cell strainer 40 µm	Falcon
Columns (MACS, LS and MS)	Miltenyi
Cryovials 1.5 ml	Sarstedt
Cuvettes	Roth
E-plate 96	ACEA
Filters, 0.45 µm	Sartorius

## Material & Methods

Gloves (nitril, latex)	Sempermed
MultiScreen-HA Filter Plates	Merck Millipore
Parafilm	Pechiney Plastic Packaging
Pipettes (25, 10 and 5 ml)	VWR
Pipette filter tips (1000, 200, 100, 10 µl)	Thermo Scientific
Pipette tips (1000, 200, 100, 10 µl)	Molecular BioProducts
Plates for qRT-PCR (96 well)	Applied Biosystems
Reagent reservoirs (50 ml)	Falcon
Reagent reservoir (for 12 channel pipette)	VWR
Tubes for cell culture (polypropylene, 15 ml and 50 ml)	Greiner Bio-One
Tubes for cell culture (polystyrene, 15 ml)	Falcon
Tubes for flow cytometry (5 ml)	Sarstedt
Tubes for PCR	Sarstedt
Safelock tubes for molecular biology (1.5 ml and 2 ml)	Roth
Syringes (5 ml)	B. Braun
Syringes (29 G 0.33 mm x 12.7 mm)	B. Braun

### 2.3 List of instruments and equipment

Device	Specification	Manufacturer
Autoclave	V95	Systec
Bacteria shaker	Certomat BS-T	Sartorius
Ice maker	AF 100	Scotsman
Cell counting chamber	Neubauer	Brand
Centrifuge	Multifuge 3 S-R	Heraeus
Centrifuge	Biofuge fresco	Heraeus
Controlled-freezing box	Mr. Frosty	Nalgene
Electroporator	Nucleofactor I	Amaxa biosystems

---

**Material & Methods**

---

Electrophoresis chamber		BioRad
ELISpot reader	AID-ELIRIFL04	Autoimmun Diagnostika
Flow cytometer	FACScalibur™	Becton Dickinson
Freezer (-80°C)	Hera freeze	Heraeus
Freezer (-20°C)	Cool vario	Siemens
Fridge (+4°C)	Cool vario	Siemens
Gel documentation	Gene Genius	Syngene
Heating block	Thermomixer comfort	Eppendorf
Incubator	Hera cell 150	Heraeus
Liquid nitrogen reservoir	L-240 K series	Taylor-Wharton
Luminometer	Sirius Luminometer	Berthold detection systems
Multichannel pipette	(10-100 µl)	Eppendorf
Micropipettes	(0.5 – 10 µl, 10 – 100 µl, 20 – 200 µl, 100 – 1000 µl)	Eppendorf
Microscope	DMIL	Leica
Nanophotometer		Implen
PCR cycler		Eppendorf
Pipetting assistant	Stripettor Plus	Falcon
Real-time PCR	7300 Real-Time PCR	Applied Biosystems
Rotator		GLW
Steril bench		Heraeus
Sonifier	S60H Elmasonic	Elma
Water bath		GFL GmbH
Vortexer	Vortex-Genie 2	Scientific Industries
Water purification system	TKA GenPure	TKA GmbH

## 2.4 List of chemical and biological reagents

Chemical/reagent	Manufacturer
Agar	Sigma
Agarose	Invitrogen
AIM-V Medium	Invitrogen
Ampicilin	Merck
BCP (1-bromo-3-chloropropane)	Sigma
$\beta_2$ -microglobulin	Sigma
Blue Juice Gel Loading Buffer	Invitrogen
Dimethylformamide	Roth
dNTPs	Roche
D-luciferin	Perkin Elmer
DMSO (dimethyl sulfoxide)	Merck
DMEM medium	Invitrogen
Erythrocyte Lysis Buffer	Pharmacy, Klinikum rechts der Isar
EtBr (ethidium bromid)	BioRad
Ethanol	Merck
FCS (fetal calf serum)	Biochrom
Ficoll-Paque	GE Healthcare
Formaldehyd (37%)	Merck
Glycerol	Merck
Glycin	Merck
G418	PAA
HBSS (Hank's buffered salt solution)	Invitrogen
HCl (hydrochloric acid)	Merck
HEPES	Sigma
Human IgG	Genzyme
Human male AB serum	Lonza
Isofluran	Abott
Isopropanol	Sigma

---

**Material & Methods**

---

L-glutamin	Invitrogen
MACS® BSA Stock Solution	Miltenyi
autoMACS™ Rinsing Solution	Miltenyi
Maxima™ Probe/ROX qPCR Master Mix (2x)	Fermentas
MgCl <sub>2</sub> (magnesium chloride)	Invitrogen
NaN <sub>3</sub> (sodium azide)	Merck
NaOH (sodium hydroxide)	Merck
Na-pyruvate	Invitrogen
Non-essential amino acids (100x, NEAA)	Invitrogen
PBS 10 x (phosphate buffered saline)	Invitrogen
PCR buffer (10x)	Invitrogen
Pepton	Invitrogen
PFA (paraformaldehyde)	Merck
PGE <sub>2</sub> (prostaglandin E <sub>2</sub> )	Cayman Chemical Company
Proleukin (recombinant human interleukin 2)	Novartis
Propidium iodide	Sigma
Puromycin	PAA
Ready-Load 1Kb plus DNA Ladder	Invitrogen
rhGM-CSF (recombinant human granulocyte-macrophage colony-stimulating factor)	Genzyme
rhIFN $\gamma$ (recombinantes humanes interferon- $\gamma$ )	R&D
rhIL-1 $\beta$ (recombinant human interleukin 1 $\beta$ )	R&D
rhIL-4 (recombinant human interleukin 4)	Peptotech
rhIL-6 (recombinant human interleukin 6)	R&D
rhIL-7 (recombinant human interleukin 7)	R&D
rhIL-12 (recombinant human interleukin 12)	PanB
rhIL-15 (recombinant human interleukin 15)	Peptotech
rhIL-21 (recombinant human interleukin 21)	Peptotech
Retronectin	TaKaRa

---

**Material & Methods**

---

RPMI 1649 medium	Invitrogen
rhTNF $\alpha$ (recombinant human tumor necrosis factor $\alpha$ )	R&D
Streptavidin-Horse Radish Peroxidase	Mabtech
<i>TransIT</i> ®-293	Mirus
Trypan blue	Sigma
Trypsin/EDTA	Invitrogen
Tween 20	Sigma
TWS119	Merck
X-VIVO 15 medium	Lonza

## 2.5 List of commercial reagent kits

Name	Manufacturer
AccuPrime Taq DNA Polymerase System	Invitrogen
CD8 <sup>+</sup> T cell Isolation Kit, human	Miltenyi
Cell Line Nucleofector® Kit R	Lonza
High-Capacity cDNA Reverse Transcription Kit	Applied Biosystems
JETSTAR 2.0 Plasmid Maxiprep Kit	Genomed
MycoAlert™ Mycoplasma Detection Kit	Lonza
Naive Pan T Cell Isolation Kit	Miltenyi
NucleoSpin® Plasmid Kit	Macherey-Nagel
StrataPrep® DNA Gel Extraction Kit	Stratagene
TaqMan® Gene Expression Assays	Applied Biosystems
TRI Reagent RNA Isolation Kit	Ambion

## 2.6 Antibodies

### 2.6.1 List of antibodies for ELISpot assays

Name	Specification	Manufacturer
Anti-human Granzyme B mAB	GB10, purified	Mabtech
Anti-human Granzyme B mAB	GB11, biotinylated	Mabtech
Anti-human IFN $\gamma$ mAB	1-D1K, purified	Mabtech
Anti-human IFN $\gamma$ mAB	7-B6-1, biotinylated	Mabtech

### 2.6.2 List of antibodies for flow cytometry

Name	Conjugation	Clone	Manufacturer
Anti-human CD3	PE	MOPC-21	BD Biosciences
Anti-human CD4	FITC	RPA-T4	BD Biosciences
Anti-human CD8	APC	RPA-T8	BD Biosciences
Anti-human CD8	FITC	RPA-T8	BD Biosciences
Anti-human CD14	FITC	M5E2	BD Biosciences
Anti-human CD45	APC	HI30	BD Biosciences
Anti-human CD45R0	PE	UCHL1	BD Biosciences
Anti-human CD45RA	PE	T6D11	Miltenyi
Anti-human CD62L	APC	SK11	BD Biosciences
Anti-human CD80	FITC	L307.4	BD Biosciences
Anti-human CD83	APC	HB15e	BD Biosciences
Anti-human CD86	FITC	2331	BD Biosciences
Anti-human CD95	APC	DX2	BD Biosciences
Anti-human CD197 (CCR7)	PE	150503	BD Biosciences
Anti-human HLA-A2	FITC	BB7.2	BD Biosciences
Anti-human HLA-DR	PE	L243	BD Biosciences

Anti-mouse IgG	APC	X40	BD Biosciences
Anti-mouse IgG	FITC	X40	BD Biosciences
Anti-mouse IgG	PE	X40	BD Biosciences
Anti-mouse IgG2a, $\kappa$ , isotype	FITC	X39	BD Biosciences

### 2.6.3 Antibodies for MHC-I blockade

For the blocking of MHC-I molecules on the surface of tumor cells, an azide free anti-human MHC-I antibody (W6.32, Abcam) was used.

## 2.7 Buffer, Media and Solutions

### 2.7.1 List of cell culture media and universal solutions

Name	Ingredients
Standard tumor medium	500 ml RPMI 1640 medium or DMEM medium, 10% FCS, 100 U/ml penicillin and 100 $\mu$ g/ml streptomycin
T cell medium (TCM)	500 ml AIM-V medium, 5% hAB serum, 100 U/ml penicillin and 100 $\mu$ g/ml streptomycin
NSO medium	500 ml DMEM medium, 10% FCS, 1mM Na-pyruvate, 1mM NEAAs, 100 U/ml penicillin and 100 $\mu$ g/ml streptomycin
LCL medium	500 ml RPMI 1640 medium, 10% FCS, 1mM Na-pyruvate, 1mM NEAAs, 100 U/ml penicillin and 100 $\mu$ g/ml streptomycin
4% formaldehyde	4% Formalin, 55 mM Na <sub>2</sub> HPO <sub>4</sub> , 12 mM NaH <sub>2</sub> PO <sub>4</sub> -H <sub>2</sub> O
4% paraformaldehyde	4% PFA in PBS, adjusted to pH 7.4
LB medium	10 g peptone, 5 g yeast extract, 10 g NaCl, in 1000 ml distilled water
LB agar medium	LB medium, 2% Select agar
FACS staining buffer	0.5% BSA in PBS

Freezing medium (tumor cells)	FCS, 10% DMSO
Freezing medium (human cells)	hAB serum, 10% DMSO

## 2.7.2 List of buffer and gel for DNA electrophoresis

Name	Ingredients
TAE running buffer	50 x TAE: 2 M Tris, 10% EDTA (0.5 M), 5.71% HCl
Electrophoresis gel	200 ml TAE buffer (1 x), 0.7-3% agarose, 3 µl EtBr

## 2.8 Oligonucleotides

### 2.8.1 List of primers for polymerase chain reaction (PCR)

Name	Sequence (5'-3')
STEAP1 P2A5 Va2sN	5'-TAG CGG CCG CCA CCA TGA TGA AAT CCT TGA GAG TTT TAC-3'
STEAP1 P2A5 VA2 asE	5'-TGG AAT TCT CAG CTG GAC CAC AGC CGC AGC-3'
STEAP1 P2A5 Va14sN	5'-TAG CGG CCG CCA TGG CAT GCC CTG GCT TCC TG-3'
STEAP1 P2A5 Va14 asE	5'-TGG AAT TCT CAG CTG GAC CAC AGC CGC AG-3'
STEAP1 P2A5 Vb6sN	5'-TAG CGG CCG CCA CCA TGG GCA CCA GCC TCC TCT GC-3'
STEAP1 P2A5 Vb6asE	5'-TGG AAT TCT AGC CTC TGG AAT CCT TTC TC-3'
STEAP1 P2A5 Vb6sN_2	5'-TAG CGG CCG CCA CCA TGG GCA CCA GCC TCC TCT GCT GG-3'
STEAP1 P2A5 Vb6asE2	5'-TGG AAT TCT AGC CTC TGG AAT CCT TTC TCT TG-3'
STEAP1 P2A5 Vb6-P2A	5'-GTC TCC TGC TTG CTT TAA CAG AGA GAA GTT CGT GGC GCC GCT TCC GCC TCT GGA ATC CTT TCT CTT GAC CAT GGC-3'
STEAP1 P2A5 P2A- Va14	5'-TCT CTG TTA AAG CAA GCA GGA GAC GTG GAA GAA AAC CCC GGT CCC ATG GCA TGC CCT GGC TTC CTG TGG GCA CTT-3'

---

**Material & Methods**

---

P-5'aST	5'-CTG TGC TAG ACA TGA GGT CT-3'
P-3'aST	5'-CTT GCC TCT GCC GTG AAT GT-3'
3'T-Ca	5'-GGT GAA TAG GCA GAC AGA CTT GTC ACT GGA-3'
PanVa1	5'-AGA GCC CAG TCT GTG ASC CAG-3'
PanVa1.1	5'-AGA GCC CAG TCR GTG ACC CAG-3'
Va2	5'-GTT TGG AGC CAA CRG AAG GAG-3'
Va3	5'-GGT GAA CAG TCA ACA GGG AGA-3'
Va4	5'-TGA TGC TAA GAC CAC MCA GC-3'
Va5	5'-GGC CCT GAA CAT TCA GGA-3'
Va6neu	5'-GGT CAC AGC TTC ACT GTG GCT A-3'
Va7	5'-ATG TTT CCA TGA AGA TGG GAG-3'
Va8	5'-TGT GGC TGC AGG TGG ACT-3'
Va9	5'-ATC TCA GTG CTT GTG ATA ATA-3'
Va10	5'-ACC CAG CTG CTG GAG CAG AGC CCT-3'
Va11	5'-AGA AAG CAA GGA CCA AGT GTT-3'
Va12	5'-CAG AAG GTA ACT CAA GCG CAG ACT-3'
Va13	5'-GAG CCA ATT CCA CGC TGC G-3'
Va.14.1	5'-CAG TCC CAG CCA GAG ATG TC-3'
Va14	5'-CAG TCT CAA CCA GAG ATG TC-3'
Va15	5'-GAT GTG GAG CAG AGT CTT TTC-3'
Va16	5'-TCA CGC GAA GAT CAG GTC AAC-3'
Va17	5'-GCT TAT GAG AAC ACT GCG T-3'
Va18	5'-GCA GCT TCC CTT CCA GCA AT-3'
Va19	5'-AGA ACC TGA CTG CCC AGG AA-3'
Va20	5'-CAT CTC CAT GGA CTC ATA TGA-3'
Va21	5'-GTG ACT ATA CTA ACA GCA TGT-3'
Va22	5'-TAC ACA GCC ACA GGA TAC CCT TCC-3'
Va23	5'-TGA CAC AGA TTC CTG CAG CTC-3'
Va24neu	5'-GAA CTG CAC TCT TCA ATG C-3'
Va25	5'-ATC AGA GTC CTC AAT CTA TGT TTA-3'

---

**Material & Methods**

---

Va26	5'-AGA GGG AAA GAA TCT CAC CAT AA-3'
Va27	5'-ACC CTC TGT TCC TGA GCA TG-3'
Va28	5'-CAA AGC CCT CTA TCT CTG GTT-3'
Va29	5'-AGG GGA AGA TGC TGT CAC CA-3'
Va30	5'-GAG GGA GAG AGT AGC AGT-3'
Va31neu	5'-TCG GAG GGA GCA TCT GTG ACT A-3'
Va32	5'-CAA ATT CCT CAG TAC CAG CA-3'
P-5'bST	5'-AAG CAG AGA TCT CCC ACA C-3'
P-3'bST	5'-GAG GTA AAG CCA CAG TTG CT-3'
P-3CbII	5'-GAT GGC TCA AAC ACA GCG ACC TC-3'
Vb1	5'-GCA CAA CAG TTC CCT GAC TTG GCA C-3'
Vb2	5'-TCA TCA ACC ATG CAA GCC TGA CCT-3'
Vb3	5'-GTC TCT AGA GAG AAG AAG GAG GCG-3'
Vb4	5'-ACA TAT GAG AGT GGA TTT GTC ATT-3'
Vb5.1	5'-ATA CTT CAG TGA GAC ACA GAG AAA C-3'
Vb5.2	5'-TTC CCT AAC TAT AGC TCT GAG CTG-3'
Vb5.2T	5'-TTC CCT AAT TAT AGC TCT GAG CTG-3'
Vb6.1neu	5'-GCC CAG AGT TTC TGA CTT ACT TC-3'
Vb6.2	5'-ACT CTG ASG ATC CAG CGC ACA-3'
Vb6.3	5'-ACT CTG AAG ATC CAG CGC ACA-3'
Vb7	5'-CCT GAA TGC CCC AAC AGC TCT C-3'
Vb8	5'-ATT TAC TTT AAC AAC AAC GTT CCG-3'
Vb8S3	5'-GCT TAC TTC CGC AAC CGG GCT CCT-3'
Vb9neu	5'-CCT AAA TCT CCA GAC AAA GCT-3'
Vb10	5'-CTC CAA AAA CTC ATC CTG TAC CTT-3'
Vb11	5'-TCA ACA GCT TCC AGA ATA AGG ACG-3'
Vb12	5'-AAA GGA GAA GTC TCA GAT-3'
Vb12S3	5'-GCA GCT GCT GAT ATT ACA GAT-3'
Vb13neu	5'-TCG ACA AGA CCC AGG CAT GG-3'
Vb13.1	5'-CAA GGA GAA GTC CCC AAT-3'

---

**Material & Methods**

---

Vb13.2	5'-GGT GAG GGT ACA ACT GCC-3'
Vb13S5	5'-ATA CTG CAG GTA CCA CTG GCA-3'
Vb14	5'-GTC TCT CGA AAA GAG AAG AGG AAT-3'
Vb15	5'-AGT GTC TCT CGA CAG GCA CAG GCT-3'
Vb16	5'AAA GAG TCT AAA CAG GAT GAG TCC-3'
Vb17	5'-CAG ATA GTA AAT GAC TTT CAG-3'
Vb18	5'-GAT GAG TCA GGA ATG CCA AAG GAA-3'
Vb19	5'-AA TGC CCC AAG AAC GCA CCC TGC-3'
Vb20	5'-AGC TCT GAG GTG CCC CAG AAT CTC-3'
Vb21	5'-AAA GGA GTA GAC TCC ACT CTC-3'
Vb22.1	5'-CAT CTC TAA TCA CTT ATA CT-3'
Vb22.2	5'-AAG TGA TCT TGC GCT GTG TCC CCA-3'
Vb22.3	5'-CTC AGA GAA GTC TGA AAT AAT CG-3'
Vb23	5'-GCA GGG TCC AGG TCA GGA CCC CCA-3'
Vb24neu	5'-ATC CAG GAG GCC GAA CAC TTC T-3'

### **2.8.2 TaqMan Gene Expression Assays**

The TaqMan Gene Expression Assays for STEAP1 (Hs00248742\_m1) and GAPDH (Hs99999905\_m1) were obtained from Applied Biosystems and primers and probes used with concentrations of 900 and 250 nM, respectively.

## 2.9 List of human cancer cell lines

Name	HLA A2 status	Description
293T	unknown	Highly transfectable derivative of cell line 293 transduced with the SV40 T-antigen. Capable of producing high retrovirus titers.
293VecGalv	unknown	Galv envelope plasmid transfected GP21C cells (293SF-derived clone expressing MLV Gag-Pol).
293VecRD114	unknown	Simian derived RD114 envelope plasmid transfected GP21C cells (293SF-derived clone expressing MLV Gag-Pol).
697	positive	B cell precursor leukemia cell line, established from a 12-year-old boy with relapsed ALL in 1979.
A673	positive	ES cell line (type 1 translocation) with additional p53 mutation, established from the primary tumor of a 15-year-old girl.
A673-Luc	positive	ES cell line A673 transfected in our lab, to express firefly luciferase for bioluminescent measurements.
A673 pSI neg	positive	ES cell line A673 transfected with control small interfering RNA (siRNA).
A673 pSI STEAP1	positive	ES cell line A673 transfected with STEAP1 siRNA.
CHP126	negative	Neuroblastoma cell line, established in 1973 from a stage III tumor of a 14-month-old girl.
Cos7	negative	Simian virus 40 (SV40) transformed derivative of simian kidney cell line.

---

**Material & Methods**

---

EW7	positive	ES cell line established from a shoulder-blade tumor; characterized by O. Delattre (Institute Curie, Paris, France).
K562	negative	Established from the pleural effusion of a 53-year-old woman with chronic myelogenous leukemia.
LCL	positive	Lymphoblastoid cell line, established by EBV transformation of peripheral blood B cells from healthy donors by use of a mini-EBV plasmid.
MHH-ES1	positive	ES cell line (type 2 translocation), established from the ascites of a 12-year-old Turkish boy with a tumor of the left pelvis and additional peritoneal metastases.
MHH-NB11	positive	Neuroblastoma cell line established from an adrenal metastasis of a 4-year-old Caucasian boy.
RD-ES	negative	ES cell line (type 2 translocation) established in 1984 from the primary tumor of a 19-year-old caucasian man.
SB-KMS-KS1	negative	Ewing Tumor (ET) cell line (type 1 translocation), established from an extra osseous inguinal metastasis of a 17-year old girl (formerly, SBSR-AKS).
SBSY5Y	negative	Neuroblastoma cell line, established from a bone marrow biopsy of a 4-year-old girl with metastatic neuroblastoma.
SIMA	negative	Neuroblastoma cell line, established in 1991 from a stage III tumor of a 20-month-old caucasian boy.

SK-N-MC	negative	ES cell line (type 1 translocation), established from the supraorbital metastases of a 14-year-old girl with Askin's tumor (related to ET).
T2	positive	TAP-transporter deficient hybrid of a T and a B lymphoblastoid cell line.
TC-71	positive	ES cell line (type 1 translocation) established in 1981 from a locally relapsed ES of a 22-year-old man.

### 2.10 Bacterial strain for plasmid multiplication

For the multiplication of plasmids the chemically competent One Shot® TOP 10 *E. coli* strain (Invitrogen) with the following genotype was used: F-*mcrA*  $\Delta$ (*mrr-hsdRMS-mcrBC*)  $\phi$ 80*lacZ* $\Delta$ M15  $\Delta$ *lacX74* *recA1* *araD139*  $\Delta$ (*araleu*) 7697 *galU* *galK* *rpsL* (StrR) *endA1* *nupG*.

### 2.11 Vectors

The retroviral vectors pMP71STEAP1humm (Fig. 3) and pMP71STEAP1wt (Fig. 4) were obtained from GeneArt. The expression vector pCMVTag4A was from Origene and STEAP1 previously integrated into the vector in our lab (Fig. 5). The pCDN3.1 / Zeo(-) / HLA-A2 (Fig. 6) vector was a gift from the laboratory of Prof. Dr. Helga Bernhard, Department of Hematology / Oncology, Klinikum rechts der Isar, Technische Universität München, 81664 Munich, Germany. The pmaxGFP vector is a control vector included in the Cell Line Nucleofector® Kit R.

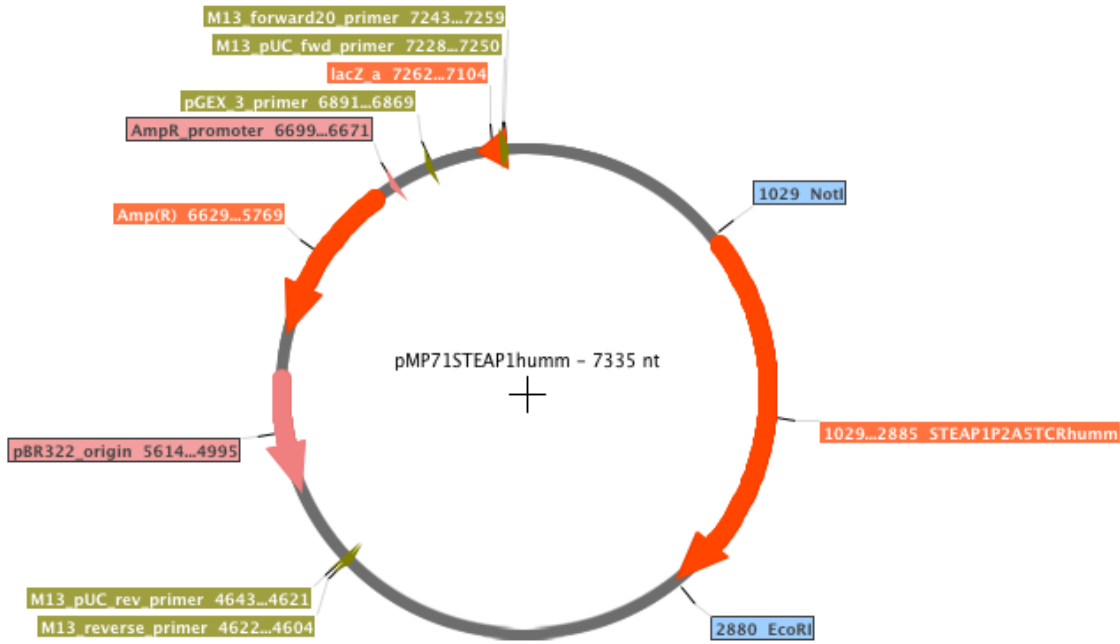


Figure 3: Vector map of the retroviral pMP-71 vector containing the codon optimized and minimal murinized STEAP1<sup>P2A5</sup>TCR.

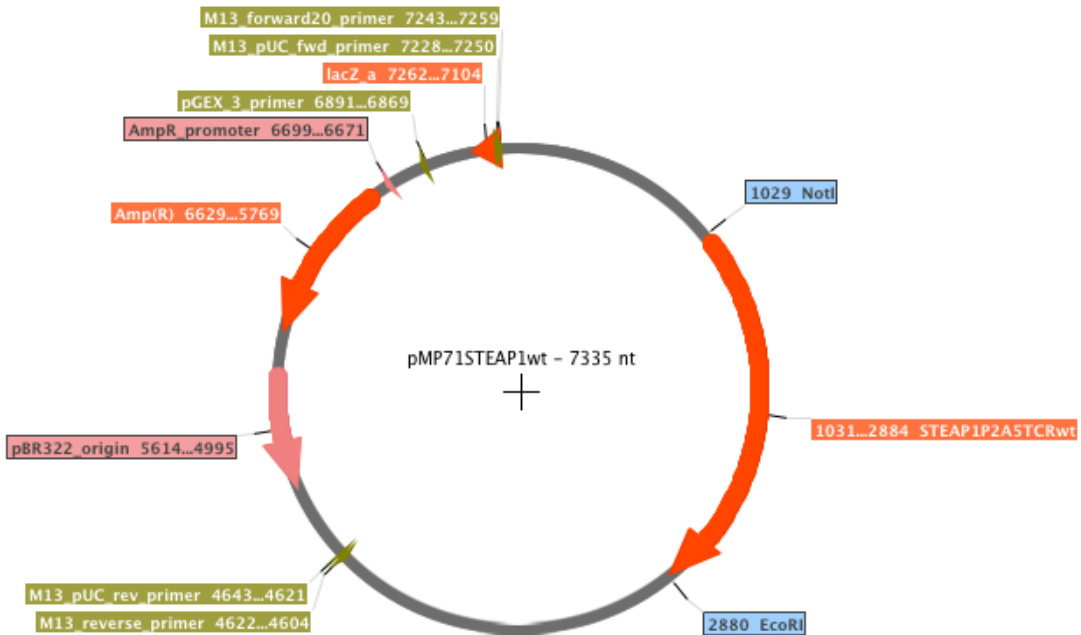


Figure 4: Vector map of the retroviral pMP-71 vector containing the wildtype STEAP1<sup>P2A5</sup>TCR.

## Material & Methods

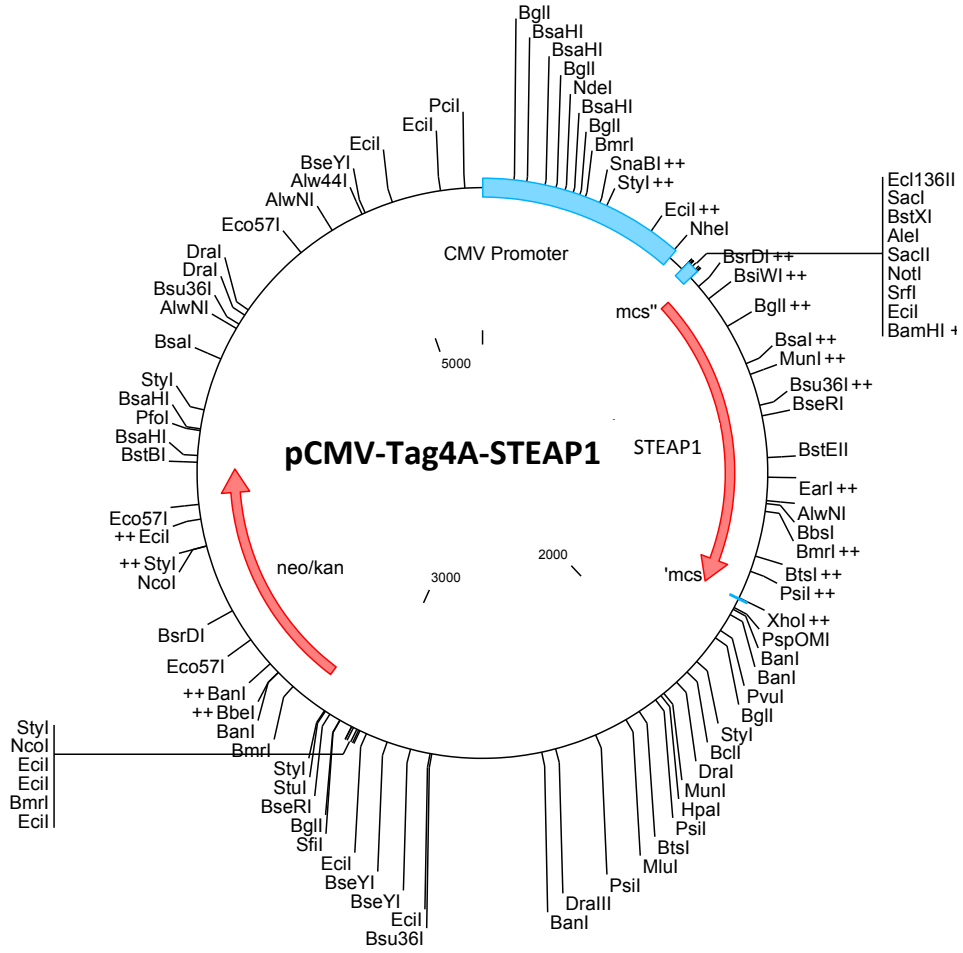


Figure 5: Vector map of the STEAP1 expression vector

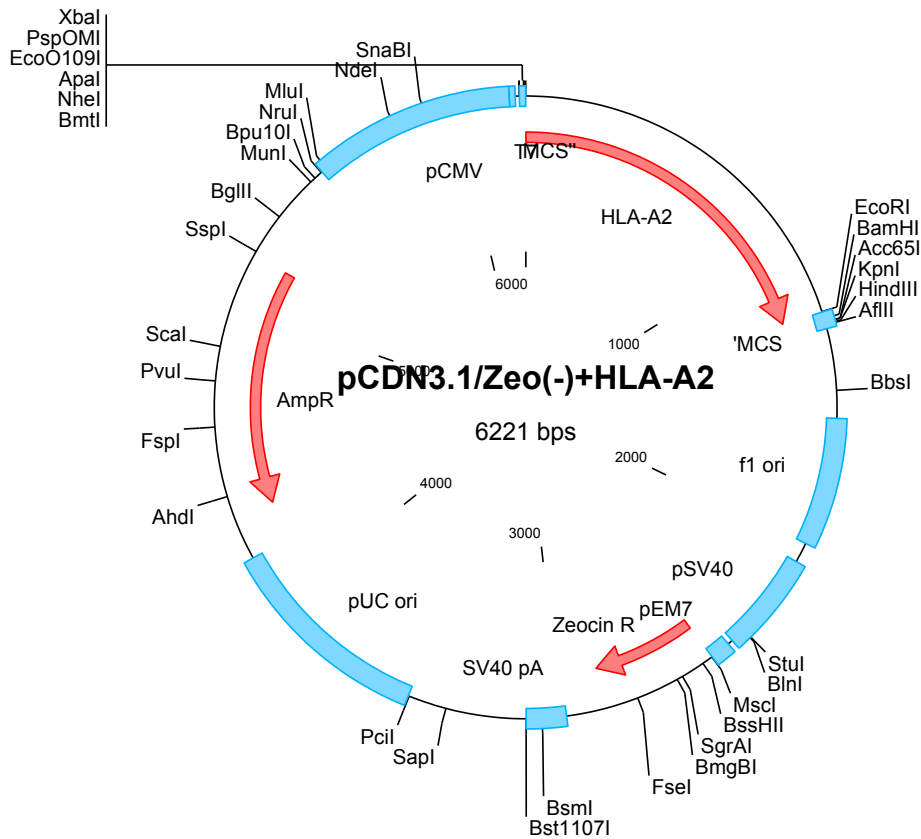


Figure 6: Vector map of the HLA-A\*02:01 expression vector.

## 2.12 Mouse model

The mouse model on a BALB/c background used in the experiments has knockouts in the *Rag2* as well as in the *gamma(c)* locus. Deletion of the *Rag2* locus leads to a complete loss of peripheral B-lymphocytes as well as thymus-derived T-lymphocytes. The common cytokine receptor gamma chain ( $\gamma c$ ) is a functional subunit of a variety of cytokine receptors including the IL-2, IL-7 and IL-15 receptor. Loss of this gene leads to an impaired development of NK cells and hampers survival of NK cells and T lymphocytes. As a result the *Rag2*<sup>-/-</sup>*γc*<sup>-/-</sup> mouse model is completely abolished from NK cells as well as B- and T-lymphocytes and can be claimed as immunodeficient (90). The animals were obtained from the Central Institute for Experimental Animals

---

## Material & Methods

---

(Kawasaki, Japan) and kept in the Zentrum für Präklinische Forschung (Klinikum rechts der Isar, München) under pathogen free conditions.

### 3 Methods

#### 3.1 Cultivation of adherent and suspension tumor cell lines

All Ewing Sarcoma (ES) and neuroblastoma cell lines were cultured in RPMI 1640 medium (Invitrogen) containing 10% FCS (Biochrom), 100 U/ml penicillin and 100 µg/ml streptomycin (Invitrogen). For LCL and T2 cells RPMI 1640 medium was additionally provided with 1mM Na-pyruvate and non-essential amino acids (Invitrogen). Dendritic cells were cultivated in X-VIVO 15 medium (Lonza) enriched with 1% human AB serum (hAB) without antibiotics. 293T, 293VecGalv (Galv), 293VecRD114 (RD114) packaging cell lines and hIL-15 producing NSO cells were cultured in DMEM (Invitrogen) containing 10% FCS, 1mM Na-pyruvate, 1mM non-essential amino acids and antibiotics. T cells were cultured in AIM-V medium (Invitrogen) containing 5% human AB serum and antibiotics. All cells were cultivated in T25, T75 or T175 culture flasks (Greiner Bio One) at 37 °C and 5% CO<sub>2</sub>.

Suspension cell lines were split every 3 - 4 days 1:2 to 1:10. Adherent cells received fresh medium every 3 - 4 days and cells were split 1:5 to 1:10 once a week. Therefore, medium was aspirated completely and cells were washed once with PBS. Subsequently, Trypsin/EDTA (Invitrogen) was added and cells incubated at 37 °C until they were detached from the bottom of the culture flask. Cell numbers were determined with a Neubauer hemocytometer using Trypan-Blue (Sigma) exclusion method of dead cells and an appropriate amount of cells afterwards transferred into fresh cell culture flasks.

To detect mycoplasma contamination all cell lines were tested regularly with the MycoAlert™ Mycoplasma Detection Kit according to the manufacturer's instructions (Lonza). If there was a contamination with mycoplasmas, cells were discarded and replaced by freshly thawed aliquots. Additionally tumor cell lines were routinely tested for their HLA-A2 status by flow cytometry.

### **3.2 Freezing and thawing**

Depending on the given tumor cell line, cell concentrations between  $1 \times 10^6$  and  $1 \times 10^7$  cells/ml were cryopreserved in FCS/10% DMSO. Human T cell clones as well as transgenic T cells were frozen in aliquots containing  $3 \times 10^5$  cells in hAB serum/10% DMSO. After re-suspension of pelleted cells in the desired volume of the appropriate pre-cooled freezing medium, 1 ml aliquots of the cell suspension were transferred into pre-cooled cryovials. The cryovials were placed into controlled freezing boxes, stored for 12 - 18h at  $-80 \text{ }^\circ\text{C}$  and were then transferred into a liquid nitrogen reservoir ( $-192 \text{ }^\circ\text{C}$ ) for long-term storage. For recovery of cryopreserved cells, cryovials were thawed at  $37 \text{ }^\circ\text{C}$ , afterwards washed with appropriate medium to remove cytotoxic DMSO and transferred into T75 cell culture flasks.

### **3.3 *In silico* prediction of HLA-A\*02:01 peptide binding properties**

An *in silico* analysis of STEAP1 peptide nonamers was executed to find feasible adoptive T cell transfer (ACT) targets. We used BIMAS ([http://www-bimas.cit.nih.gov/molbio/hla\\_bind/](http://www-bimas.cit.nih.gov/molbio/hla_bind/)), NetCTL1.2 (<http://www.cbs.dtu.dk/services/NetCTL/>) and SYFPEITHI (<http://www.syfpeithi.de/bin/MHCServer.dll/EpitopePrediction.htm>) web based algorithm tools to check for HLA-A\*02:01 binding and proteasomal cleavage as well as TAP-transport of STEAP1 peptides. Top binders of all three web tools were further tested in a HLA-A\*02:01 binding assay.

### **3.4 HLA-A\*02:01 binding assay**

To confirm the suitable presentation of STEAP1 specific peptides on HLA-A\*02:01 (HLA-A2) predicted by the *in silico* analysis, a binding assay using the TAP-transporter deficient T2 cell line was performed.  $50 \text{ }\mu\text{M}$  and  $100 \text{ }\mu\text{M}$  as well as titrated amounts of various STEAP1 peptide nonamers were loaded onto T2 cells for 16h at  $37 \text{ }^\circ\text{C}$  and 5%  $\text{CO}_2$ . Therefore, T2 cells were washed twice with PBS and re-suspended in RPMI 1640 medium. Afterwards peptides were added in appropriate concentrations ranging

from  $10^{-10}$   $\mu\text{M}$  – 100  $\mu\text{M}$ . Subsequently, stabilized HLA-A2 molecules on the cell surface were stained with a FITC-conjugated anti-HLA-A2 antibody (BD Bioscience) and fluorescence intensity compared to T2 cells loaded with a well-established influenza peptide (GILGFVFTL).

### **3.5 Isolation of peripheral blood mononuclear cells from buffy coats**

For the isolation of peripheral blood mononuclear cells (PBMCs), human peripheral blood samples (obtained with IRB approval and informed consent from the DRK-Blutspendedienst Baden-Wuerttemberg-Hessen, Ulm, Germany) were separated via density gradient centrifugation using Ficoll-Paque (GE Healthcare) according to the supplier's instructions. Therefor whole blood samples were diluted 1:2 with PBS and 10 ml Ficoll-Paque were overlaid with 20 ml of the diluted blood. After centrifugation for 30 min at 400 x g without active deceleration, the PBMC containing interlayer was collected and washed twice with PBS. When there was any contamination with erythrocytes, the cell pellet was re-suspended in Erythrocyte Lysis Buffer and incubated for 5 min at 37 °C before the reaction was stopped with PBS. Cells were pelleted and re-suspended in 10 ml PBS for determination of cell numbers.

### **3.6 Generation of monocyte derived dendritic cells (moDCs)**

After isolation of PBMCs out of a healthy HLA-A\*02:01<sup>+</sup> donor, CD14<sup>+</sup> monocytes were isolated using anti-human CD14 magnetic particles (BD Bioscience), according to the supplier's instructions. Briefly, PBMCs were washed with an excess volume of 1 x BD Imag Buffer (BD Bioscience) and re-suspended at a concentration of  $4 \times 10^8$  cells/ml in magnetic particle containing solution. Suspension was mixed thoroughly and incubated for 30 min at 4 °C. Cells were expanded to a volume of 9 ml with 1 x BD Imag buffer and placed onto a magnet for 8 - 10 min. Supernatant was aspirated and cells washed twice with 1 x BD Imag buffer. Cells were then cultivated at a concentration of  $5 \times 10^5$  cells/ml in X-VIVO 15 medium containing 1% hAB serum, 1000 U/ml rhIL-4 (Peprotech) and 800 U/ml GM-CSF (Genzyme), for the transformation of monocytes into moDCs. Cytokines were refreshed on day 3. On day 5, medium was

exchanged and maturation induced by adding a cytokine cocktail consisting of 1000 U/ml rhIL-6, 10 ng/ml rhIL-1 $\beta$ , 10 ng/ml rhTNF- $\alpha$  (all R&D) and 1  $\mu$ g/ml PGE<sub>2</sub> (Cayman Chemicals). DCs were designated as mature when they detached from the cell culture flask and stained positive for the markers CD80, CD83 and HLA-DR in flow cytometry on day 7.

### **3.7 Isolation of T cell subpopulations**

To obtain an unlabeled CD8<sup>+</sup> T cell population, the irrelevant cell populations of healthy HLA-A\*02:01<sup>-</sup> donor PBMCs were magnetically labeled using the human CD8<sup>+</sup> T cell isolation kit (Miltenyi) and subsequently depleted on LS columns (Miltenyi), following the manufacturer's instructions. Therefor PBMCs were isolated, washed twice with 1 x PBS and re-suspended in 40  $\mu$ l/10<sup>7</sup> cells MACS buffer. 10  $\mu$ l/10<sup>7</sup> cells of the respective biotinylated antibody cocktail were added and the mixture was incubated for 10 min at 4 °C. Subsequently another 30  $\mu$ l/10<sup>7</sup> cells buffer and 20  $\mu$ l/10<sup>7</sup> cells microbead cocktail were added. After incubation of 15 min at 4 °C, cells were washed and re-suspended in 500  $\mu$ l/10<sup>8</sup> cells MACS buffer before separating the cells on a column by gravity-flow. After washing the column 3 times with MACS buffer, the flow-through was collected containing the desired enriched CD8<sup>+</sup> T cell population. For further isolation of untouched naïve CD8<sup>+</sup> T cells, such T cells were enriched for CCR7<sup>+</sup>CD45RA<sup>+</sup> cells, using the Naive Pan T Cell Isolation Kit (Miltenyi) with a similar isolation protocol.

### **3.8 Expansion of allo-restricted, peptide specific, cytotoxic T cells (CTL)**

Mature moDCs of a healthy HLA-A\*02:01<sup>+</sup> donor were pulsed with 38  $\mu$ M STEAP1<sup>130</sup> peptide, supported by 20  $\mu$ g/ml  $\beta$ 2-microglobulin, in TCM for 4h at 37 °C and 5% CO<sub>2</sub> under continuous rotation. Subsequently, untouched CD8<sup>+</sup> T cells from a HLA-A\*02:01<sup>-</sup> healthy donor were co-cultured with pulsed moDCs in TCM, containing 10 ng/ml rhIL-12 and 1000 U/ml rhIL-6 for one week at a effector to target rate of 1:20 in 96 well plates. After one week, T cells were re-primed with the same amount of freshly generated, peptide loaded moDCs together with 100 U/ml rhIL-2 and 5 ng/ml rhIL-7. After two

weeks STEAP1<sup>130</sup> specific, HLA-A\*02:01 restricted CD8<sup>+</sup> T cells were sorted for further expansion.

### **3.9 Sorting and expansion of STEAP1<sup>130</sup> multimer positive CTLs**

For FACS sorting of STEAP1<sup>130</sup> specific T cells, cells were pooled after two weeks of co-culture with moDCs and stained with STEAP1<sup>130</sup> specific phycoerythrin (PE) labeled multimer (Dirk Busch) and anti-CD8 mAb. Isotype IgG and irrelevant multimer served as controls. Sorting was performed on a FACS Aria (BD Bioscience) at the institute of medical microbiology (TUM) and STEAP1<sup>130</sup>/HLA-A\*02:01 multimer<sup>+</sup> CD8<sup>+</sup> T cells collected in hAB serum. Subsequently, cells were expanded in 96 well plates containing  $5 \times 10^4$  irradiated (30 Gy) PBMCs (pooled from 5 different donors) and  $1 \times 10^5$  irradiated (100 Gy) LCLs as well as 30 ng/ml anti-CD3 mAb (OKT3), 100 U/ml rhIL-2 and 2 ng/ml rhIL-15. Cells were diluted to statistically one cell per well using the limiting dilution approach. Cells were expanded for two weeks with replacement of medium and cytokines on day 7, before analyzing T cell lines in functional assays.

### **3.10 Generation of stem cell memory like T cells (T<sub>SCM</sub>)**

For the generation of stem cell like memory T cells (T<sub>SCM</sub>), naïve T cells were activated with anti-CD3/CD28 microbeads (Invitrogen) at a bead: cell ratio of either 3:1 (Cieri *et al.*) or 1:1 (Gattinoni *et al.*). When the protocol of Cieri *et al.* (91) was used  $5 \times 10^5$  cells/ml were cultivated in T cell medium (TCM) containing moderate amounts of rhIL-7 and rhIL-15 (5ng/ml). For the generation of T<sub>SCM</sub> using the protocol of Gattinoni *et al.* (92)  $5 \times 10^5$  cells/ml were cultivated together with 5  $\mu$ M of the GSK-3 $\beta$  Inhibitor XII TWS119 (Merck) and 300 U/ml rhIL-2. Cytokines and TWS119 were replaced every 3 - 4 days and medium exchanged whenever necessary. T cells were designated as stem cell memory like T cells staining positive for the surface markers CD45RA, CCR7, CD62L, CD95 and CD45R0, as verified by flow cytometry.

### **3.11 Transduction of PBMCs and T<sub>SCM</sub> with STEAP1 specific TCRs**

Cells were transduced using a retroviral infection system. On day one,  $3 \times 10^5$  RD114,  $3 \times 10^5$  Galv or  $2 \times 10^5$  293T packaging cells were seeded in 3 ml RD114 medium in a 6 well plate. One day later the TCR encoding retroviral plasmid was applied to the cells. For each approach 200  $\mu$ l DMEM without supplements were incubated with 9  $\mu$ l TansIT (Mirus) transfection reagent for 20 min at RT. Then 1  $\mu$ g retroviral plasmid was added and incubated for another 30 min to enable complex formation between plasmid and transfection reagent. When 293T cells were used as packaging cell line, additionally plasmids encoding the envelope glycoprotein (*env*) and the reverse transcriptase as well as the retroviral core proteins (*pol/gag*), had to be added. On the same day PBMCs and T<sub>SCM</sub> were isolated, respectively, and activated either via OKT3 and 100 U/ml rhIL-2, via anti-CD3/CD28 microbeads (bead: cell ratio 3:1) together with rhIL-7 and rhIL-15 (5 ng/ml) or via anti-CD3/CD28 microbeads (bead: cell ratio 1:1) together with 300 U/ml rhIL-2 and 5  $\mu$ M TWS119. On day 3 non-tissue culture 24 well plates were coated with 5  $\mu$ g Retronectin to support transduction efficacy by bringing virus and cells in close proximity. On day 4, spin transduction was performed by incubating  $1 \times 10^6$  T cells with 1 ml virus supernatant, cytokines, 1% HEPES and 4  $\mu$ g/ml protaminsulfate. Co-culture was centrifuged for 90 min at 32 °C. One day later, cells were split 1:2 and spin transduction procedure repeated. Transduction efficacy was verified on day 10 via multimer staining and analysis in flow cytometry. A scheme of the transduction procedure can be found in Figure 7.

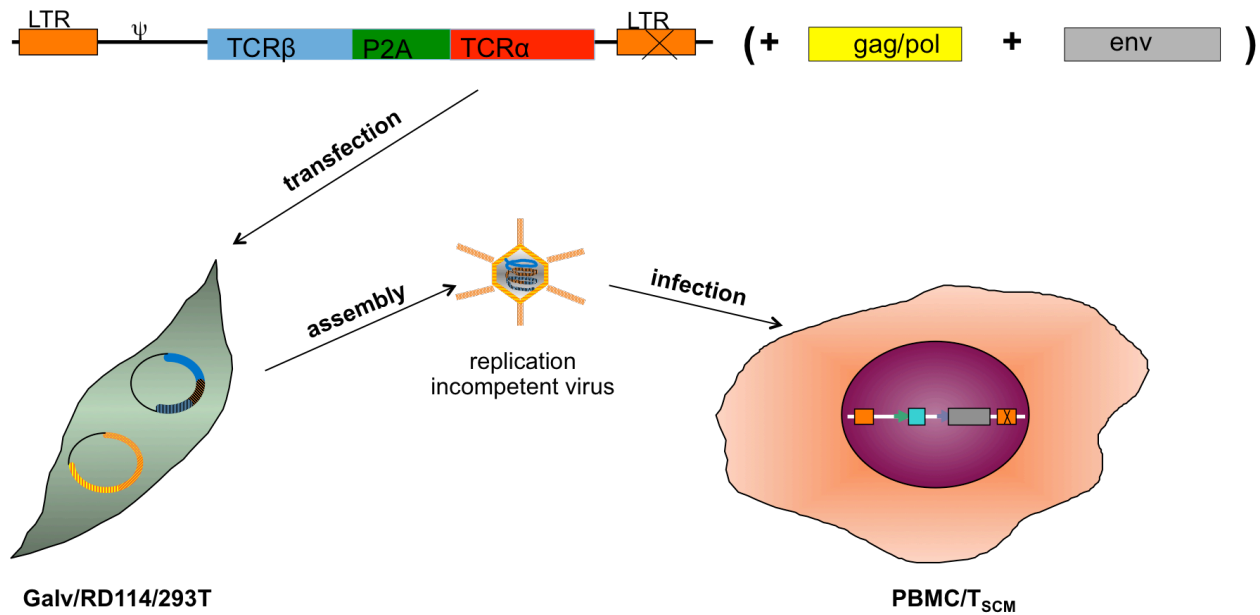


**Figure 7: Transduction scheme for TCR  $\alpha$ - and  $\beta$ -chains into various target cells.** TCR  $\alpha$ - and  $\beta$ -chains are linked with a self-cleaving P2A element and added either alone or together with *gag/pol* and *env* encoding vectors to the packaging cell lines 293VecGalv (Galv), 293VecRD114 (RD114) or 293T. Afterwards PBMCs or T<sub>SCM</sub> were cultivated with virus supernatant. Procedure was repeated once to increase transduction efficacy.

### 3.12 Flow cytometry

Cells were harvested, washed two times with staining buffer (0.5% BSA in PBS) and re-suspended at a concentration of  $4 \times 10^6$  cells/ml staining buffer. Then samples were incubated with specific fluorochrome-labeled monoclonal antibodies (mAb) for 30 min at 4 °C. Respective isotype antibodies served as negative controls. After washing twice again, cells were re-suspended in 300  $\mu$ l PBS and analyzed on a FACScalibur flow cytometer (Becton Dickinson) with at least 25000 events/sample recorded. Analysis was performed using the Cellquest software (Becton Dickinson).

Dendritic cells were analyzed using CD80, CD83 and HLA-DR specific antibodies. CD45R0, CD45RA (Miltenyi), CD62L, CD95 and CCR7 (except CD45RA all from BD Biosciences) specific antibodies were used to confirm the stem cell memory like phenotype of T cells. HLA status of tumor cells was checked using an anti-HLA-A2 mAb (BD Biosciences). Cytotoxic T cells were stained using human CD8 specific antibodies (BD Biosciences) and specific multimers (handmade, Dirk Busch, Institute of Medical

Microbiology and Hygiene). At the end of the *in vivo* experiments blood, spleen and tumors of animals were analyzed using human CD45 and human CD8 (both BD Biosciences) specific mAb.

### **3.13 ELISpot**

96 well mixed cellulose ester plates (MultiScreen-HA Filter Plate) were coated overnight with 10 µg/ml 1-D1K (for detection of IFN $\gamma$  release) or GB10 (for detection of granzyme B release) mAb per well, respectively. On day two, plates were washed 4 times with 200 µl PBS, followed by blocking with 150 µl TCM for at least 1 h at 37 °C and 5% CO $_2$  to avoid unspecific binding. In the meantime, T cells were harvested and washed three times with TCM. T cells were incubated without targets for 30 min at 37 °C before adding tumor cells. To avoid dispersion of T cells, target cells were carefully dripped on top and plates were incubated for 20 h at 37 °C and 5% CO $_2$ . On day three, plates were washed 6 times with PBS/0.05% Tween, followed by incubation with 2 µg/ml 7-B6-1 (IFN $\gamma$ ) or GB11 (granzyme B) biotinylated mAb for two hours at 37 °C and 5% CO $_2$ . After incubation, plates were washed again six times with PBS/0.05% Tween and incubated with 200 µl Streptavidin-HRP (1:100 dilution) for 1 h at RT. In IFN $\gamma$  ELISpots, cells were used at an effector: target ratio of 1:20. When granzyme B was to be detected, effector: target ratios were titrated ranging from 10:1 - 0.15625:1. All experiments were performed in triplicates. T cells alone served as a negative control. Analysis was performed using an ELISpot reader (Autoimmun Diagnostika).

### **3.14 xCelligence assay**

Specific inhibition of target cell growth by candidate T cell clones was determined using the impedance based xCELLigence system. The system detects cellular changes in real-time by measuring electrical impedance using golden microelectrodes. To allow target cell adhesion to the surface of the electrodes, cells were seeded 48 h in advance compared to T cells. For A673 cells  $1 \times 10^4$  cells per well were seeded, for SK-N-MC  $2.5 \times 10^4$  cells per well. Target specific T cells were added in titrated amounts ranging from an effector: target ratio of 20: 1 – 0.3: 1 on top of tumor cells and analysis

performed over a total time period of 5 days with measurements every 15 min. Untreated target cells and medium alone served as controls. Experiments were executed in quintuplicates.

### **3.15 RNA isolation**

For mRNA analysis up to  $1 \times 10^7$  cells were re-suspended in TriReagent and either further used for immediate mRNA isolation or frozen if isolation was performed later. Cells in TriReagent were mixed with 100  $\mu$ l BCP/ml of TRI Reagent for 5 - 15 min and subsequently phases were separated at 12000 x g for 10 - 15 min at 4 °C. The RNA containing aqueous phase was transferred into new tubes and the RNA thereafter precipitated with 500  $\mu$ l isopropanol for 5 - 10 min at RT and subsequently centrifuged at 12000 x g for 8 min. Then the RNA was washed with 1 ml 75% ethanol, centrifuged at 7500 x g for 5 min and briefly air dried, before resuspended in DEPC-treated ddH<sub>2</sub>O. RNA content was measured using a nanophotometer.

### **3.16 Reverse transcription**

To analyze the expression profile of different genes within cells via quantitative real-time polymerase chain reaction (qRT-PCR), RNA was reverse transcribed into complementary DNA (cDNA) using the High-Capacity cDNA Reverse Transcription Kit (Applied Biosystems). Therefore, 5.8  $\mu$ l reverse transcription master mix containing dNTPs, MultiScribe™ Reverse Transcriptase, reverse transcription random primers and buffer were mixed with 14.2  $\mu$ l RNA solution (containing 1  $\mu$ g purified RNA).

### cDNA synthesis

PCR mix:	RT Buffer (10x)	2.0 $\mu$ l
	RT random primers (10x)	2.0 $\mu$ l
	dNTP Mix (100 mM)	0.8 $\mu$ l
	RNA (1 $\mu$ g)	in 14.2 $\mu$ l ddH <sub>2</sub> O
	Multiscribe® Reverse Transcriptase (50 U/ $\mu$ l)	1 $\mu$ l

Cycling conditions:	25 °C	10 min
	37 °C	120 min
	85 °C	5 min
	4 °C	$\infty$

### 3.17 Quantitative Real Time PCR (qRT-PCR)

qRT-PCR was performed using Maxima™ Probe/ROX qPCR Master Mix (2x) and specific TaqMan® Gene Expression Assays (Applied Biosystems), consisting of two unlabeled PCR primers and a FAM™ dye-labeled TaqMan® MGB probe. Reaction mixes were prepared in 96 well plates according to the manufacturer's instructions (Fermentas PureExtreme™ Insert). Briefly, 10  $\mu$ l of Maxima™ Probe/ROX qPCR Master Mix (2x), 1  $\mu$ l TaqMan® Gene Expression Assays, 0.5  $\mu$ l cDNA template and 8.5  $\mu$ l RNase-free water were mixed. Final concentrations of primers and probe were 0.9 and 0.25  $\mu$ M respectively. Gene expression profiles were normalized to mRNA levels of the *glyceraldehyde 3-phosphate dehydrogenase (GAPDH)* housekeeping gene and calculated using the 2-ddCt method. Fluorescence measurement was performed in an AB 7300 Real-Time PCR system using a three-step cycling protocol: 1 s 50 °C; 10 min 95 °C; (15 s 95 °C; 1 min 60 °C) 40x (Applied Biosystems).

### **3.18 Identification of TCR $\alpha$ - and $\beta$ -repertoire**

To identify the TCR  $\alpha$ - and  $\beta$ -chains of the STEAP1<sup>130</sup> specific T cell clone P2A5, a PCR based approach was used. Therefore, RNA was isolated out of a monoclonal T cell population, cDNA synthesized and 34 degenerate alpha chain specific primers and 35 beta chain specific primers as well as two constant internal controls per chain used to amplify the TCR repertoire. The PCR was performed using the AccuPrime Taq DNA Polymerase System (Invitrogen).

#### **Identification of P2A5 T cell line V $\alpha$ - and V $\beta$ -repertoire**

Ingredients for V $\alpha$ -repertoire:	ddH <sub>2</sub> O	18 $\mu$ l
	Buffer I (10x)	2.5 $\mu$ l
	P-5'aST (5 $\mu$ M)	0.5 $\mu$ l
	P-3'aST (5 $\mu$ M)	0.5 $\mu$ l
	3'T-Ca (5 $\mu$ M)	1 $\mu$ l
	Variable $\alpha$ -chain Primers (5 $\mu$ M)	1.5 $\mu$ l
	AccuPrime polymerase (2 U/ $\mu$ l)	0.5 $\mu$ l

Ingredients for V $\beta$ -repertoire:	ddH <sub>2</sub> O	18 $\mu$ l
	Buffer I (10x)	2.5 $\mu$ l
	P-5'bST (5 $\mu$ M)	0.5 $\mu$ l
	P-3'bST (5 $\mu$ M)	0.5 $\mu$ l
	3'T-CbII (5 $\mu$ M)	1 $\mu$ l
	Variable $\beta$ -chain Primers (5 $\mu$ M)	1.5 $\mu$ l
	AccuPrime polymerase (2 U/ $\mu$ l)	0.5 $\mu$ l

---

## Material & Methods

---

Cycling conditions:	94 °C	6 min		
	94 °C	1 min	}	40x
	54 °C	1 min		
	68 °C	1 min		
	68 °C	7 min		
	4 °C	∞		

PCR products were analyzed on a 2% agarose gel, specific bands eluted using the StrataPrep® DNA Gel Extraction Kit (Stratagene) and sequenced (Sequiseve). Subsequently, sequences were aligned with the IMGT database and productive TCR sequences cloned into plasmids to confirm the *in silico* alignment. To do this the predicted variable chains were completed in frame with the corresponding constant chains and primers covering the whole TCR  $\alpha$ - and  $\beta$ -chains designed. For the  $\alpha$ -chain the primers STEAP1 P2A5 Va14sN and STEAP1 P2A5 Va14asE were used, for the  $\beta$ -chain STEAP1 P2A5 Vb6sN and STEAP1 P2A5 Vb6asE (all 5  $\mu$ M). The PCR product was again sequenced and checked for integrity before designing a construct for the infection of T cells.

### PCR conditions for amplification of TCR P2A5 $\alpha$ -chain

Ingredients:	ddH <sub>2</sub> O	31.5 $\mu$ l
	Native Plus Buffer (10x)	5 $\mu$ l
	STEAP1P2A5Va14sN Primer	5 $\mu$ l
	STEAP1 P2A5 Va14asE Primer	5 $\mu$ l
	dNTPs	2 $\mu$ l
	P2A5 cDNA	1 $\mu$ l
	Pfu polymerase	1 $\mu$ l

---

## Material & Methods

---

PCR conditions:	94 °C	2 min		
	94 °C	30 s	}	5x
	58 °C	30 s		
	72 °C	2 min	}	40x
	94 °C	30 s		
	62 °C	30 s	}	40x
	72 °C	2 min		
	72 °C	10 min		
	4 °C	∞		

### PCR conditions for amplification of TCR P2A5 $\beta$ -chain

Ingredients:	ddH <sub>2</sub> O	31.5 $\mu$ l
	Native Plus Buffer (10x)	5 $\mu$ l
	STEAP1P2A5Vb6sN Primer	5 $\mu$ l
	STEAP1 P2A5 Vb6asE Primer	5 $\mu$ l
	dNTPs (100 mM)	2 $\mu$ l
	P2A5 cDNA	1 $\mu$ l
	Pfu polymerase (2.5 U/ $\mu$ l)	1 $\mu$ l

PCR conditions:	94 °C	2 min		
	94 °C	30 s	}	5x
	62 °C	30 s		
	72 °C	2 min	}	40x
	94 °C	30 s		
	64 °C	30 s	}	40x
	72 °C	2 min		
	72 °C	10 min		
	4 °C	∞		

### 3.19 Design of retroviral TCR construct

For infection of target cells, the complete TCR was synthesized and subcloned into a pMP-71 retroviral backbone by GeneArt, using the identified TCR  $\alpha$ - and  $\beta$ -chains connected by a self-cleaving P2A element. To increase expression and avoid misspairing of exo- and endogenous TCR chains, a second construct with human codon optimized and minimal murinized (hummm)  $\alpha$ - and  $\beta$ -chains was designed, complying with the results of Sommermeyer *et al.* (93). Sequences of both constructs are shown in the Appendix.

### 3.20 Agarose gelelectrophoresis

To separate DNA fragments, agarose gelelectrophoresis was performed. Therefore, agarose was dissolved in 150 ml TAE buffer and supplemented with 4  $\mu$ l EtBr. DNA was mixed with 6x Blue Juice Gel Loading Buffer (Invitrogen) and gel pockets filled with up to 20  $\mu$ l DNA containing suspension. The 1kb plus ladder (Invitrogen) was used as size standard. Electrophoresis was performed at 90 V for 45 min. To isolate DNA from agarose gels, bands were excised and purified using the StrataPrep® DNA Gel Extraction Kit, following the supplier's instructions.

### 3.21 Mini and maxi plasmid preparation

To expand plasmid DNA, chemically competent One Shot® TOP 10 *E. coli* bacteria (Invitrogen) were transformed by the originate plasmid using a heat shock. Briefly, plasmid and bacteria were incubated for 30 min on ice, followed by a heat shock at 42 °C for 30 s. Afterwards the suspension was placed back on ice. Then 250  $\mu$ l of pre-warmed S.O.C medium were added and cells recovered at least 1 h at 275 rpm and 37 °C. To check for successful integration of the plasmid into bacteria, cells were spread on LB plates containing either ampicillin or kanamycin as selection markers. Bacterial plates were incubated at 37 °C over night and clones containing the plasmids picked and further amplified in either 5 ml or 400 ml LB medium supplemented with antibiotics. The plasmid preparations were performed according to manufacturers guidelines using

the NucleoSpin® Plasmid Kit (Machery & Nagel) for small-scale plasmid isolation. When large amounts of plasmid should be obtained the JETSTAR 2.0 Plasmid Maxiprep Kit was used. DNA content was checked via spectrophotometry and plasmids analyzed via restriction enzyme analysis and sequencing. For control digestion of plasmids, DNA was incubated for 1 - 2 h at 37 °C together with EcoRI and NotI restriction enzymes and subsequently analyzed after agarose gel electrophoresis.

### **Digestive analysis**

Ingredients:	ddH <sub>2</sub> O	14 µl
	plasmid DNA	< 1 µg in 3 µl
	Buffer (10x)	2 µl
	EcoRI (10 U/µl)	0.5 µl
	NotI (10 U/µl)	0.5 µl

Digestion was performed for 2 h at 37 °C.

### **3.22 *In vivo* experiments**

Two *in vivo* experiments were carried out. In the first experiment Rag2<sup>-/-</sup>γc<sup>-/-</sup> immunodeficient mice were inoculated with 2 x 10<sup>6</sup> A673 cells subcutaneously into the groin. On day three, the animals were sublethally irradiated (3.5 Gy). One day later we injected 3 x 10<sup>6</sup> human codon optimized and minimally murinized (humm) STEAP1<sup>P2A5</sup> TCR transgenic T<sub>SCM</sub> together with 5 x 10<sup>6</sup> CD8 depleted autologous PBMCs or 3 x 10<sup>6</sup> HLA-A\*02:01<sup>-</sup> PBMCs or no cells at all intra peritoneally (i.p.). Additionally, cells were provided with hIL-15 by injecting 1.5 x 10<sup>7</sup> hIL-15 producing NSO cells (NSO-IL15) i.p. twice a week. The experiments were stopped when tumors of any treatment group reached 1 cm<sup>3</sup>. At the end of the experiment tumors were weighted and analyzed via flow cytometry analysis and immunohistochemistry.

In a second experiment mice received  $2 \times 10^6$  luciferase expressing A673 cells were again irradiated on day three and received either  $5 \times 10^6$  humm or wild type (wt) STEAP1<sup>P2A5</sup>TCR transgenic T<sub>SCM</sub> together with  $5 \times 10^6$  CD8 depleted autologous PBMCs,  $5 \times 10^6$  unspecific CD8<sup>+</sup>HLA-A\*02:01<sup>-</sup> T cells or were left untreated. Here also  $1.5 \times 10^7$  NSO-IL15 cells were injected twice a week. After 17 days tumors were analyzed for their weight. Additionally, tumors were evaluated by measuring total photon flux after administration of 150 mg luciferin/kg body weight (Caliper life science). A scheme of the *in vivo* experimental procedure is shown in Figure 8.

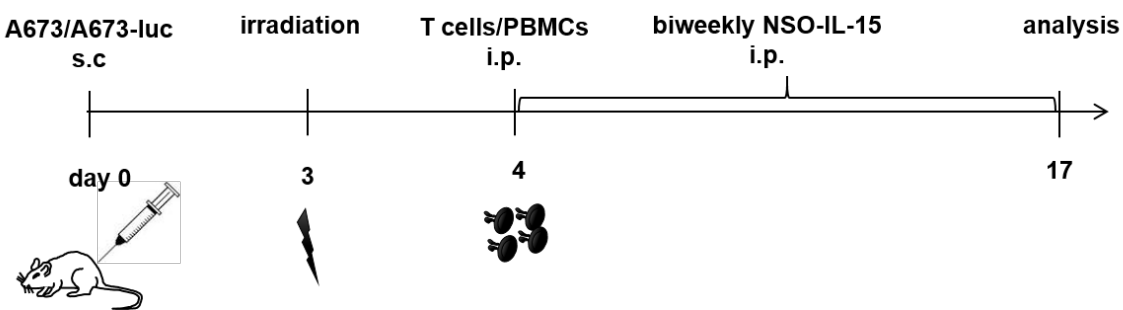


**Figure 8: Experimental set-up for *in vivo* experiments.** Animals were inoculated with  $2 \times 10^6$  A673 or A673-luc cells. On day 3 animals were irradiated and received T cells or PBMCs one day later. Twice a week hIL-15 producing NSO cells were injected i.p.. Tumor size was evaluated twice a week by measuring total photon flux of luciferase expressing tumor cells. At day 17 tumors and organs of mice were analyzed.

### 3.23 Bioluminescent measurements

Bioluminescent measurements of A673-luc cells were performed in cooperation with Dr. Dirk Wohlleber (Institute of Molecular Immunology/ Experimental Oncology, Klinikum rechts der Isar, Technische Universität München). First measurement was done one day before T cells were injected and thereafter twice a week. To do this 150 mg/kg body weight luciferin were injected i.p. 15 min prior to the measurement, to allow a sufficient distribution of the substrate within the animals. To avoid movement during the recording, animals were narcotized with 2% isofluran. Exposure time of the camera was 10 s and luminescence analyzed in photons/seconds (p/s).

### **3.24 Immunohistochemistry**

Histological analyses were performed in cooperation with Dr. Thomas Grünewald (Institute of pathology, Medical department, Ludwig-Maximilians-Universität München). IHC analyses of tumors were performed on formalin fixed, paraffin-embedded samples. All tissue slides were collected at the Department of Pathology of the Ludwig-Maximilians-Universität München. The following primary antibodies were used: CD8 (1:100, SP16, DCS) and CD3 (1:150, Dako).

### **3.25 Statistics**

Descriptive statistics were used to determine parameters like mean, standard deviation and standard error of the mean (SEM). Differences were analyzed by unpaired two-tailed student's t-test using Prism 5 (GraphPad Software); p values < 0.05 were considered as statistically significant (\*p < 0.05; \*\*p < 0.005; \*\*\*p < 0.0005).

## 4 Results

### 4.1 Identification of *STEAP1*<sup>130</sup> as suitable target for adoptive T cell therapy in Ewing Sarcomas

To evaluate *STEAP1* as adoptive T cell therapy target (ACT), its expression profile in Ewing Sarcoma and other tumor entities as well as in normal tissues was assessed. Therefore, the microarray dataset of Staeger *et al.* (37) was used and expression reassured via qRT-PCR. DNA microarray analysis identified *STEAP1* as one of multiple genes being highly overexpressed in ES, whereas it is only minimally expressed in normal tissues, except prostate and urothelium (Fig. 9 A). The expression of *STEAP1* within ES cell lines was further confirmed by qRT-PCR. Additionally, its expression in various neuroblastoma and leukemia cell lines was assessed. Whereas *STEAP1* is strongly expressed in ES cell lines, especially in SK-N-MC and TC-71, it is almost not detectable in neuroblastomas and the leukemic cell line 697 (Fig. 9 B).

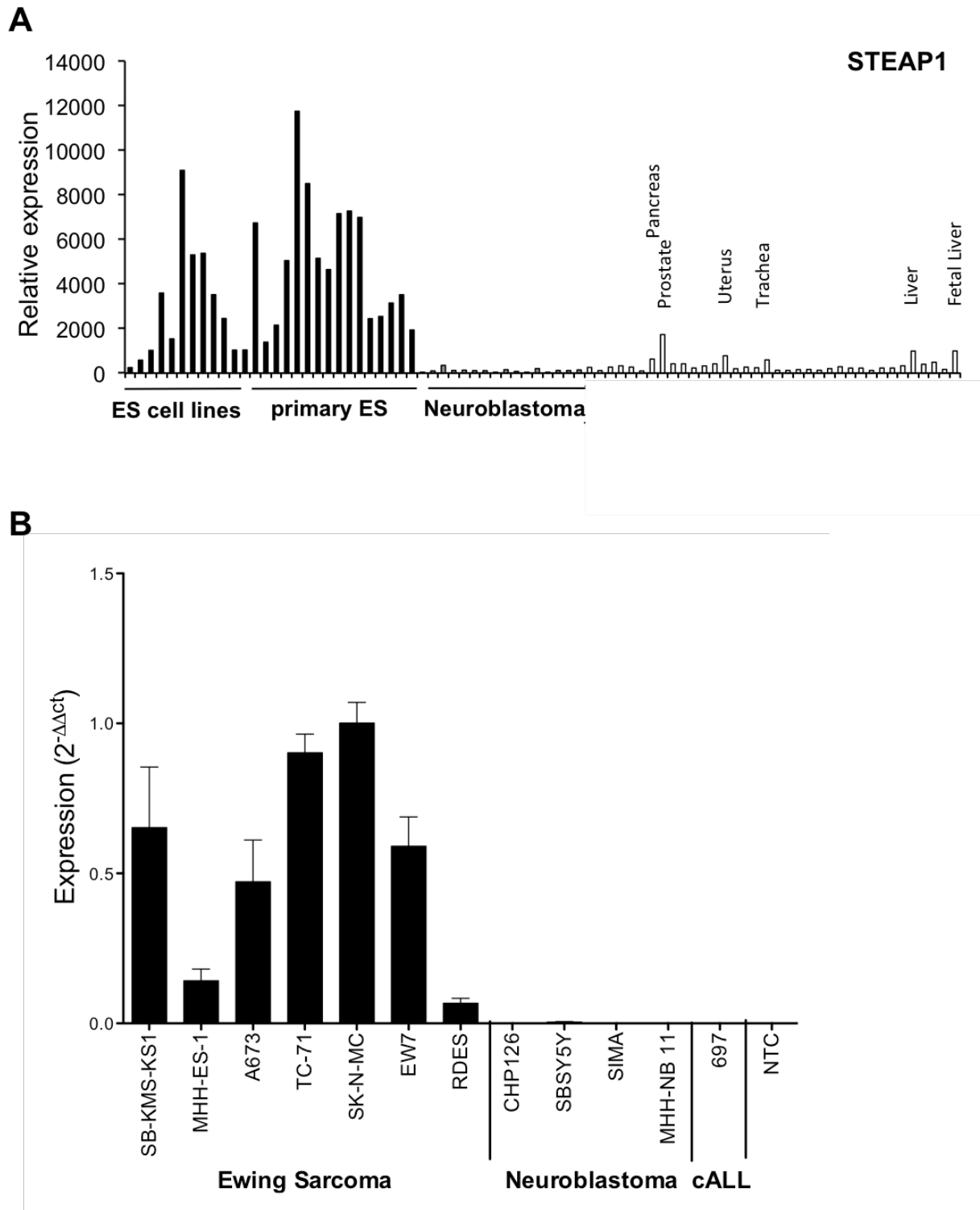


**Figure 9: STEAP1 expression profile.** STEAP1 is highly overexpressed in Ewing Sarcoma (ES). **(A)** DNA microarrays of 26 Ewing Sarcomas and 16 neuroblastomas (GSE1824, GSE1825 and GSE15757) were compared with 36 normal tissues (GSE2361) for *STEAP1* expression. **(B)** Quantification of *STEAP1* expression was analyzed by qRT-PCR in Ewing Sarcoma (type 1 and 2 *EWS/FLI1* translocation), neuroblastoma and leukemia cell lines. Mean  $\pm$  SEM of 3 experiments (duplicates/group). NTC: non template control.

## Results

To identify those STEAP1 peptides that are properly processed within cells and presented on top of tumor cells in a HLA-A\*02:01 (HLA-A2) context, an *in silico* analysis was performed, using BIMAS, NetCTL and SYFPEITHY web tools. Among others STEAP1<sup>86</sup> and STEAP1<sup>130</sup> were predicted to be appropriate HLA-A\*02:01 binders (Tab. 5) and further tested in a HLA-A\*02:01 binding assay.

**Table 1: *In silico* binding scores of various STEAP1 peptides, predicted by NetCTL1.2, Bimas and SYFPEITHY web algorithms.**

STEAP1		Score		
Starting AA	Sequence	NetCTL1.2	Bimas	SYFPEITHI
	Influenza	1,2885	550,927	30
165	GLLSFFFAV	1,4595	10776,47	25
<b>86</b>	<b>FLYTLRELV</b>	<b>1,3046</b>	<b>470,951</b>	<b>29</b>
262	LLLGTIHAL	1,2756	309,05	32
<b>130</b>	<b>YLPGVIAAI</b>	<b>1,3477</b>	<b>110,379</b>	<b>29</b>
270	LIFAWNKWI	0,8349	49,627	18
252	YIQSKLGIV	0,7658	9,405	25

Therefore, TAP transporter deficient T2 cells were pulsed with 100  $\mu$ M and 50  $\mu$ M of the respective peptide for 16 h and amount of stabilized HLA-A\*02:01 molecules on the cell surface measured via flow cytometry. Furthermore, T2 cells were pulsed with titrated concentrations of the peptides. All binding properties of STEAP1 peptides were compared to a well-described influenza peptide (GILGFVFTL) and other ES associated epitopes (Appendix). Additionally, to avoid target nonamers that are likely phosphorylated within tumor cells, an *in silico* analysis using NetPhos 2.0 (<http://www.cbs.dtu.dk/services/NetPhos/>) was performed. STEAP1<sup>130</sup> turned out to be

an appropriate binder to HLA-A\*02:01 with binding properties similar to the influenza peptide (Fig. 10) and low likelihood for phosphorylation (data not shown) and was used for further *in vitro* priming of CD8<sup>+</sup> T cells.

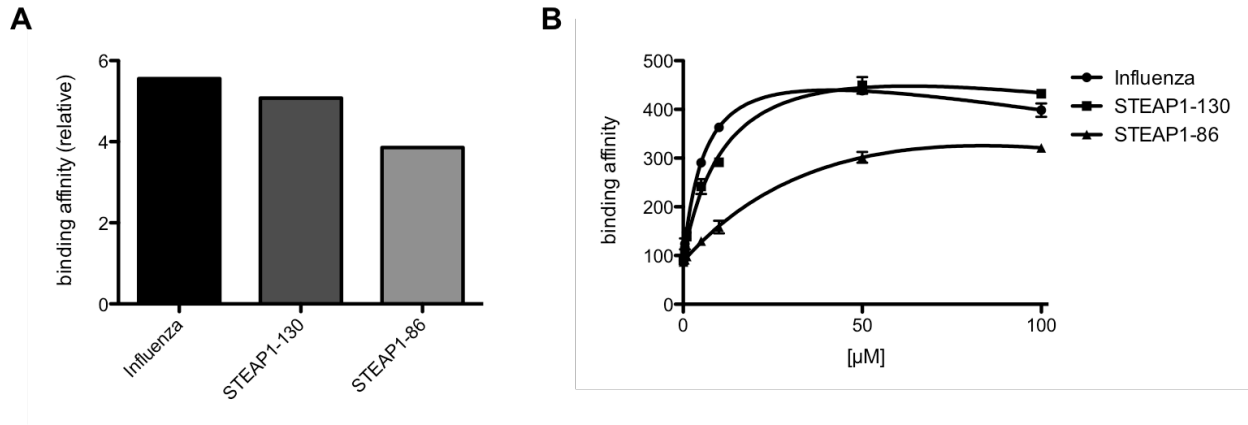


**Figure 10: HLA-A\*02:01 specific binding of STEAP1 peptides.** FACS analysis of STEAP1<sup>130</sup> peptide (YLPGVIAAI) binding to TAP transporter deficient HLA-A\*02:01<sup>+</sup> T2 cells. T2 cells were pulsed for 16 h with 50 μM of peptide. Influenza peptide (GILGFVFTL) and STEAP1<sup>130</sup> are assumed as strong binders. **(A)** Shown is the relative HLA-A\*02:01 binding affinity compared to unloaded T2 cells and **(B)** the concentration dependent binding of STEAP1<sup>130</sup>, STEAP1<sup>86</sup> and influenza peptide to T2 cells, quantified via flow cytometry.

## 4.2 STEAP1<sup>130</sup> specific T cell clone P2A5 specifically recognizes target cells

To generate allo-restricted, STEAP1<sup>130</sup> specific, cytotoxic T cells, CD8<sup>+</sup> T cells of a HLA-A\*02:01<sup>-</sup> healthy donor were co-incubated with STEAP1<sup>130</sup> peptide pulsed HLA-A\*02:01<sup>+</sup> mature dendritic cells (Fig. 11) for two weeks.

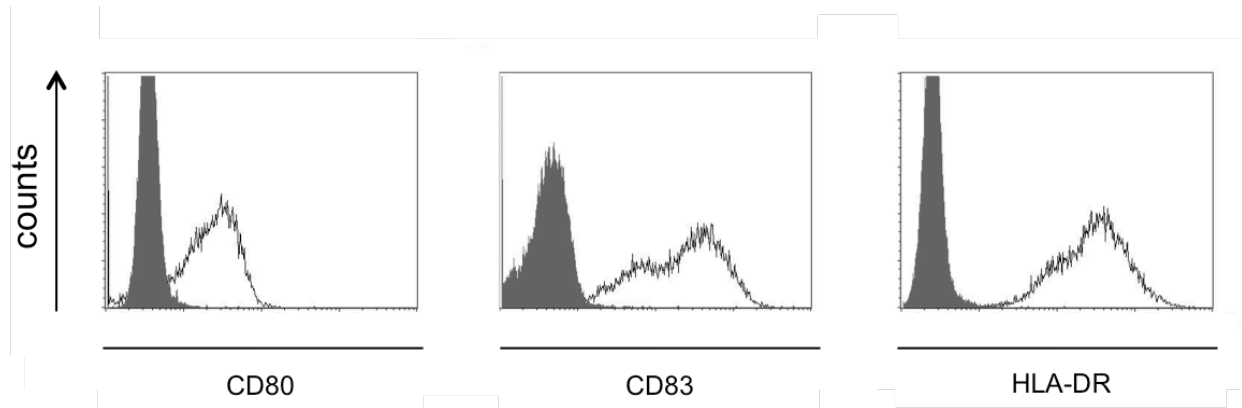


**Figure 11: Maturation status of moDCs.** MoDCs were stained with CD80, CD83 and HLA-DR specific monoclonal antibodies. Gray histograms represent fluorochrome-matched isotype controls.

After 14 days cells were specifically stained by a HLA-A\*02:01/STEAP1<sup>130</sup> multimer and anti-human CD8 monoclonal antibodies (mAb). Out of  $3 \times 10^7$  cells deployed for FACS sorting, 1788 were specifically stained by the STEAP1 multimer and CD8 (Fig. 12), which accounts for 0.00006% of all cells. Double positive cells were subsequently sorted at the facility of medical microbiology (Technische Universität München) and expanded via limiting dilution.

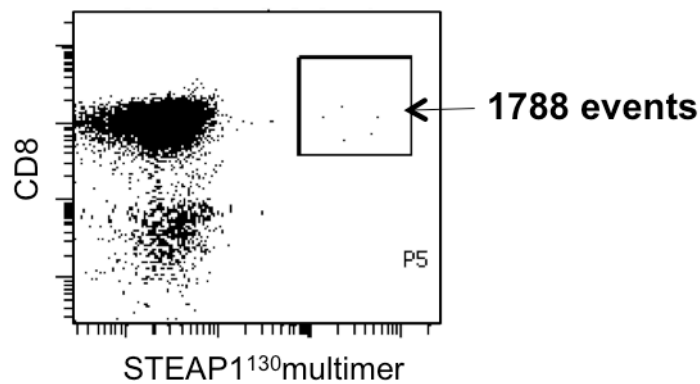


**Figure 12: Staining of *in vitro* primed CD8<sup>+</sup> T cells for FACS sorting.** HLA-A\*02:01<sup>-</sup> CD8<sup>+</sup> T cells of a healthy donor were primed with STEAP1<sup>130</sup> pulsed moDCs of a HLA-A\*02:01<sup>+</sup> healthy donor for two weeks. Antigen specific cytotoxic T cells were stained with HLA-A\*02:01/STEAP1<sup>130</sup> multimer and anti-CD8 antibody for subsequent sorting and expansion.

## Results

The expanded STEAP1<sup>130</sup> multimer<sup>+</sup> CD8<sup>+</sup> T cells were then screened for their target recognition (Appendix). Several lines specifically recognized STEAP1<sup>130</sup> peptide pulsed T2 cells and HLA-A\*02:01<sup>+</sup> ES cells in an IFN $\gamma$  ELISpot. The T cell lines P2A7, P2F2 and P2C7 showed either background recognition of influenza pulsed T2 cells or no recognition of target cells at all (Fig. 13). T cell lines P1A3, P1C4 and P2A5 were expanded for further analysis.

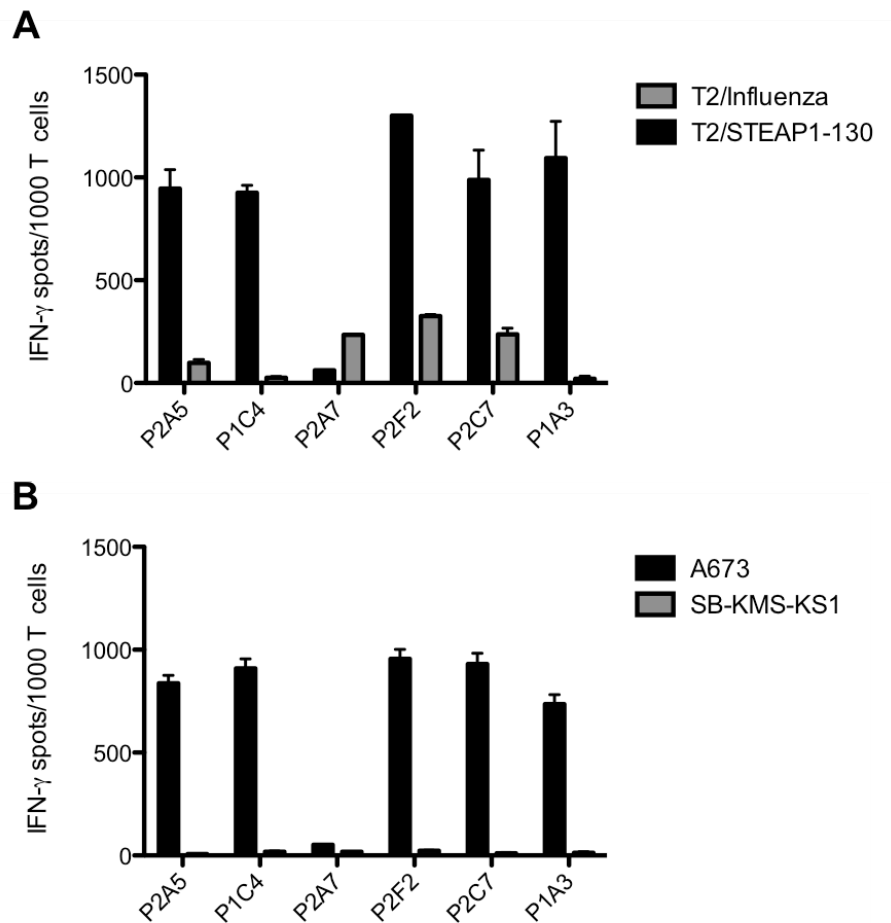


**Figure 13: Target recognition of STEAP1<sup>130</sup> specific T cell lines.** (A) IFN $\gamma$  release of FACS sorted STEAP1<sup>130</sup> specific CTLs upon co-culture with influenza or STEAP1<sup>130</sup> peptide pulsed T2 cells, (B) as well as HLA-A\*02:01<sup>+</sup> (A673) and HLA-A\*02:01<sup>-</sup> (SB-KMS-KS1) ES cell lines, analyzed in triplicates via IFN $\gamma$  ELISpot. Error bars indicate SEM.

To check the three clones for TCR similarity, the receptors of all three T cell lines were analyzed by PCR. Identification of TCR V $\alpha$ - and V $\beta$ -chains using degenerated primers, followed by sequencing showed TCR clonality of all three investigated cell lines (data not shown). Therefore, characterization was further focused on T cell clone P2A5 (STEAP1<sup>P2A5</sup>) by use of FACS staining, IFN $\gamma$  ELISpot and xCELLigence assays. T cell clone STEAP1<sup>P2A5</sup> was specifically stained by the HLA-A\*02:01/STEAP1<sup>130</sup> multimer (Fig. 14 A) and was able to recognize peptide pulsed T2 cells (Fig 14 B) and HLA-A\*02:01<sup>+</sup>, STEAP1 expressing ES cell lines (A673, TC-71), whereas HLA-A\*02:01<sup>-</sup> (SB-KMS-KS-1, SK-N-MC, K562) or STEAP1<sup>-</sup> (MHH-NB11) cell lines were not detected (Fig. 14 C). Blocking the MHC-I molecules of the target cell line TC-71 with a MHC-I (W6.32) specific mAB reversed the HLA-A\*02:01 restricted recognition (Fig. 14 D). The amount of IFN $\gamma$  release was dependent on the quantities of presented peptide, as less IFN $\gamma$  spots were detectable after specific siRNA mediated knock down of STEAP1 in the ES cell line A673 (Fig. 14 E). Furthermore, IFN $\gamma$  release was reduced after titration of STEAP1<sup>130</sup> peptide onto T2 cells (Fig. 14 F). To verify accurate processing of STEAP1<sup>130</sup> within cells, Cos7 cells were co-transfected with HLA-A\*02:01 and *STEAP1* or *GFP* cDNA, respectively. Markedly more IFN $\gamma$  was secreted after co-culture of T cells with Cos7 cells expressing HLA-A\*02:01 and STEAP1 compared to the GFP expressing target cells (Fig. 14 G).

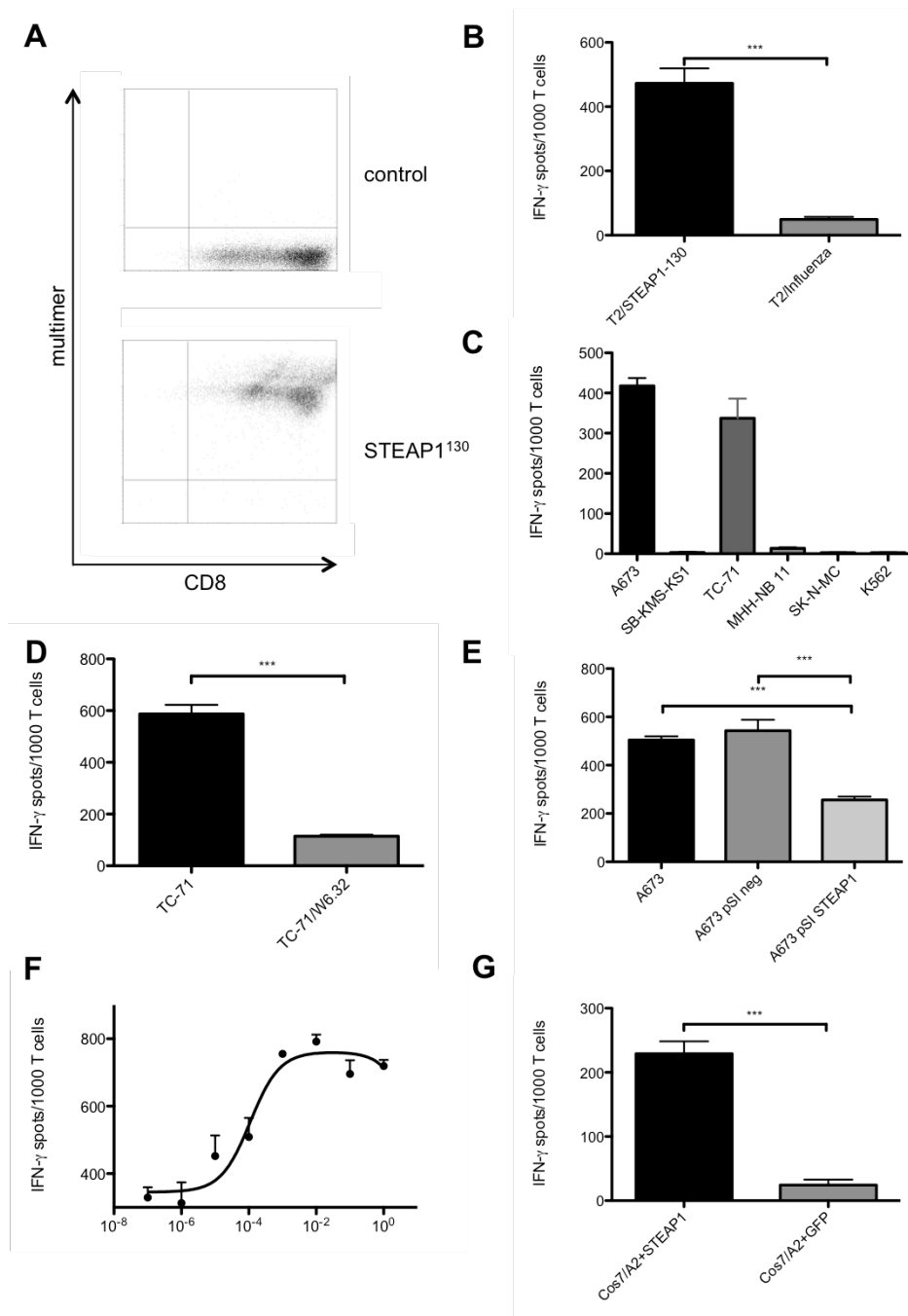


**Figure 14: ES specificity of STEAP1<sup>130</sup> specific T cell line P2A5.** (A) STEAP1<sup>P2A5</sup> was stained with anti-human CD8 mAb and HLA-A\*02:01/STEAP1<sup>130</sup> multimer (bottom) or irrelevant multimer as control (top) and analyzed by flow cytometry. (B) IFN $\gamma$  release of STEAP1<sup>P2A5</sup> during co-culture with STEAP1<sup>130</sup> and influenza pulsed T2 cells, respectively, (C) HLA-A\*02:01<sup>+</sup> (A673, TC-71) and HLA-A\*02:01<sup>-</sup> (SB-KMS-KS1, SK-N-MC, K562) tumor cells expressing STEAP1 or lacking STEAP1 expression (MHH-NB11), (D) TC-71 cells with and without MHC-I specific blocking mAb W6.32, (E) A673 cells with and without siRNA mediated STEAP1 knock down, (F) T2 cells pulsed with titrated amounts of STEAP1<sup>130</sup> peptide, and (G) Cos 7 cells transfected with HLA-A\*02:01 and either STEAP1 or GFP, analyzed in triplicates via IFN $\gamma$  ELISpot. Error bars indicate SEM. P values < 0.05 were considered as statistically significant (\*p < 0.05; \*\*p < 0.005; \*\*\*p < 0.0005).

### 4.3 T cell clone STEAP1<sup>P2A5</sup> inhibits growth of target structures

To show the lytic activity of T cell clone STEAP1<sup>P2A5</sup>, granzyme B (GB) release upon co-culture with target cell lines was examined via ELISpot. Therefore, titrated amounts of T cells were incubated with HLA-A\*02:01<sup>+</sup> ES cell lines A673 and TC-71 or HLA-A\*02:01<sup>-</sup> cell lines SK-N-MC, SB-KMS-KS1 and K562 (used as NK cell control). A T cell concentration dependent release of GB was visible upon co-culture with HLA-A\*02:01<sup>+</sup> cells, whereas only baseline secretion was observed after stimulation with negative controls (Fig. 15 A). To further demonstrate direct inhibition of target cell growth, an impedance based xCELLigence assay was performed. Target cells were seeded 65 h in advance before adding 2.5 x 10<sup>4</sup> T cells. The HLA-A\*02:01<sup>+</sup> ES cell line A673 was rapidly lysed by the cytotoxic STEAP1<sup>P2A5</sup> T cells, though growth of HLA-A\*02:01<sup>-</sup> ES cell line SK-N-MC was not affected (Fig. 15 B). The rate of lysis was dependent on the effector: target ratio, as the timeframe needed to lyse 50% of the plated cells was increased after titrating T cell numbers (Fig. 15 C).

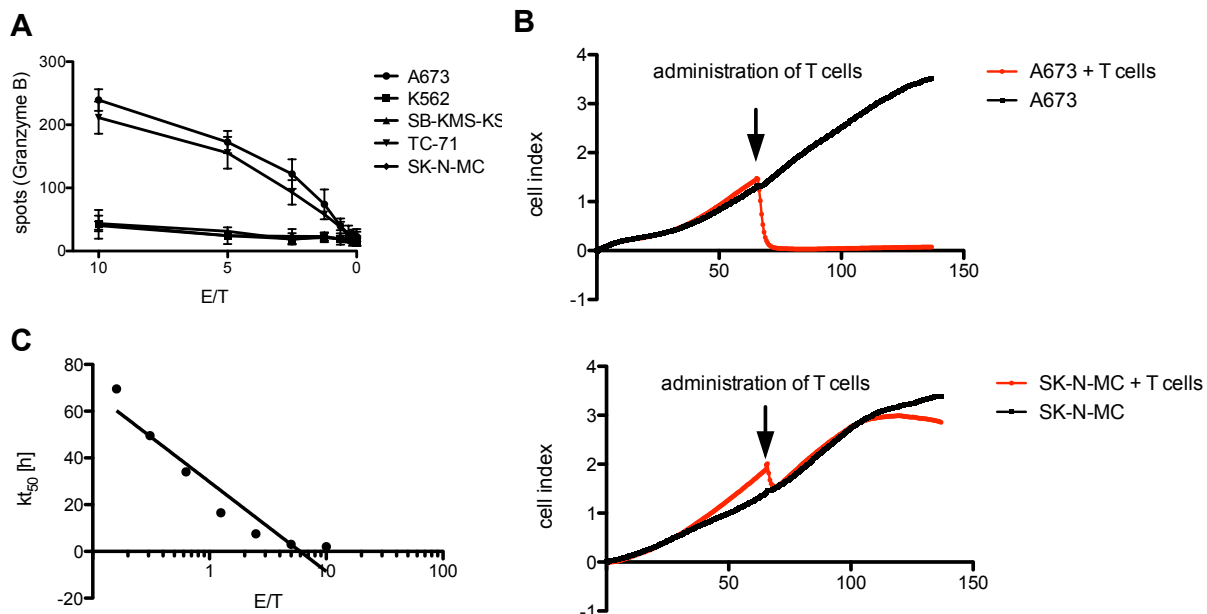


**Figure 15: Anti-tumor reactivity of STEAP1<sup>130</sup> specific T cell clone P2A5.** (A) Effector: target ratio (E/T) dependent granzyme B release of STEAP1<sup>130</sup>P2A5 after co-culture with various tumor cell lines was analyzed via ELISpot in triplicates. Error bars indicate SEM. (B) Target-specific tumor cell lysis of A673 and SK-N-MC (E/T: 10) by STEAP1<sup>130</sup>P2A5 and (C) E/T-dependent timeframe needed for killing of 50% of tumor cells (kt<sub>50</sub>) by STEAP1<sup>130</sup>P2A5, detected via a xCELLigence assay in quintuplicates.

#### 4.4 Identification of V $\alpha$ - and V $\beta$ -chains of T cell clone STEAP1<sup>P2A5</sup>

A set of degenerated primers was used for a PCR based amplification of the STEAP1<sup>P2A5</sup> specific V $\alpha$ - and V $\beta$ -chains. The resulting PCR products were loaded onto an agarose gel and fragments of the right size eluted and sequenced (Fig 16).

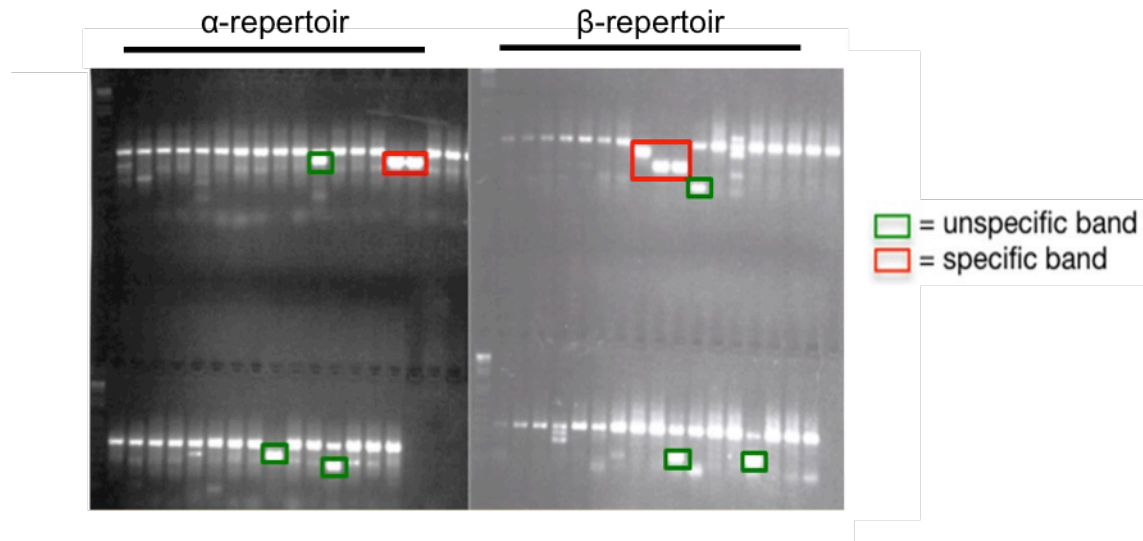


**Figure 16: Identification of the STEAP1<sup>130</sup>P2A5 TCR  $\alpha$ - and  $\beta$ -chains.** STEAP1<sup>P2A5</sup> TCR specific  $\alpha$ - and  $\beta$ -chains were amplified and analyzed with variable chain specific RT-PCR primers. Fragments of the right size (red and green frames) were eluted and sequenced.

The resulting sequences were analyzed using the international ImMunoGeneTics (IMGT) information system database and TRAV38-2 ( $\alpha$ -chain) and TRBV7-9 ( $\beta$ -chain) chains unambiguously identified. The resulting  $\alpha$ - and  $\beta$ -chain sequences were completed with corresponding constant chains and signaling sequence using the IMGT database. To verify the correct assembly of the chains, the generated sequences were confirmed by PCR with primers covering the complete chains (Fig. 17 A).

Afterwards constructs containing  $\alpha$ - and  $\beta$ -chain linked by a self-cleaving P2A element were designed and synthesized by GeneArt, either as an unmodified (wt) or as a human codon optimized and minimal murinized version (hummm) (Fig. 17 A + B). GeneArt also accomplished the subcloning into a pMP-71 retroviral backbone.

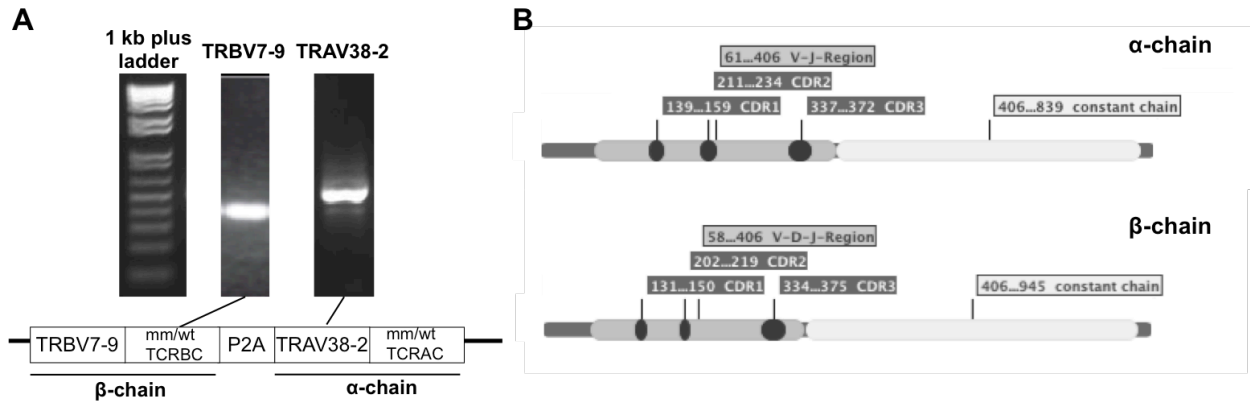


**Figure 17: Generation of STEAP1<sup>130</sup> TCR transgenic T<sub>SCM</sub>.** (A) Identification of TCR α- (TRAV38-2) and β- (TRBV7-9) chains via PCR. Additionally a scheme of the TCR construct either codon optimized and containing a minimal murinized constant chain (mm) or unmodified (wt) is shown. TCR α- and β-chains are linked with a self-cleaving P2A element and integrated into the pMP-71 vector. (B) Structural information of TCR α- and β-chains are provided.

#### 4.5 Generation of STEAP1<sup>P2A5</sup> transgenic cytotoxic T<sub>SCM</sub>

Since there are two different methods for the generation of T<sub>SCM</sub>, both were tested to find the optimal protocol for the production of transgenic T<sub>SCM</sub>. While the protocol of Gattinoni *et al.*, uses anti-CD3/CD28 microbeads, TWS119 and rhIL-2, the protocol of Cieri *et al.*, uses anti-CD3/CD28 microbeads and moderate amounts of rhIL-7 and rhIL-15. Both protocols were compared for phenotypic markers of the resulting cells and their sensibility for retroviral transduction with an endogenous TCR. There was almost no differential expression of the surface markers CD45R0, CD62L, CCR7, CD95 and CD8, but cells generated with the protocol of Cieri *et al.* showed a higher expression of CD45RA (Fig. 18 A). Transduction efficacy of the STEAP1<sup>P2A5</sup> TCR into both populations was similar (Fig. 18 B), but the cells stimulated with IL-7 and IL-15 grew markedly faster (Fig. 18 C).

## Results

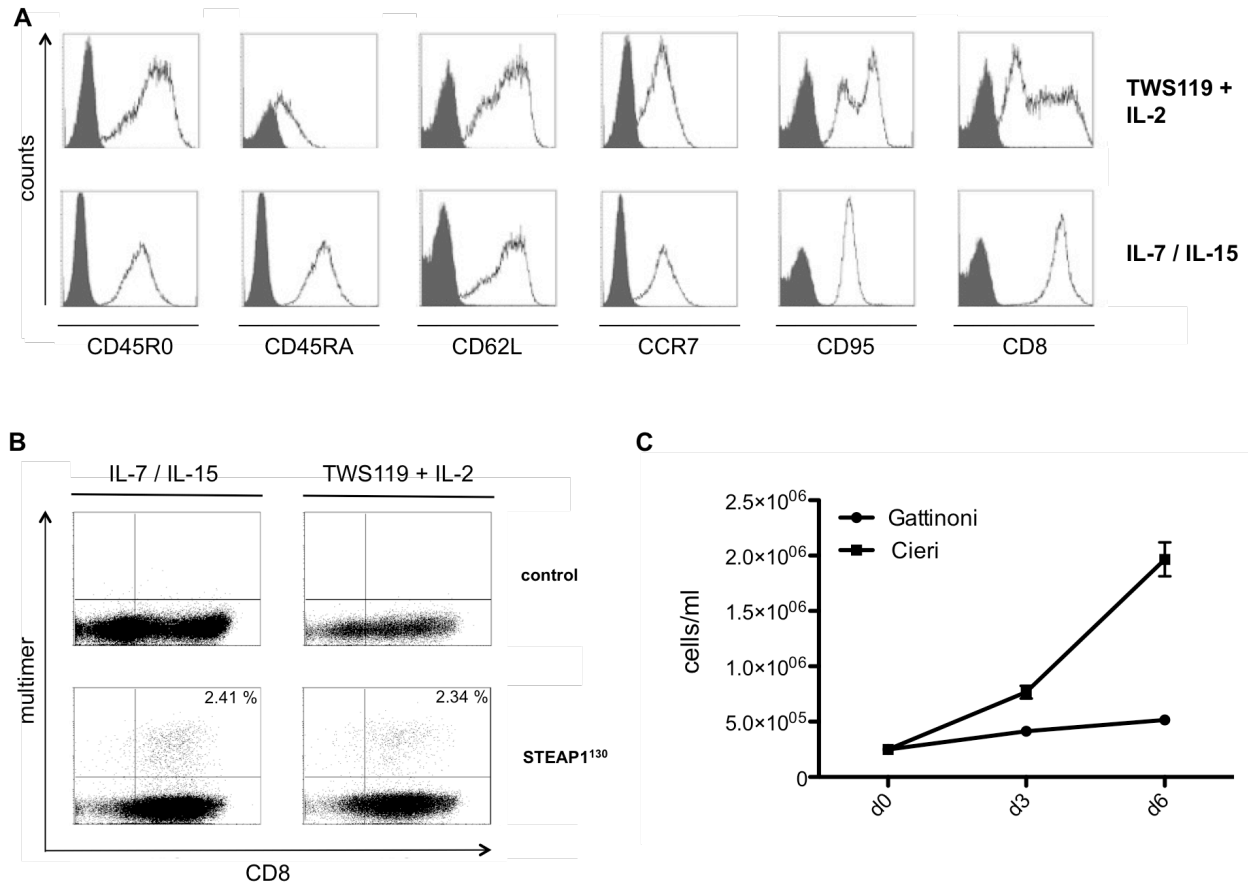


**Figure 18: Generation of STEAP1<sup>P2A5</sup> transgenic cytotoxic T<sub>SCM</sub>.** Phenotype, transduction efficacy and proliferative capacity of transduced T<sub>SCM</sub> generated with two different protocols were assessed. **(A)** T<sub>SCM</sub> generated either with TWS119 and IL-2 (Gattinoni *et al.*) or IL-7 and IL-15 (Cieri *et al.*) were analyzed for their surface markers CD45R0, CD45RA, CD62L, CCR7, CD95 and CD8, and **(B)** transduced T<sub>SCM</sub> generated with both protocols stained with STEAP1<sup>130</sup>/HLA-A\*02:01 multimer or irrelevant multimer, respectively, and anti-CD8 mAb, and analyzed via flow cytometry. **(C)** Growth of transduced cells was evaluated over 7 days by counting cells in triplicates. Error bars indicate SEM.

To maximize transduction efficacy, various packaging cell lines (293T, 293VecGalv and 293VecRD114) were tested for their ability to produce high virus titers. To do this, the cell lines were transfected with the pMP-71 plasmid encoding the STEAP1<sup>P2A5</sup><sub>wt</sub> TCR and subsequently PBMCs infected with the retrovirus. Numbers of transduced cells were then analyzed by flow cytometry. Where virus produced with 293T cells reached a fraction of 39.3% transduced CD8<sup>+</sup> T cells, 293VecGalv (Galv) and 293VecRD114 (RD114) had much higher transduction rates (65.2% and 74.0%) (Fig. 19). RD114 was used for subsequent infection of primary donor T cells.

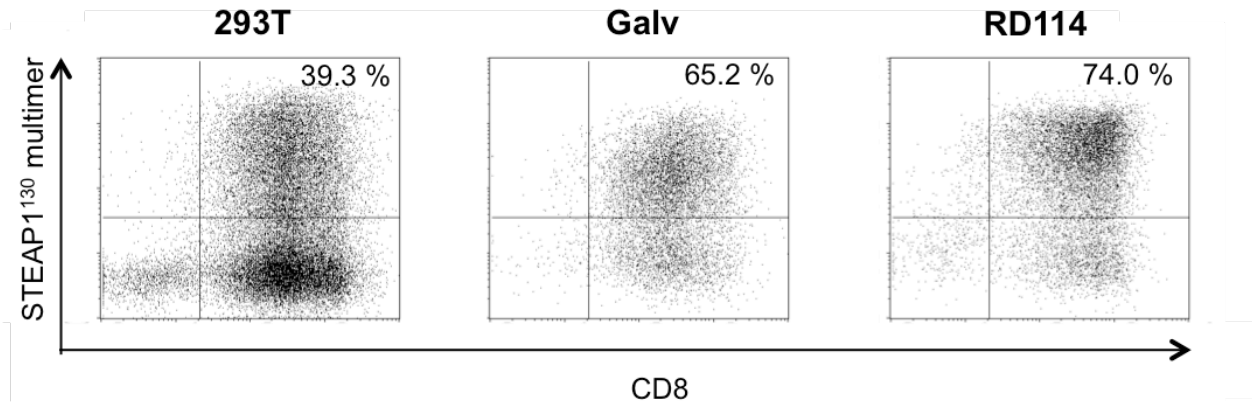


**Figure 19: Transduction efficacy of virus supernatant obtained from different packaging cell lines.** Packaging cell lines 293T, 293VecGalv (Galv) and 293VecRD114 (RD114) were transfected with pMP71STEAP1wt and human PBMCs infected with virus supernatant. PBMCs were stained with STEAP1<sup>130</sup>/HLA-A\*02:01 multimer and human CD8 specific mAb and transduction efficacy analyzed via flow cytometry. Percentages of STEAP1<sup>130</sup>multimer<sup>+</sup> CD8<sup>+</sup> cells are given.

To compare the expression and ability of correct pairing of the exogenous STEAP1<sup>P2A5</sup> TCR  $\alpha$ - and  $\beta$ -chain within T cells, PBMCs were transduced with either the humm or the wt TCR. There were only small differences between the transduction efficacies between the humm or the wt constructs (87.99% vs. 97.45%), with the wt TCR being slightly higher expressed compared to the humm TCR (Fig. 20).

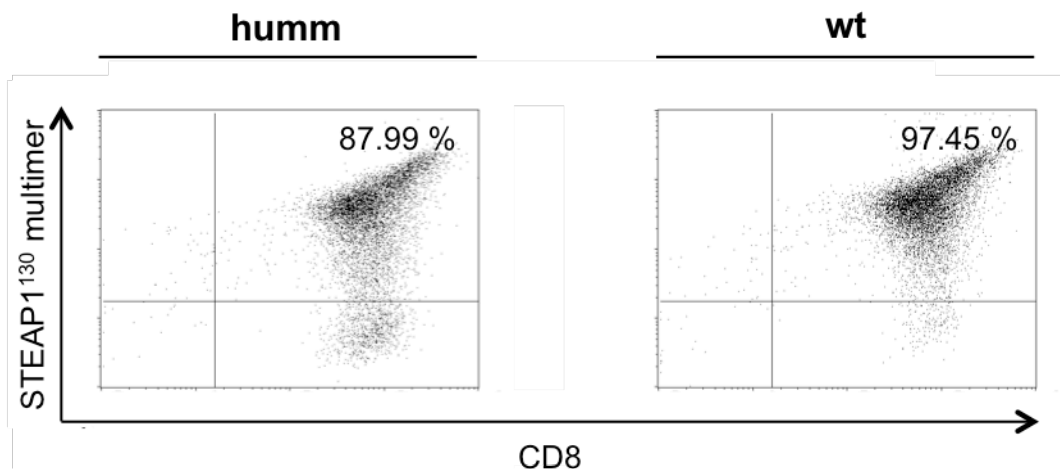


**Figure 20: Transduction efficacy of humm and wt TCRs into human CD8<sup>+</sup> T cells.** FACS staining of human CD8<sup>+</sup> T cells transduced with either humm or wt TCR containing vectors. Cells were stained with STEAP1<sup>130</sup>/HLA-A\*02:01 multimer and anti-human CD8 mAb one week after the transduction procedure. Percentages of STEAP1<sup>130</sup>/HLA-A\*02:01 multimer<sup>+</sup> CD8<sup>+</sup> cells are given.

#### 4.6 Functionality of STEAP1<sup>P2A5</sup> TCR transgenic T cells

To test *in vitro* functionality of STEAP1<sup>P2A5</sup> TCR transgenic (tg) T cells, human HLA-A\*02:01<sup>-</sup> PBMCs of healthy donors were transduced with the humm TCR construct and tested for specificity and lytic activity in ELISpot and xCELLigence assays. The tg T cells were able to recognize STEAP1<sup>130</sup> peptide pulsed T2 cells (Fig. 21 A) as well as HLA-A\*02:01<sup>+</sup> ES cells, whereas HLA-A\*02:01<sup>-</sup> cell lines were not detected (Fig. 21 B) in an IFN $\gamma$  ELISpot assay. IFN $\gamma$  release was dependent on the quantities of presented peptide as shown in an experiment where titrated amounts of STEAP1<sup>130</sup> peptide were loaded onto T2 cells (Fig. 21 C). An xCELLigence assay showed the lytic ability of tg T cells as vital A673 cells were rapidly killed after administration of T cells, whereas the HLA-A\*02:01<sup>-</sup> cell line SK-N-MC was not affected (Fig. 21 D).

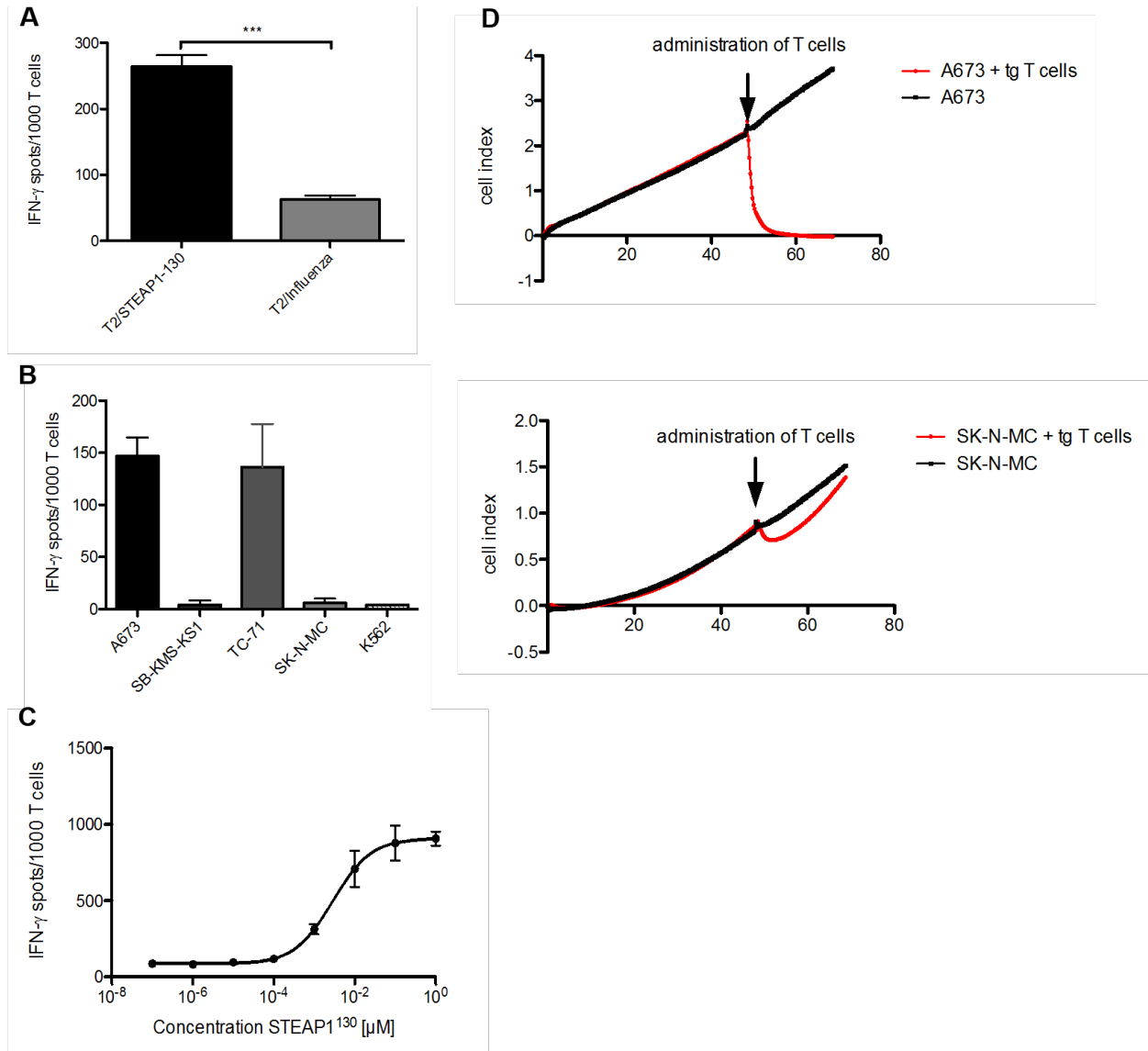


**Figure 21: Antigen specific target cell recognition of STEAP1<sup>P2A5</sup> TCR transgenic CD8<sup>+</sup> T cells.** (A) IFN $\gamma$  release of STEAP<sup>P2A5</sup> TCR transgenic T cells during co-culture with STEAP1<sup>130</sup> and influenza peptide pulsed T2 cells, respectively, (B) HLA-A\*02:01<sup>+</sup> (A673, TC71) and HLA-A\*02:01<sup>-</sup> (SB-KMS-KS1, SK-N-MC, K562) tumor cells expressing STEAP1 and (C) T2 cells pulsed with titrated amounts of STEAP1<sup>130</sup> peptide, analyzed in triplicates via IFN $\gamma$  ELISpot. Error bars indicate SEM. P values < 0.05 were considered as statistically significant (\*\*\*p < 0.0005). (D) Target-specific tumor cell lysis of A673 and SK-N-MC (E/T: 10) by STEAP1<sup>P2A5</sup> TCR transgenic T cells was detected via xCELLigence assay.

#### 4.7 Potential cross reactivity of STEAP1<sup>P2A5</sup> TCR transgenic T cells

To screen STEAP1<sup>P2A5</sup> TCR transgenic T cells for possible cross reactivity, an alanine/threonine scan was performed. Single amino acids of the STEAP1 peptide were exchanged by either an alanine or a threonine. The resulting peptides were then loaded onto T2 cells (100  $\mu$ M) and IFN $\gamma$  secretion measured via an ELISpot assay. The tg T cells recognized the STEAP1<sup>130</sup> peptide even when amino acid 4, 5 or 6 were replaced by alanine and when amino acid 4, 5 or 7 were replaced by threonine. The resulting recognition motifs generated with the ScanProsit database **X(3)-G-V-X-A-X(2)** or **X(3)-G-V-I-A-X(2)**, added up to 5096 or 264 naturally occurring peptide nonamers, respectively (Fig. 22 A). Furthermore, when STEAP1<sup>130</sup> peptide was loaded onto LCL cell lines bearing different HLA-A subtypes on their surface, tg T cells recognized peptide pulsed HLA-A\*02:09 and HLA-A\*02:17 cells, but did not react to other tested HLA molecules or unloaded cells (Fig. 22 B).

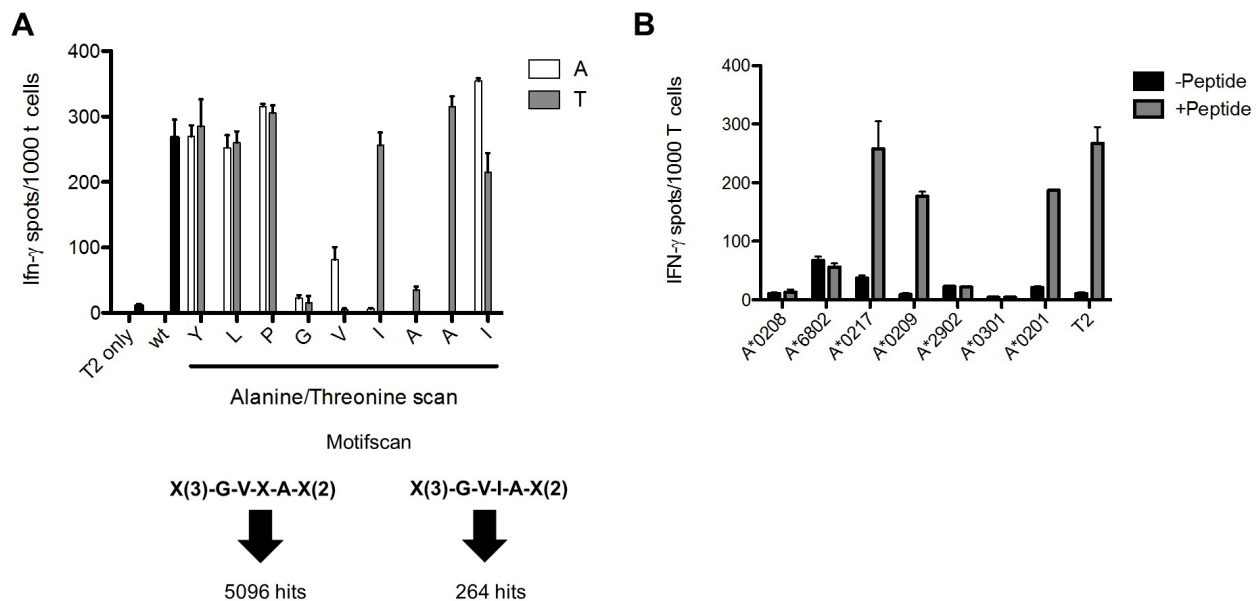


**Figure 22: Cross-reactivity screen for STEAP1<sup>P2A5</sup> TCR transgenic T cells.** (A) Unspecific recognition of natural occurring peptides was examined by an IFN $\gamma$  ELISpot based alanine/threonine scan. Resulting motifs were aligned with the ScanProsit database. (B) Off-target recognition of different HLA subtypes was assessed via IFN $\gamma$  ELISpot. All cross-reactivity screens were carried out in triplicates and error bars indicate SEM.

#### 4.8 *In vivo* reactivity of STEAP1<sup>P2A5</sup> TCR transgenic T cells in Rag2<sup>-/-</sup>γc<sup>-/-</sup> mice

To demonstrate *in vivo* efficacy of STEAP1<sup>P2A5</sup> TCR transgenic T<sub>SCM</sub>, Rag2<sup>-/-</sup>γc<sup>-/-</sup> mice were inoculated with ES tumor cells and animals treated with transgenic T cells 4 days later. Therefore, 2 x 10<sup>6</sup> A673 cells were injected subcutaneously (s.c.) into the groin of Rag2<sup>-/-</sup>γc<sup>-/-</sup> mice. On day 3, animals were sublethally irradiated (3.5 Gy) and received 3 x 10<sup>6</sup> transgenic T<sub>SCM</sub> humm together with 5 x 10<sup>6</sup> autologous CD8 depleted PBMCs or unspecific HLA-A\*02:01<sup>-</sup> PBMCs, respectively, the day after. 1.5 x 10<sup>7</sup> hIL-15 producing NSO cells were injected twice a week to provide T cells with human IL-15. The phenotype of the infused T<sub>SCM</sub> cells was examined prior to the injection into the animals by flow cytometry (Fig. 23).

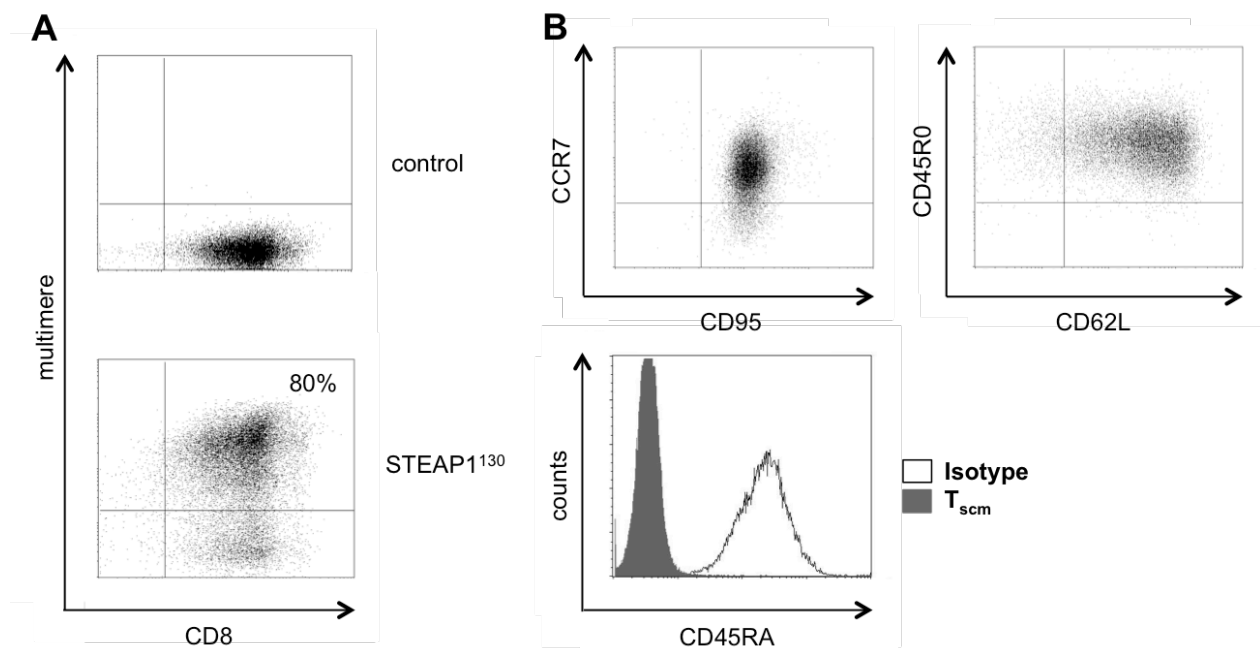


**Figure 23: Verification of the T<sub>SCM</sub> phenotype of STEAP1<sup>130</sup> TCR transgenic T cells prior to injection into animals.** (A) STEAP1<sup>130</sup> TCR transgenic T cells were stained with CD8-APC and HLA-A\*02:01/STEAP1<sup>130</sup> multimer (bottom) or irrelevant multimer as control (top) and (B) T cells co-stained with CCR7/CD95 (upper dot plot), CD45R0/CD62L (lower dot plot) and CD45RA (histogram plot), all analyzed via flow cytometry.

After 17 days total tumor weight was analyzed and blood, spleen and tumors of the mice monitored for T cell engraftment. Tumors of mice treated with tgSTEAP1hum T<sub>SCM</sub> cells were markedly smaller compared to tumors of animals treated with unspecific PBMCs (Fig. 24 A). Furthermore, CD8<sup>+</sup> T cells were found within blood (17.5% of whole blood cells), spleen (4.09% of splenocytes) and tumor (0.02% of tumor cells) of specific T<sub>SCM</sub> cell treated animals. Mice treated with unspecific PBMCs also demonstrated T cell infiltrations into blood (2.05%) and spleen (1.14%), but to a much lesser extent and no infiltration of tumors was detectable in flow cytometry analysis (Fig. 24 B). Immunohistochemistry at day 17 indicated a strong infiltration of CD3<sup>+</sup> lymphocytes into the tumors; both in animals treated with PBMCs and in animals treated with STEAP1 specific tg T cells (Fig. 24 C). However, there was almost no abundance of CD8<sup>+</sup> T cells within the tumors after 17 days (Appendix).

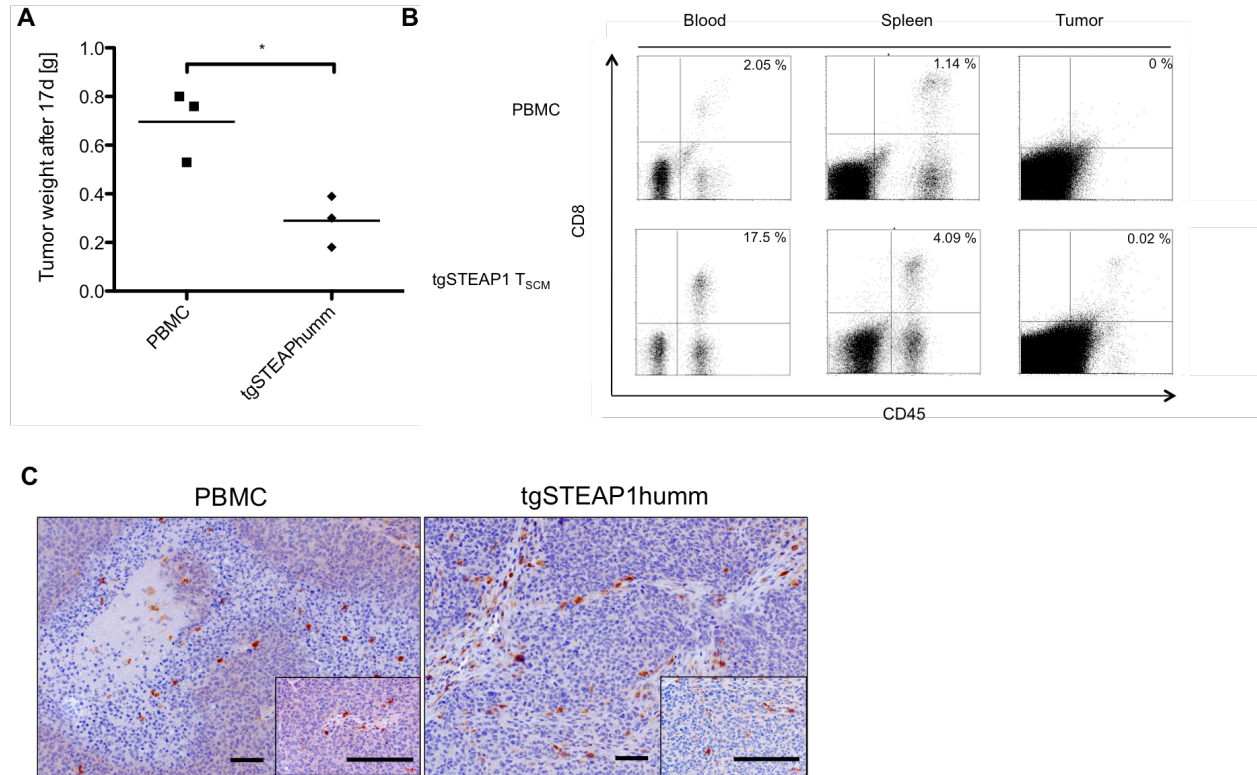


**Figure 24: *In vivo* activity and tumor infiltration of STEAP1<sup>P2A5</sup> TCR transgenic T<sub>SCM</sub>.**  $2 \times 10^6$  A673 cells were injected into the groin of Rag2<sup>-/-</sup>γc<sup>-/-</sup> mice. Animals were irradiated on day 3 (3.5 Gy) and received  $3 \times 10^6$  tg STEAP1humM T<sub>SCM</sub> cells the day after via i.p. injection.  $1.5 \times 10^7$  hIL-15 producing cells were injected twice a week i.p.. Analysis of animals treated with either human codon optimized/minimal murinized (humM) STEAP<sup>P2A5</sup> TCR transgenic (tg) T cells or unspecific PBMCs 17 days after inoculation with A673 cells. **(A)** Total tumor weight and **(B)** blood, spleen and tumor of treated animals were analyzed via flow cytometry. Whole blood was stained with anti-human CD45 mAb and anti-human CD8 mAb. Percentages of double positive cells are given. **(C)** Representative immunohistochemistry staining of CD3<sup>+</sup> cells within tumors from animals treated either with PBMCs or with tgSTEAP1humM T<sub>SCM</sub>.

In a second experiment  $2 \times 10^6$  luciferase expressing A673 cells were injected into the groin of Rag2<sup>-/-</sup>γc<sup>-/-</sup> mice and animals treated with either  $5 \times 10^6$  unspecific CD8<sup>+</sup> T cells or humM/wt tgSTEAP1 T<sub>SCM</sub>. Photon flux of the tumor cells was assessed after administration of 150 mg/kg body weight luciferin. Total photon flux was significantly reduced 3 days after administration of either humM or wt T<sub>SCM</sub> cells (Fig. 25 B + C) compared to tumors treated with unspecific CD8<sup>+</sup> T cells. At the end of the experiment total photon flux was not significantly reduced in animals treated with tgSTEAP1 T<sub>SCM</sub>

## Results

cells, but mice that received tgSTEAP1hummm or tgSTEAP1wt T<sub>SCM</sub> cells had smaller tumors than mice receiving unspecific T cells (Fig. 25 A + D).

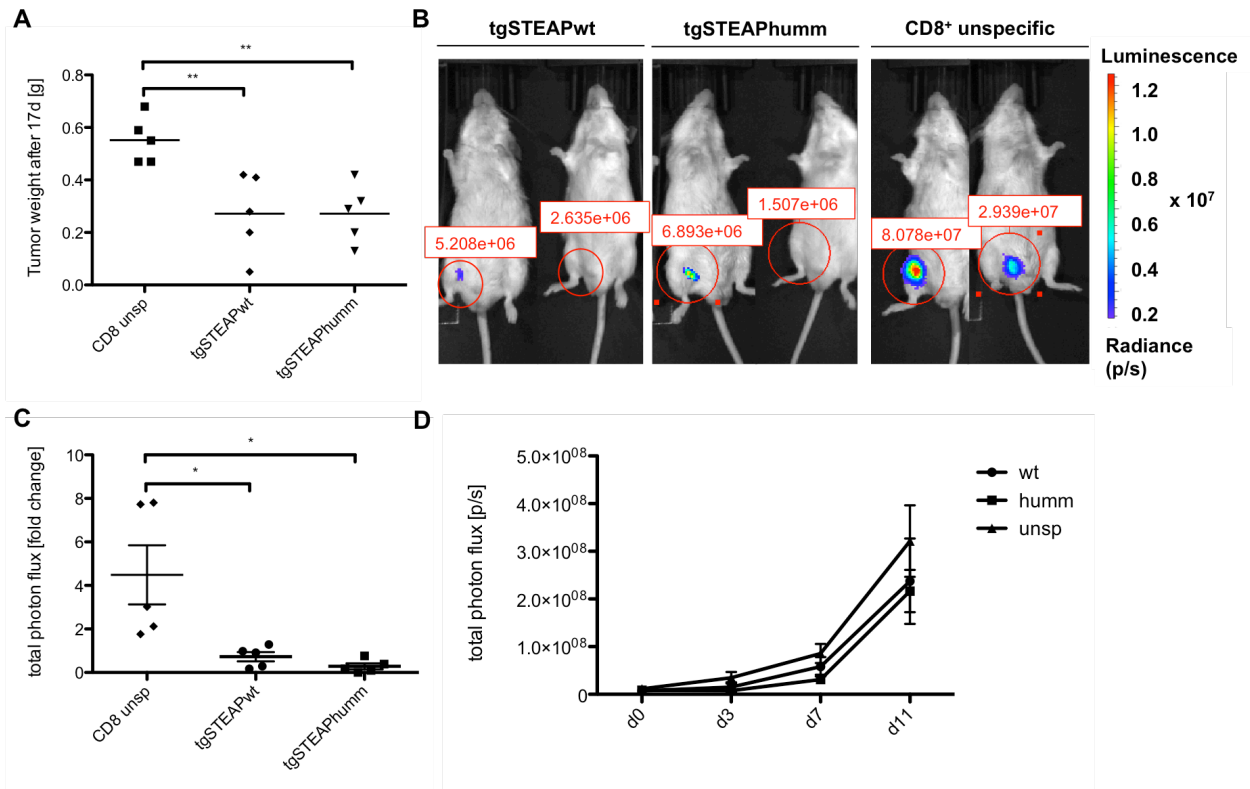


**Figure 25: *In vivo* anti ES reactivity of STEAP1<sup>130</sup> TCR transgenic T<sub>SCM</sub> cells.** Animals received  $2 \times 10^6$  luciferase expressing A673 cells and were irradiated on day 3 (3.5 Gy). One day later  $5 \times 10^6$  wt or humm STEAP<sup>P2A5</sup> TCR transgenic T<sub>SCM</sub> were injected i.p.. **(A)** Absolute tumor weight was analyzed 17 days after initial tumor cell injection. **(B)** Representative total photon flux (p/s) and **(C)** fold change of total photon flux of luciferase expressing A673 cells, was assessed three days after i.p injection of either STEAP1 transgenic T<sub>SCM</sub> or unspecific CD8<sup>+</sup> T cells, respectively. **(D)** A time curve of total photon flux was recorded over a time period of 11 days.

## 5 Discussion

Therapy options for Ewing Sarcoma (ES) patients with recurrent disease are limited and the search for additional therapeutic devices is essential. Immunotherapy has had enormous success over the last couple of years, constituting it an interesting opportunity also for ES (56, 77, 89). The most promising approach seem to be TILs, but ES appear weakly immunogenic, mainly due to the low mutation rate, compared to other tumor entities (94, 95). Other possible reasons for the low immunogenicity of ES are inhibitory cell types within the tumor, like tumor-associated macrophages or bone marrow derived regulatory T cells ( $T_{REG}$ ) (96, 97). Nevertheless, the success with allogeneic hematopoietic stem cell transplantation (allo-HSCT) as well as immune-stimulating additives during therapy illuminates the opportunities of immunotherapy in ES (12, 98).

To develop an efficient adoptive T cell therapy (ACT) approach the right target for the cytotoxic T cells is essential, to avoid antigen escape mechanisms of the tumor or reactivity of the injected T cells against self-antigens (63). The best target would be the driver mutation of ES, namely the balanced chromosomal *EWS/ETS* translocation that gives rise to the most common EWS-FLI1 fusion protein (99-101). There has been some achievement with major histocompatibility complex class II (MHC-II) binding peptides of the EWS-FLI1 fusion regions able to induce a  $CD4^+$  response (102). However, there have no natural occurring epitopes of the fusion region been identified, that bind to MHC-I molecules with high enough affinities (103) to initiate a  $CD8^+$  anti-tumor response. Therefore, the search for other suitable targets is essential. *STEAP1* is one of the genes that is part of the ES specific molecular signature, previously identified by Staeger *et al.* (37). It is induced by EWS-FLI1 and its expression is associated with the invasive, tumorigenic and metastatic phenotype of ES (27). Besides its important role in propagation and survival of the tumor, it is only weakly expressed in normal tissue, except of minimal expression in prostate and urothelium. The overexpression in ES and only minimal expression in tissues that are not essential for survival, together with the importance for tumor survival, make *STEAP1* a suitable target for ACT. As high affinity of the target peptide is a prerequisite of successful tumor rejection after ACT (104), *STEAP1*<sup>130</sup> is an optimal candidate for CTL based immunotherapy. Its binding affinities to HLA-A\*02:01 are almost equal to the well described influenza peptide and superior to

other STEAP1 nonamer peptides, like STEAP1<sup>86</sup> which has been published as an antigen capable to induce anti-tumor responses *in vitro* (53). Although, the STEAP1<sup>86</sup> specific T cells generated in their study recognized the antigen in an HLA-A\*02:01 restricted manner, IFN $\gamma$  release and lytic potential after co-culture with STEAP1 expressing target cells was rather low. Thus, the use of a STEAP1 antigen with higher affinities might increase the therapeutic potential. Furthermore, there are no phosphorylation sites predicted for the STEAP1<sup>130</sup> peptide, which might influence the binding of a TCR to the peptide/MHC complex or the binding of the peptide to HLA-A\*02:01 itself.

Treatment of high risk or recurrent ES patients with autologous stem cell therapy delivered controversial results. On the one hand some studies showed improved disease free survival compared with historical controls (105, 106), on the other hand some studies demonstrated no long-term benefit compared to standard treatment (7, 107). The recognition of autologous and allogeneic antigens by T cells share many similarities, like the recognition of the MHC complex by the TCR and the generation of peptide specific T cells (81). However, the allo-restricted recognition of foreign peptide is a strong reaction, generating T cells with high avidity against their target structures and in the case of tumor associated antigens (TAA) higher avidity than their autologous counterpart, enabling them to recognize and react against those antigens. That makes allo-restricted TCRs a possible tool for the treatment of a variety of cancer entities (108). Allo-restricted T cells are now routinely isolated from allogeneic T cell populations with multimer technologies (88). With this approach it was possible to isolate T cell lines directed against STEAP1<sup>130</sup> in a HLA-A\*02:01 restricted manner. Those cells could be stained with STEAP1<sup>130</sup>/HLA-A\*02:01 multimer and released IFN $\gamma$  upon co-culture with STEAP1 expressing HLA-A\*02:01<sup>+</sup> target cells. Furthermore, those cells were able to specifically lyse HLA-A\*02:01<sup>+</sup> ES target cells *in vitro*, whereas negative controls were not killed. The identified peptide was not only specifically recognized, it was also properly processed and presented on HLA-A\*02:01, shown by co-transfection of HLA-A\*02:01 and *STEAP1* cDNA in Cos-7 cells, suggesting it to be a natural processed antigen on tumor cells.

The characterization of the respective STEAP1<sup>130</sup> specific TCRs resulted in the identification of a dominant T cell clone, as all 3 analyzed T cell lines encoded the same TCR. Based on the higher affinity of murine sequences to human CD3 (109), we codon-optimized variable and constant chains of the TCR to improve the expression in human T cell populations. A problem that might rise with TCR engineered T cells is mispairing of exo- and endogenous TCR  $\alpha$ - and  $\beta$ -chains, that could result in unpredicted cross-reactivity against self-tissues. Although this phenomenon has not been seen in clinical trials, studies in animal models indicate that possibility (110, 111). To avoid such mispairing, a minimal murinization of the constant chain was performed by exchanging 9 amino acids with their counterparts of the murine constant chain. In contrast to fully murinized constant chains, the likelihood of an antibody response to the TCR constant chains is reduced (93). However, the proposed enhanced expression of a humm TCR compared to a wt construct has not been observed in these experiments. Furthermore, as up to 90% of TCR transduced PBMCs could be stained with a TCR specific multimer, the risk of mispairing of the STEAP1<sup>P2A5</sup>  $\alpha$ - and  $\beta$ -chains with chains of the endogenous TCR seems rather low. For both constructs the use of a RD114 pseudotyped retrovirus producing high titer viruses, increased transduction efficacy compared to the MLV-10A1 pseudotyped retroviruses (112). Although the STEAP1<sup>P2A5</sup> TCR transgenic T cells showed a little lower affinity towards the STEAP1 peptide, which has also been recognized in previous studies (68), the *in vitro* recognition, as well as the killing of target cells, occurred with similar efficacy as for the original T cell clone P2A5.

There is an ongoing debate about the right subpopulation of T cells that should be used for ACT. The use of unselected peripheral blood lymphocytes as targets for genetic modification has shown impressive antitumor efficacy, but also unexplainable toxicities and low persistence have been observed (113, 114). Since the peripheral blood consists of different T cell subtypes a selection of the most effective one, prior to genetic modification with TCRs, seems reasonable. On the one hand there are antigen inexperienced naïve T cells ( $T_N$ ), expressing the surface molecules CD62L and CCR7, which enable them to home to secondary lymph organs. Those kind of cells cover the biggest diversity of TCRs (115) and effector T cells ( $T_{EFF}$ ) generated out of  $T_N$  seem to have superior proliferative capacity and longer telomers compared to other progenitor

populations. Additionally they show no acquisition of late differentiation markers (116) and have the ability to give rise to  $T_{EFF}$ , effector memory ( $T_{EM}$ ) and central memory ( $T_{CM}$ ) T cells when transferred as single cells into immunocompetent mice (117). The clear disadvantage of the use of  $T_N$  for ACT is that this T cell subset has been shown to be the primary reason for Graft versus Host Disease (GvHD) (118). To avoid the risk of causing a GvHD by introducing a foreign TCR into T cells that cross-pairs with the endogenous TCR, the use of virus specific memory T cells as donor cells has been advocated. Due to their specificity towards viral antigens, their TCR repertoire is restricted, which limits the possibilities of crosspairing. Furthermore, those cells could be activated through their endogenous TCR via vaccination, which might prevent tolerance mechanisms (119, 120). A population that lies somewhat in between naïve and memory T cells are the most recently in humans described stem cell memory T cells ( $T_{SCM}$ ) (121). Those cells are on top of their activation but at the same time show features of early differentiated cells. They have the ability to self-renew and at the same time to differentiate into all other memory and effector subtypes upon antigen encounter (91). There are different ways of generating those kind of cells. Gattinoni *et al.*, generated  $T_{SCM}$  by inducing the Wnt/ $\beta$ -catenin pathway with the GSK-3 $\beta$  Inhibitor XII TWS119. This induction prevents the differentiation into  $T_{EFF}$  and promotes the generation of a self-renewing, multipotent  $T_{SCM}$  population with anti-tumor efficacy superior to other T cell subtypes (92). Another possibility to generate those cells is by the use of low amounts of IL-7 and IL-15 after activation of  $T_N$  via anti-CD3/CD28 magnetic beads, as described by Cieri *et al.*. Although, this procedure creates cells with a similar phenotype, those cells show a higher proliferative capacity (91), which was also observed in this study. Even though it is not clear what kind of numbers are necessary for ACT with  $T_{SCM}$ , a sufficient multiplication of antigen specific T cells is mandatory.

When  $T_{SCM}$  generated with the Cieri protocol and transduced with the STEAP1<sup>P2A5</sup> TCR were injected into RAG2<sup>-/-</sup> $\gamma$ c<sup>-/-</sup>, an enhanced engraftment of those cells was observed in blood, spleen and also within the tumor when compared to unspecific PBMCs. Although tumor eradication was superior with the antigen specific  $T_{SCM}$  cells, the tumors seem to recover after the first line attack of the transferred T cells, as seen in the changes of total photon flux of those tumors over 11 days. Furthermore, in histological staining almost no

infiltrate of transgenic T cells was visible after 17 days. A possible explanation for that might be the rudimentary secondary lymphoid organs of the RAG2<sup>-/-</sup>γc<sup>-/-</sup> mouse model, the species specificity of homing molecules and the missing cytokines, preventing a sustained support of transferred T cells to develop a long lasting anti-tumor reactivity (122). Although a source of human IL-15 was provided twice a week, there is still a lack of e.g. IL-7 and IL-2 within those animals. There might be some mechanisms of T cell exhaustion as well that prevent the infused T cells from sustained anti-tumor reactivity and infiltration. Those kind of T cell inhibitions have been reported before in a variety of chronic infections (123) and cancer entities (124-126). Molecules that might play a role in the prevention of anti-tumor response are programmed cell death protein 1 (PD-1), cytotoxic T lymphocyte antigen 4 (CTLA-4), lymphocyte activation gene 3 protein (LAG3) and T cell immunoglobulin and mucin domain-containing protein 3 (TIM3). There has recently been impressive success by blocking those inhibitory molecules with specific antibodies, especially against PD-1 (pembroluzimab, nivolumab) and CTLA-4 (ipilimumab) (127). Moon *et al.* for example, showed a reversion of T cell hypofunction after combination therapy with an anti-human PD-1 antibody in immunodeficient mice (128). Whether there is any PD-1 expression in the phenotypically young T<sub>SCM</sub> cells used in this study needs to be assessed. This would be a prerequisite for combination therapy of anti-PD1 antibodies and the STEAP1<sup>P2A5</sup> TCR transgenic T cells.

Although there was no sustained anti-tumor activity of the infused transgenic T cells, a strong short term effect was visible, but at the same time no adverse effects or tissue toxicities have been observed as in other *in vivo* experiments before (129). This might be due to the mediocre affinity of the P2A5 TCR. It has been reported that a very high affinity does not increase anti-tumor efficacy, but might lead to autoimmune reactions (130, 131). Thus on-target as well as off-target toxicity is a great concern. In a clinical trial with autologous MART-1 specific T cells, on-target toxicity against melanocytes in the skin, eye and ear, which naturally express this antigen, was observed, requiring the treatment with corticosteroids (131). In another clinical trial, where high affinity carcinoembryonic antigen (CEA) specific autologous T cells were infused into patients to treat colorectal cancer, severe colitis resulted in the termination of this clinical study after only 3 patients (132). This on-target toxicity of high affinity TCRs makes the choice of

antigen important. If, like in the case of ES, no tumor specific antigen is available, TAAs with only minimal expression in normal tissues like STEAP1 may open a therapeutic window. Another, more complicated toxicity is off-target toxicity as observed by Morgan *et al.* in 2013. Infusion of autologous MAGE-A3 specific TCR transgenic T cells led to coma and ultimately death of two patients immediately after administration of those cells. The reason for that was the expression of MAGE-A12 in the brain of those patients, crossrecognized by the MAGE-A3 targeting T cells (133). Another severe case of crossreactivity was reported by Linette *et al.*, in 2013, where affinity enhanced TCR transgenic T cells directed against HLA-A\*01 restricted MAGE-A3, caused severe cardiovascular toxicity leading to the death of 2 patients a few days after administration of those cells. In this case the reason was an unexpected reactivity against the striated muscle specific protein titin, which has not been predicted in extensive preclinical studies (80). As the number of MHC binding peptides surpasses the diversity of TCRs by log scales, cross-reactivity of TCRs seems to be a logical event and has been shown in previous experiments (134). The T cell receptor diversity of humans is, due to combinatorial and junctional processes, theoretically estimated as  $10^{18}$ . This number exceeds the actual number by far, because of negative selection and other processes during development. The individual repertoire is estimated to be less than  $10^8$  in humans (135). Nonetheless,  $10^{15}$  different possible MHC binding peptides have to be recognized with this TCR repertoire (136). Unfortunately, so far there are no predictions based on the structure or composition of peptide/MHC complexes or TCRs, respectively, available to perform an *in silico* prediction of possible TCR crossreactivity (137), so that provisional tests have to be performed. By doing so, the STEAP1<sup>P2A5</sup> TCR seems not to be reactive against HLA-A\*02:01 itself or other MHC-I molecules, as LCLs with different HLA-A subtypes were not recognized without the STEAP1 peptide. Nonetheless, when LCLs containing the HLA-A2 subtypes A\*02:17 and A\*02:09 were loaded with peptide they were recognized by the TCR, indicating promiscuous binding of the peptide to other HLA molecules. To further analyze the reactivity of the TCR against other peptides, an alanine/threonine scan was performed. The resulting motifs depended on the kind of exchanged amino acid and add up to over 5000 different possible recognized proteins. This number does clearly not recapitalize the amount of possible TCR targets, as not all of those peptides bind to HLA-A\*02:01. Furthermore, this assay gives just a hint for

possible cross-reactivity, as no real occurring peptides are tested but artificial, structurally related nonamers. Next to that the STEAP1<sup>P2A5</sup> TCR transgenic T cells showed no recognition of HLA-A\*02:01<sup>+</sup> cells not expressing STEAP1. Nonetheless, further validation has to be performed.

To handle unwanted toxicity of the transferred cells, inducible suicide genes may be incorporated into the TCR transgenic T cells. In this way the cells can be ablated immediately by giving either a drug or a specific antibody. Currently, there are several suicide genes under investigation. One is CD20, which leads to a rapid ablation of co-transfected T cells after administration of rituximab (138). Another approach is the introduction of a truncated epidermal growth factor receptor (EGFR), which induces cell death after administration of the anti-EGFR mAB Erbitux (139). A very elegant way to induce apoptosis is the inducible Caspase-9 suicide gene, which is already evaluated in several clinical trials. Therein, the administration of the receptor cross-linking drug AP1903 leads to dimerization of caspase 9 and further to cell death via caspase 3 (140, 141). By incorporating a suicide gene into the STEAP1<sup>P2A5</sup> TCR transgenic T<sub>SCM</sub> cells, severe on- and off-target toxicity destroying normal tissue, could be prevented.

## 6 Conclusion and future perspectives

This study shows the generation and efficiency of transgenic, STEAP1 specific, HLA-A\*02:01 restricted, cytotoxic T cells. Those cells are able to specifically recognize and lyse ES target cells *in vitro* in a highly restricted manner and to proliferate, persist and show anti-tumor efficiency in an immunodeficient mouse model. As STEAP1 is not only overexpressed in ES, but also in bladder, prostate and pancreatic cancer, among others, those TCRs allow for an off the shelf production for patients with those kind of tumors, expressing the antigen.

Nonetheless, before using those cells in the clinic several characterizing steps have to be performed. As the predicted cross-reactivity is incompletely analyzed so far, further verification has to be done. One possibility for that might be the use of HLA-A\*02:01 transgenic mice. Those animals carry the human  $\alpha 1$  and  $\alpha 2$  domain, but contain a murine  $\alpha 3$  domain (142). This mouse model would allow a preclinical *in vivo* cross-reactivity study with fully competent immune system. Furthermore, this model would allow for a closer look onto persistence and long-term anti-tumor reactivity of the infused cells. Problems like missing secondary lymphoid organs, species specific homeostatic cytokines and homing receptors could be prevented. Moreover, in a system with an intact immune system, cells have to compete with other cells for the available amount of cytokines, making engraftment more comparable to the clinical situation.

To improve anti-tumor activity of the STEAP1<sup>P2A5</sup> TCR transgenic T<sub>SCM</sub> cells, a combination with checkpoint inhibitors, especially anti-PD1 antibodies, might be a promising approach. Although the T cells used in this study strongly engraft within the animals, they showed no prolonged anti-tumor reactivity, maybe because of exhaustion. Combining ACT with checkpoint inhibitors might reverse this phenomenon. However, this strategy only works if tumor stroma cells express PD-L1 on their surface. So far no studies on that topic have been published and it remains unclear if blocking the PD-1/PD-L1 interaction boosts the anti-tumor reactivity of transferred T cells in ES.

In a clinical setting the conditioning of patients might be crucial. There are several chemotherapeutic drugs stimulating the immune system. Current chemotherapeutic treatment of patients in Europe includes vincristine, ifosfamide, doxorubicin and

---

## Conclusion

---

etoposide. Doxorubicin for example boosts the proliferation of CD8<sup>+</sup> T cells recognizing tumor antigen and supports their tumor infiltration with the help of IL-17 secreting  $\gamma\delta$  T cells (143). Furthermore, vincristine and doxorubicin have been shown to increase the amount of antigen presenting DCs as well as the expression of IL-12 (144), a cytokine important for a variety of anti-tumor effects, including proper CD8<sup>+</sup> T cell function. So it seems like chemotherapeutic treatment might enhance the patient's own immune system and might also support adoptively transferred T cells. But there is an ongoing debate about the right timing of both therapies. There are some studies indicating an advantage of chemotherapy prior to immunotherapy to make tumor cells more susceptible for T cells and others showing an improve of immunotherapy followed by chemotherapy (145). Another possibility to support infused T<sub>SCM</sub> cells is a lymphoablation prior to T cell administration. Thereby, not only the access for homeostatic cytokines is increased, but also immunosuppressive regulatory T cells are depleted (146).

Thus, in this thesis generated STEAP1<sup>P2A5</sup> TCR transgenic T cells are potentially useful for immunotherapy also for other STEAP1 expressing tumors and may open the avenue for new therapeutic strategies for the treatment of patients with STEAP1-positive tumors. Nonetheless, further characterizing steps have to be performed to increase the safety and efficacy of those cells.

## 7 Summary

Only 65% - 70% of Ewing Sarcoma (ES) patients with primary disease are cured and almost all patients with bone marrow involvement die irrespective of the therapy, prompting the search for new therapeutic treatment modalities. Based on expression profiling technology targetable tumor associated antigens (TAA) are identified and exploited for engineered T cell therapy. Here, the specific recognition and lytic potential of transgenic, allo-restricted, CD8<sup>+</sup> T cells directed against the ES-associated antigen STEAP1 was examined.

Following repetitive STEAP1<sup>130</sup> peptide-driven stimulations with HLA-A\*02:01<sup>+</sup> dendritic cells, allo-restricted, HLA-A\*02:01<sup>-</sup> CD8<sup>+</sup> T cells were isolated with HLA-A\*02:01/peptide multimers and expanded by limiting dilution. After functional analysis of suitable T cell clones via ELISpot, flow cytometry and xCELLigence assays, TCR  $\alpha$ - and  $\beta$ -chains were identified. They were cloned into retroviral vectors, codon optimized, transfected into HLA-A\*02:01<sup>-</sup> primary T cell populations and tested again for specificity and lytic capacity *in vitro* and in a Rag2<sup>-/-</sup>  $\gamma$ c<sup>-/-</sup> mouse model. Additionally, the transgenic cells were screened for possible off-target toxicity against other HLA molecules or peptides.

Initially generated and transgenic T cells specifically recognized STEAP1<sup>130</sup> pulsed or transfected cells in the context of HLA-A\*02:01. They lysed cells and inhibited growth of HLA-A\*02:01<sup>+</sup> ES lines more effectively than HLA-A\*02:01<sup>-</sup> ES lines. *In vivo* tumor growth was inhibited more effectively with transgenic STEAP1<sup>130</sup> specific T cells than with unspecific T cells. The transgenic T cells showed some unspecific IFN $\gamma$  release against artificially generated, STEAP1 related peptides and other STEAP1<sup>130</sup> loaded HLA-A2 subclasses.

In summary the results of this thesis identify TCRs capable of recognizing and inhibiting growth of STEAP1 expressing ES cells *in vitro* and *in vivo* in a HLA-A2 restricted manner. As STEAP1 is overexpressed in a wide variety of cancers, we anticipate these STEAP1 specific TCRs to be potentially useful for immunotherapy of other STEAP1 expressing tumors. To avoid unpredicted off-target toxicity further cross-reactivity studies are necessary.

## 8 References

1. J. Ewing, Classics in oncology. Diffuse endothelioma of bone. James Ewing. Proceedings of the New York Pathological Society, 1921. *CA Cancer J Clin* **22**, 95-98 (1972).
2. M. Bernstein *et al.*, Ewing's sarcoma family of tumors: current management. *Oncologist* **11**, 503-519 (2006).
3. A. G. Glass, J. F. Fraumeni, Jr., Epidemiology of bone cancer in children. *J Natl Cancer Inst* **44**, 187-199 (1970).
4. S. A. Burchill, Ewing's sarcoma: diagnostic, prognostic, and therapeutic implications of molecular abnormalities. *J Clin Pathol* **56**, 96-102 (2003).
5. P. Jedlicka, Ewing Sarcoma, an enigmatic malignancy of likely progenitor cell origin, driven by transcription factor oncogenic fusions. *Int J Clin Exp Pathol* **3**, 338-347 (2010).
6. B. Widhe, T. Widhe, Initial symptoms and clinical features in osteosarcoma and Ewing sarcoma. *J Bone Joint Surg Am* **82**, 667-674 (2000).
7. S. J. Cotterill *et al.*, Prognostic factors in Ewing's tumor of bone: analysis of 975 patients from the European Intergroup Cooperative Ewing's Sarcoma Study Group. *J Clin Oncol* **18**, 3108-3114 (2000).
8. G. Bacci *et al.*, Therapy and survival after recurrence of Ewing's tumors: the Rizzoli experience in 195 patients treated with adjuvant and neoadjuvant chemotherapy from 1979 to 1997. *Ann Oncol* **14**, 1654-1659 (2003).
9. N. Gaspar *et al.*, Ewing Sarcoma: Current Management and Future Approaches Through Collaboration. *J Clin Oncol* **33**, 3036-3046 (2015).

---

## References

---

10. S. Burdach, H. Jurgens, High-dose chemoradiotherapy (HDC) in the Ewing family of tumors (EFT). *Crit Rev Oncol Hematol* **41**, 169-189 (2002).
11. S. Burdach *et al.*, High-dose therapy for patients with primary multifocal and early relapsed Ewing's tumors: results of two consecutive regimens assessing the role of total-body irradiation. *J Clin Oncol* **21**, 3072-3078 (2003).
12. S. Burdach *et al.*, Total body MRI-governed involved compartment irradiation combined with high-dose chemotherapy and stem cell rescue improves long-term survival in Ewing tumor patients with multiple primary bone metastases. *Bone Marrow Transplant* **45**, 483-489 (2010).
13. G. Bacci *et al.*, Neoadjuvant chemotherapy for osteosarcoma of the extremities with metastases at presentation: recent experience at the Rizzoli Institute in 57 patients treated with cisplatin, doxorubicin, and a high dose of methotrexate and ifosfamide. *Ann Oncol* **14**, 1126-1134 (2003).
14. T. Klingebiel *et al.*, Treatment of children with relapsed soft tissue sarcoma: report of the German CESS/CWS REZ 91 trial. *Med Pediatr Oncol* **30**, 269-275 (1998).
15. U. Thiel *et al.*, No improvement of survival with reduced- versus high-intensity conditioning for allogeneic stem cell transplants in Ewing tumor patients. *Ann Oncol* **22**, 1614-1621 (2011).
16. L. Granowetter *et al.*, Dose-intensified compared with standard chemotherapy for nonmetastatic Ewing sarcoma family of tumors: a Children's Oncology Group Study. *J Clin Oncol* **27**, 2536-2541 (2009).
17. A. Schuck *et al.*, Local therapy in localized Ewing tumors: results of 1058 patients treated in the CESS 81, CESS 86, and EICESS 92 trials. *Int J Radiat Oncol Biol Phys* **55**, 168-177 (2003).

---

## References

---

18. C. Juergens *et al.*, Safety assessment of intensive induction with vincristine, ifosfamide, doxorubicin, and etoposide (VIDE) in the treatment of Ewing tumors in the EURO-E.W.I.N.G. 99 clinical trial. *Pediatr Blood Cancer* **47**, 22-29 (2006).
19. J. L. Felgenhauer *et al.*, A pilot study of low-dose anti-angiogenic chemotherapy in combination with standard multiagent chemotherapy for patients with newly diagnosed metastatic Ewing sarcoma family of tumors: A Children's Oncology Group (COG) Phase II study NCT00061893. *Pediatr Blood Cancer* **60**, 409-414 (2013).
20. H. E. Grier *et al.*, Addition of ifosfamide and etoposide to standard chemotherapy for Ewing's sarcoma and primitive neuroectodermal tumor of bone. *N Engl J Med* **348**, 694-701 (2003).
21. J. R. Downing *et al.*, Detection of the (11;22)(q24;q12) translocation of Ewing's sarcoma and peripheral neuroectodermal tumor by reverse transcription polymerase chain reaction. *Am J Pathol* **143**, 1294-1300 (1993).
22. O. Delattre *et al.*, Gene fusion with an ETS DNA-binding domain caused by chromosome translocation in human tumours. *Nature* **359**, 162-165 (1992).
23. A. Uren, J. A. Toretsky, Ewing's sarcoma oncoprotein EWS-FLI1: the perfect target without a therapeutic agent. *Future Oncol* **1**, 521-528 (2005).
24. N. Riggi *et al.*, EWS-FLI1 utilizes divergent chromatin remodeling mechanisms to directly activate or repress enhancer elements in Ewing sarcoma. *Cancer Cell* **26**, 668-681 (2014).
25. G. H. Richter *et al.*, EZH2 is a mediator of EWS/FLI1 driven tumor growth and metastasis blocking endothelial and neuro-ectodermal differentiation. *Proc Natl Acad Sci U S A* **106**, 5324-5329 (2009).

---

## References

---

26. G. H. Richter *et al.*, G-Protein coupled receptor 64 promotes invasiveness and metastasis in Ewing sarcomas through PGF and MMP1. *J Pathol* **230**, 70-81 (2013).
27. T. G. Grunewald *et al.*, STEAP1 is associated with the invasive and oxidative stress phenotype of Ewing tumors. *Mol Cancer Res* **10**, 52-65 (2012).
28. L. Cironi *et al.*, IGF1 is a common target gene of Ewing's sarcoma fusion proteins in mesenchymal progenitor cells. *PLoS One* **3**, e2634 (2008).
29. E. C. Toomey, J. D. Schiffman, S. L. Lessnick, Recent advances in the molecular pathogenesis of Ewing's sarcoma. *Oncogene* **29**, 4504-4516 (2010).
30. A. Prieur, F. Tirode, P. Cohen, O. Delattre, EWS/FLI-1 silencing and gene profiling of Ewing cells reveal downstream oncogenic pathways and a crucial role for repression of insulin-like growth factor binding protein 3. *Mol Cell Biol* **24**, 7275-7283 (2004).
31. L. Dauphinot *et al.*, Analysis of the expression of cell cycle regulators in Ewing cell lines: EWS-FLI-1 modulates p57KIP2 and c-Myc expression. *Oncogene* **20**, 3258-3265 (2001).
32. H. Kovar, Context matters: the hen or egg problem in Ewing's sarcoma. *Semin Cancer Biol* **15**, 189-196 (2005).
33. G. Potikyan *et al.*, Genetically defined EWS/FLI1 model system suggests mesenchymal origin of Ewing's family tumors. *Lab Invest* **88**, 1291-1302 (2008).
34. Y. Miyagawa *et al.*, Inducible expression of chimeric EWS/ETS proteins confers Ewing's family tumor-like phenotypes to human mesenchymal progenitor cells. *Mol Cell Biol* **28**, 2125-2137 (2008).

---

## References

---

35. M. Lipinski *et al.*, Phenotypic characterization of Ewing sarcoma cell lines with monoclonal antibodies. *J Cell Biochem* **31**, 289-296 (1986).
36. D. Schmidt, D. Harms, S. Burdach, Malignant peripheral neuroectodermal tumours of childhood and adolescence. *Virchows Arch A Pathol Anat Histopathol* **406**, 351-365 (1985).
37. M. S. Staeger *et al.*, DNA microarrays reveal relationship of Ewing family tumors to both endothelial and fetal neural crest-derived cells and define novel targets. *Cancer Res* **64**, 8213-8221 (2004).
38. S. Hu-Lieskovan *et al.*, EWS-FLI1 fusion protein up-regulates critical genes in neural crest development and is responsible for the observed phenotype of Ewing's family of tumors. *Cancer Res* **65**, 4633-4644 (2005).
39. C. J. Rorie *et al.*, The Ews/Fli-1 fusion gene switches the differentiation program of neuroblastomas to Ewing sarcoma/peripheral primitive neuroectodermal tumors. *Cancer Res* **64**, 1266-1277 (2004).
40. N. Riggi *et al.*, EWS-FLI-1 expression triggers a Ewing's sarcoma initiation program in primary human mesenchymal stem cells. *Cancer Res* **68**, 2176-2185 (2008).
41. F. Tirode *et al.*, Mesenchymal stem cell features of Ewing tumors. *Cancer Cell* **11**, 421-429 (2007).
42. R. S. Ohgami, D. R. Campagna, A. McDonald, M. D. Fleming, The Steap proteins are metalloreductases. *Blood* **108**, 1388-1394 (2006).
43. I. M. Gomes, C. J. Maia, C. R. Santos, STEAP proteins: from structure to applications in cancer therapy. *Mol Cancer Res* **10**, 573-587 (2012).

---

## References

---

44. R. S. Hubert *et al.*, STEAP: a prostate-specific cell-surface antigen highly expressed in human prostate tumors. *Proc Natl Acad Sci U S A* **96**, 14523-14528 (1999).
45. P. M. Challita-Eid *et al.*, Monoclonal antibodies to six-transmembrane epithelial antigen of the prostate-1 inhibit intercellular communication in vitro and growth of human tumor xenografts in vivo. *Cancer Res* **67**, 5798-5805 (2007).
46. I. Y. Cheung *et al.*, Novel markers of subclinical disease for Ewing family tumors from gene expression profiling. *Clin Cancer Res* **13**, 6978-6983 (2007).
47. R. J. Vaghjani, S. Talma, C. L. Murphy, Six-transmembrane epithelial antigen of the prostate (STEAP1 and STEAP2)-differentially expressed by murine and human mesenchymal stem cells. *Tissue Eng Part A* **15**, 2073-2083 (2009).
48. T. G. Grunewald *et al.*, High STEAP1 expression is associated with improved outcome of Ewing's sarcoma patients. *Ann Oncol* **23**, 2185-2190 (2012).
49. L. Li, J. Li, Z. Shen, W. Liu, Z. Chen, [Clinical significance of six-transmembrane epithelial antigen of the prostate expressed in prostatic carcinoma]. *Zhonghua Nan Ke Xue* **10**, 351-354 (2004).
50. M. T. Valenti *et al.*, STEAP mRNA detection in serum of patients with solid tumours. *Cancer Lett* **273**, 122-126 (2009).
51. D. Hanahan, R. A. Weinberg, Hallmarks of cancer: the next generation. *Cell* **144**, 646-674 (2011).
52. D. A. Rodeberg, R. A. Nuss, S. F. ElSawa, E. Celis, Recognition of six-transmembrane epithelial antigen of the prostate-expressing tumor cells by peptide antigen-induced cytotoxic T lymphocytes. *Clin Cancer Res* **11**, 4545-4552 (2005).

---

## References

---

53. P. M. Alves *et al.*, STEAP, a prostate tumor antigen, is a target of human CD8+ T cells. *Cancer Immunol Immunother* **55**, 1515-1523 (2006).
54. R. E. Billingham, L. Brent, P. B. Medawar, Quantitative studies on tissue transplantation immunity. II. The origin, strength and duration of actively and adoptively acquired immunity. *Proc R Soc Lond B Biol Sci* **143**, 58-80 (1954).
55. D. W. Barnes, J. F. Loutit, Treatment of murine leukaemia with x-rays and homologous bone marrow. II. *Br J Haematol* **3**, 241-252 (1957).
56. J. Couzin-Frankel, Breakthrough of the year 2013. Cancer immunotherapy. *Science* **342**, 1432-1433 (2013).
57. S. A. Rosenberg *et al.*, Use of tumor-infiltrating lymphocytes and interleukin-2 in the immunotherapy of patients with metastatic melanoma. A preliminary report. *N Engl J Med* **319**, 1676-1680 (1988).
58. M. E. Dudley *et al.*, Adoptive cell therapy for patients with metastatic melanoma: evaluation of intensive myeloablative chemoradiation preparative regimens. *J Clin Oncol* **26**, 5233-5239 (2008).
59. S. A. Rosenberg *et al.*, Durable complete responses in heavily pretreated patients with metastatic melanoma using T-cell transfer immunotherapy. *Clin Cancer Res* **17**, 4550-4557 (2011).
60. S. R. Riddell *et al.*, Restoration of viral immunity in immunodeficient humans by the adoptive transfer of T cell clones. *Science* **257**, 238-241 (1992).
61. C. M. Rooney *et al.*, Use of gene-modified virus-specific T lymphocytes to control Epstein-Barr-virus-related lymphoproliferation. *Lancet* **345**, 9-13 (1995).

---

## References

---

62. M. A. Cheever *et al.*, The prioritization of cancer antigens: a national cancer institute pilot project for the acceleration of translational research. *Clin Cancer Res* **15**, 5323-5337 (2009).
63. K. Fousek, N. Ahmed, The Evolution of T-cell Therapies for Solid Malignancies. *Clin Cancer Res* **21**, 3384-3392 (2015).
64. A. W. Goldrath, M. J. Bevan, Selecting and maintaining a diverse T-cell repertoire. *Nature* **402**, 255-262 (1999).
65. Z. Eshhar, T. Waks, G. Gross, D. G. Schindler, Specific activation and targeting of cytotoxic lymphocytes through chimeric single chains consisting of antibody-binding domains and the gamma or zeta subunits of the immunoglobulin and T-cell receptors. *Proc Natl Acad Sci U S A* **90**, 720-724 (1993).
66. G. Dotti, S. Gottschalk, B. Savoldo, M. K. Brenner, Design and development of therapies using chimeric antigen receptor-expressing T cells. *Immunol Rev* **257**, 107-126 (2014).
67. M. V. Maus, S. A. Grupp, D. L. Porter, C. H. June, Antibody-modified T cells: CARs take the front seat for hematologic malignancies. *Blood* **123**, 2625-2635 (2014).
68. N. Cieri *et al.*, Adoptive immunotherapy with genetically modified lymphocytes in allogeneic stem cell transplantation. *Immunol Rev* **257**, 165-180 (2014).
69. D. L. Porter, B. L. Levine, M. Kalos, A. Bagg, C. H. June, Chimeric antigen receptor-modified T cells in chronic lymphoid leukemia. *N Engl J Med* **365**, 725-733 (2011).
70. M. Kalos *et al.*, T cells with chimeric antigen receptors have potent antitumor effects and can establish memory in patients with advanced leukemia. *Sci Transl Med* **3**, 95ra73 (2011).

---

## References

---

71. S. A. Grupp *et al.*, Chimeric antigen receptor-modified T cells for acute lymphoid leukemia. *N Engl J Med* **368**, 1509-1518 (2013).
72. D. L. Porter *et al.*, Chimeric antigen receptor T cells persist and induce sustained remissions in relapsed refractory chronic lymphocytic leukemia. *Sci Transl Med* **7**, 303ra139 (2015).
73. S. L. Maude *et al.*, Chimeric antigen receptor T cells for sustained remissions in leukemia. *N Engl J Med* **371**, 1507-1517 (2014).
74. D. W. Lee *et al.*, T cells expressing CD19 chimeric antigen receptors for acute lymphoblastic leukaemia in children and young adults: a phase 1 dose-escalation trial. *Lancet* **385**, 517-528 (2015).
75. T. M. Clay *et al.*, Efficient transfer of a tumor antigen-reactive TCR to human peripheral blood lymphocytes confers anti-tumor reactivity. *J Immunol* **163**, 507-513 (1999).
76. R. A. Morgan *et al.*, Cancer regression in patients after transfer of genetically engineered lymphocytes. *Science* **314**, 126-129 (2006).
77. S. A. Rosenberg, N. P. Restifo, Adoptive cell transfer as personalized immunotherapy for human cancer. *Science* **348**, 62-68 (2015).
78. P. F. Robbins *et al.*, Tumor regression in patients with metastatic synovial cell sarcoma and melanoma using genetically engineered lymphocytes reactive with NY-ESO-1. *J Clin Oncol* **29**, 917-924 (2011).
79. E. Nicholson, S. Ghorashian, H. Stauss, Improving TCR Gene Therapy for Treatment of Haematological Malignancies. *Adv Hematol* **2012**, 404081 (2012).
80. G. P. Linette *et al.*, Cardiovascular toxicity and titin cross-reactivity of affinity-enhanced T cells in myeloma and melanoma. *Blood* **122**, 863-871 (2013).

---

## References

---

81. N. J. Felix, P. M. Allen, Specificity of T-cell alloreactivity. *Nat Rev Immunol* **7**, 942-953 (2007).
82. R. Childs *et al.*, Regression of metastatic renal-cell carcinoma after nonmyeloablative allogeneic peripheral-blood stem-cell transplantation. *N Engl J Med* **343**, 750-758 (2000).
83. K. G. Lucas, C. Schwartz, J. Kaplan, Allogeneic stem cell transplantation in a patient with relapsed Ewing sarcoma. *Pediatr Blood Cancer* **51**, 142-144 (2008).
84. S. Burdach *et al.*, Allogeneic and autologous stem-cell transplantation in advanced Ewing tumors. An update after long-term follow-up from two centers of the European Intergroup study EICESS. Stem-Cell Transplant Programs at Dusseldorf University Medical Center, Germany and St. Anna Kinderspital, Vienna, Austria. *Ann Oncol* **11**, 1451-1462 (2000).
85. M. Knabel *et al.*, Reversible MHC multimer staining for functional isolation of T-cell populations and effective adoptive transfer. *Nat Med* **8**, 631-637 (2002).
86. C. Yee, P. A. Savage, P. P. Lee, M. M. Davis, P. D. Greenberg, Isolation of high avidity melanoma-reactive CTL from heterogeneous populations using peptide-MHC tetramers. *J Immunol* **162**, 2227-2234 (1999).
87. A. Moris, V. Teichgraber, L. Gauthier, H. J. Buhring, H. G. Rammensee, Cutting edge: characterization of allorestricted and peptide-selective alloreactive T cells using HLA-tetramer selection. *J Immunol* **166**, 4818-4821 (2001).
88. U. Thiel *et al.*, Specific recognition and inhibition of Ewing tumour growth by antigen-specific allo-restricted cytotoxic T cells. *Br J Cancer* **104**, 948-956 (2011).
89. C. H. June, S. R. Riddell, T. N. Schumacher, Adoptive cellular therapy: a race to the finish line. *Sci Transl Med* **7**, 280ps287 (2015).

---

## References

---

90. J. P. Goldman *et al.*, Enhanced human cell engraftment in mice deficient in RAG2 and the common cytokine receptor gamma chain. *Br J Haematol* **103**, 335-342 (1998).
91. N. Cieri *et al.*, IL-7 and IL-15 instruct the generation of human memory stem T cells from naive precursors. *Blood* **121**, 573-584 (2013).
92. L. Gattinoni *et al.*, Wnt signaling arrests effector T cell differentiation and generates CD8+ memory stem cells. *Nat Med* **15**, 808-813 (2009).
93. D. Sommermeyer, W. Uckert, Minimal amino acid exchange in human TCR constant regions fosters improved function of TCR gene-modified T cells. *J Immunol* **184**, 6223-6231 (2010).
94. B. D. Crompton *et al.*, The genomic landscape of pediatric Ewing sarcoma. *Cancer Discov* **4**, 1326-1341 (2014).
95. M. S. Lawrence *et al.*, Mutational heterogeneity in cancer and the search for new cancer-associated genes. *Nature* **499**, 214-218 (2013).
96. T. Fujiwara *et al.*, Macrophage infiltration predicts a poor prognosis for human ewing sarcoma. *Am J Pathol* **179**, 1157-1170 (2011).
97. P. Brinkrolf *et al.*, A high proportion of bone marrow T cells with regulatory phenotype (CD4+CD25hiFoxP3+) in Ewing sarcoma patients is associated with metastatic disease. *Int J Cancer* **125**, 879-886 (2009).
98. C. L. Mackall *et al.*, A pilot study of consolidative immunotherapy in patients with high-risk pediatric sarcomas. *Clin Cancer Res* **14**, 4850-4858 (2008).
99. S. L. Lessnick, M. Ladanyi, Molecular pathogenesis of Ewing sarcoma: new therapeutic and transcriptional targets. *Annu Rev Pathol* **7**, 145-159 (2012).

---

## References

---

100. C. Mackintosh, J. Madoz-Gurpide, J. L. Ordonez, D. Osuna, D. Herrero-Martin, The molecular pathogenesis of Ewing's sarcoma. *Cancer Biol Ther* **9**, 655-667 (2010).
101. H. Kovar, Blocking the road, stopping the engine or killing the driver? Advances in targeting EWS/FLI-1 fusion in Ewing sarcoma as novel therapy. *Expert Opin Ther Targets* **18**, 1315-1328 (2014).
102. F. Meyer-Wentrup, G. Richter, S. Burdach, Identification of an immunogenic EWS-FLI1-derived HLA-DR-restricted T helper cell epitope. *Pediatr Hematol Oncol* **22**, 297-308 (2005).
103. C. H. Evans *et al.*, EWS-FLI-1-targeted cytotoxic T-cell killing of multiple tumor types belonging to the Ewing sarcoma family of tumors. *Clin Cancer Res* **18**, 5341-5351 (2012).
104. T. Kammertoens, T. Blankenstein, It's the peptide-MHC affinity, stupid. *Cancer Cell* **23**, 429-431 (2013).
105. S. Burdach, Treatment of advanced Ewing tumors by combined radiochemotherapy and engineered cellular transplants. *Pediatr Transplant* **8 Suppl 5**, 67-82 (2004).
106. S. Burdach *et al.*, Myeloablative radiochemotherapy and hematopoietic stem-cell rescue in poor-prognosis Ewing's sarcoma. *J Clin Oncol* **11**, 1482-1488 (1993).
107. P. A. Meyers *et al.*, High-dose melphalan, etoposide, total-body irradiation, and autologous stem-cell reconstitution as consolidation therapy for high-risk Ewing's sarcoma does not improve prognosis. *J Clin Oncol* **19**, 2812-2820 (2001).
108. S. Burdach, H. J. Kolb, The vigor of defense against non-self: potential superiority of allorestricted T cells in immunotherapy of cancer? *Front Oncol* **3**, 100 (2013).

---

## References

---

109. C. J. Cohen, Y. Zhao, Z. Zheng, S. A. Rosenberg, R. A. Morgan, Enhanced antitumor activity of murine-human hybrid T-cell receptor (TCR) in human lymphocytes is associated with improved pairing and TCR/CD3 stability. *Cancer Res* **66**, 8878-8886 (2006).
110. C. Govers, Z. Sebestyen, M. Coccoris, R. A. Willemsen, R. Debets, T cell receptor gene therapy: strategies for optimizing transgenic TCR pairing. *Trends Mol Med* **16**, 77-87 (2010).
111. G. M. Bendle *et al.*, Lethal graft-versus-host disease in mouse models of T cell receptor gene therapy. *Nat Med* **16**, 565-570, 561p following 570 (2010).
112. K. Ghani *et al.*, Efficient human hematopoietic cell transduction using RD114- and GALV-pseudotyped retroviral vectors produced in suspension and serum-free media. *Hum Gene Ther* **20**, 966-974 (2009).
113. R. A. Morgan *et al.*, Case report of a serious adverse event following the administration of T cells transduced with a chimeric antigen receptor recognizing ERBB2. *Mol Ther* **18**, 843-851 (2010).
114. R. Brentjens, R. Yeh, Y. Bernal, I. Riviere, M. Sadelain, Treatment of chronic lymphocytic leukemia with genetically targeted autologous T cells: case report of an unforeseen adverse event in a phase I clinical trial. *Mol Ther* **18**, 666-668 (2010).
115. H. S. Robins *et al.*, Comprehensive assessment of T-cell receptor beta-chain diversity in alphabeta T cells. *Blood* **114**, 4099-4107 (2009).
116. C. S. Hinrichs *et al.*, Human effector CD8+ T cells derived from naive rather than memory subsets possess superior traits for adoptive immunotherapy. *Blood* **117**, 808-814 (2011).

---

## References

---

117. C. Stemmerger *et al.*, A single naive CD8<sup>+</sup> T cell precursor can develop into diverse effector and memory subsets. *Immunity* **27**, 985-997 (2007).
118. W. D. Shlomchik, Graft-versus-host disease. *Nat Rev Immunol* **7**, 340-352 (2007).
119. C. J. Turtle, S. R. Riddell, Genetically retargeting CD8<sup>+</sup> lymphocyte subsets for cancer immunotherapy. *Curr Opin Immunol* **23**, 299-305 (2011).
120. R. M. Teague *et al.*, Peripheral CD8<sup>+</sup> T cell tolerance to self-proteins is regulated proximally at the T cell receptor. *Immunity* **28**, 662-674 (2008).
121. L. Gattinoni *et al.*, A human memory T cell subset with stem cell-like properties. *Nat Med* **17**, 1290-1297 (2011).
122. L. D. Shultz, M. A. Brehm, J. V. Garcia-Martinez, D. L. Greiner, Humanized mice for immune system investigation: progress, promise and challenges. *Nat Rev Immunol* **12**, 786-798 (2012).
123. E. J. Wherry, M. Kurachi, Molecular and cellular insights into T cell exhaustion. *Nat Rev Immunol* **15**, 486-499 (2015).
124. W. Zou, L. Chen, Inhibitory B7-family molecules in the tumour microenvironment. *Nat Rev Immunol* **8**, 467-477 (2008).
125. H. Dong *et al.*, Tumor-associated B7-H1 promotes T-cell apoptosis: a potential mechanism of immune evasion. *Nat Med* **8**, 793-800 (2002).
126. D. M. Pardoll, The blockade of immune checkpoints in cancer immunotherapy. *Nat Rev Cancer* **12**, 252-264 (2012).
127. P. Sharma, J. P. Allison, The future of immune checkpoint therapy. *Science* **348**, 56-61 (2015).

---

## References

---

128. E. K. Moon *et al.*, Blockade of Programmed Death 1 Augments the Ability of Human T cells Engineered to Target NY-ESO-1 to Control Tumor Growth after Adoptive Transfer. *Clin Cancer Res*, (2015).
129. L. D. Fast, G. DiLeone, G. Cardarelli, J. Li, R. Goodrich, Mirasol PRT treatment of donor white blood cells prevents the development of xenogeneic graft-versus-host disease in Rag2<sup>-/-</sup>-gamma c<sup>-/-</sup> double knockout mice. *Transfusion* **46**, 1553-1560 (2006).
130. S. Zhong *et al.*, T-cell receptor affinity and avidity defines antitumor response and autoimmunity in T-cell immunotherapy. *Proc Natl Acad Sci U S A* **110**, 6973-6978 (2013).
131. L. A. Johnson *et al.*, Gene therapy with human and mouse T-cell receptors mediates cancer regression and targets normal tissues expressing cognate antigen. *Blood* **114**, 535-546 (2009).
132. M. R. Parkhurst *et al.*, T cells targeting carcinoembryonic antigen can mediate regression of metastatic colorectal cancer but induce severe transient colitis. *Mol Ther* **19**, 620-626 (2011).
133. R. A. Morgan *et al.*, Cancer regression and neurological toxicity following anti-MAGE-A3 TCR gene therapy. *J Immunother* **36**, 133-151 (2013).
134. M. E. Birnbaum *et al.*, Deconstructing the peptide-MHC specificity of T cell recognition. *Cell* **157**, 1073-1087 (2014).
135. T. P. Arstila *et al.*, A direct estimate of the human alphabeta T cell receptor diversity. *Science* **286**, 958-961 (1999).
136. P. D. Holler, D. M. Kranz, T cell receptors: affinities, cross-reactivities, and a conformer model. *Mol Immunol* **40**, 1027-1031 (2004).

---

## References

---

137. G. Petrova, A. Ferrante, J. Gorski, Cross-reactivity of T cells and its role in the immune system. *Crit Rev Immunol* **32**, 349-372 (2012).
138. M. Griffioen *et al.*, Retroviral transfer of human CD20 as a suicide gene for adoptive T-cell therapy. *Haematologica* **94**, 1316-1320 (2009).
139. X. Wang *et al.*, A transgene-encoded cell surface polypeptide for selection, in vivo tracking, and ablation of engineered cells. *Blood* **118**, 1255-1263 (2011).
140. J. D. Iulucci *et al.*, Intravenous safety and pharmacokinetics of a novel dimerizer drug, AP1903, in healthy volunteers. *J Clin Pharmacol* **41**, 870-879 (2001).
141. T. Gargett, M. P. Brown, The inducible caspase-9 suicide gene system as a "safety switch" to limit on-target, off-tumor toxicities of chimeric antigen receptor T cells. *Front Pharmacol* **5**, 235 (2014).
142. M. H. Newberg *et al.*, Importance of MHC class 1 alpha2 and alpha3 domains in the recognition of self and non-self MHC molecules. *J Immunol* **156**, 2473-2480 (1996).
143. S. R. Mattarollo *et al.*, Pivotal role of innate and adaptive immunity in anthracycline chemotherapy of established tumors. *Cancer Res* **71**, 4809-4820 (2011).
144. G. V. Shurin, I. L. Tourkova, R. Kaneno, M. R. Shurin, Chemotherapeutic agents in noncytotoxic concentrations increase antigen presentation by dendritic cells via an IL-12-dependent mechanism. *J Immunol* **183**, 137-144 (2009).
145. L. Galluzzi, L. Senovilla, L. Zitvogel, G. Kroemer, The secret ally: immunostimulation by anticancer drugs. *Nat Rev Drug Discov* **11**, 215-233 (2012).

---

## References

---

146. L. Gattinoni *et al.*, Removal of homeostatic cytokine sinks by lymphodepletion enhances the efficacy of adoptively transferred tumor-specific CD8+ T cells. *J Exp Med* **202**, 907-912 (2005).

## 9 Appendix

### 9.1 Supplemental Figures

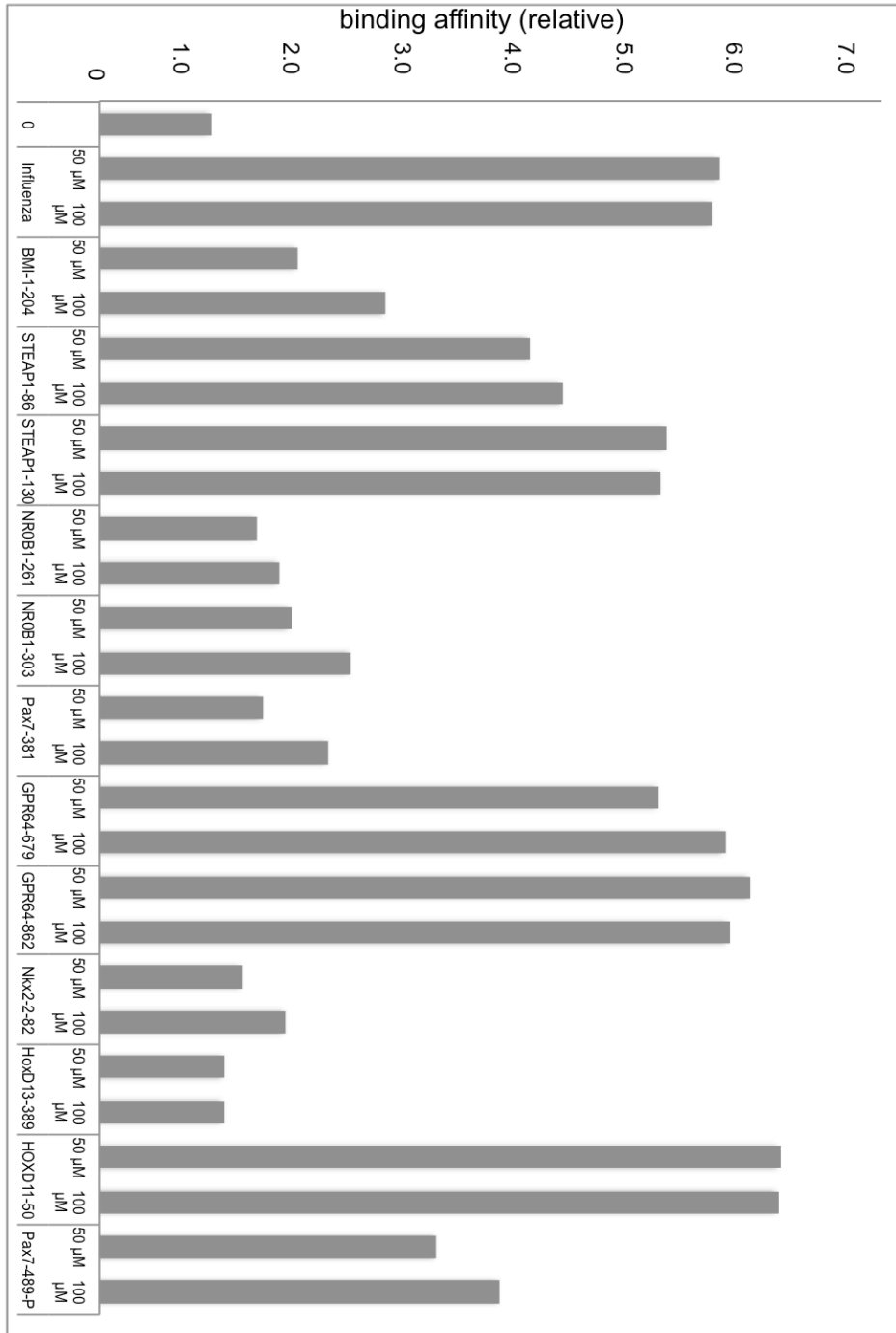


**Figure 26: Relative binding affinity of various ES associated antigen peptides.** T2 cells were loaded with 50 µM and 100 µM of the respective peptide for 16 h and subsequently stained with anti-human HLA-A2 mAb. Stabilized HLA-A\*02:01 molecules were quantified via flow cytometry.

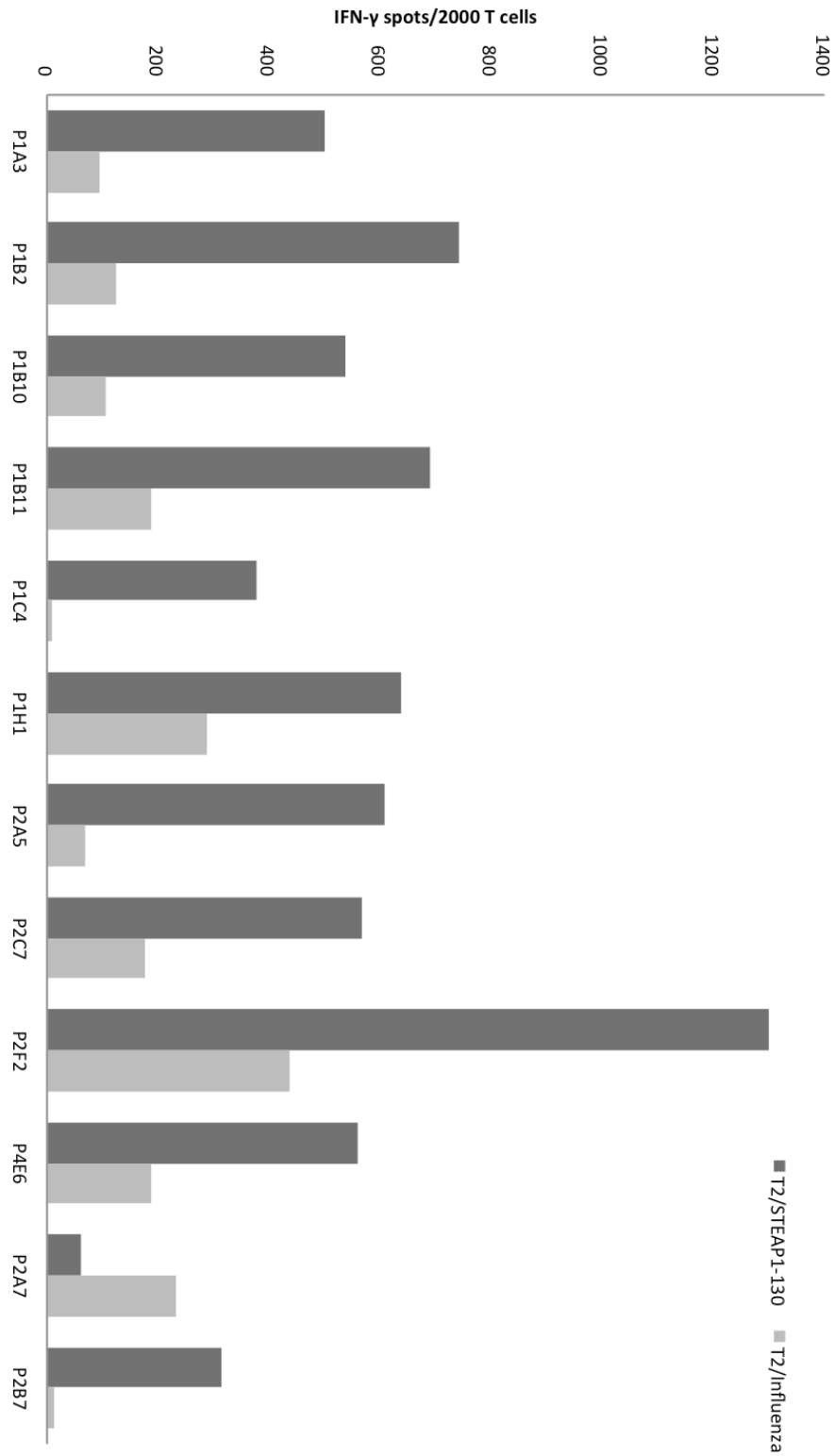


**Figure 27: Screening of FACS sorted T cell lines for specific peptide recognition.** IFN $\gamma$  release of STEAP1<sup>130</sup>/HLA-A\*02:01 multimer<sup>+</sup> CD8<sup>+</sup> T cells upon co-culture with peptide pulsed T2 cells, analyzed via ELISpot assay.

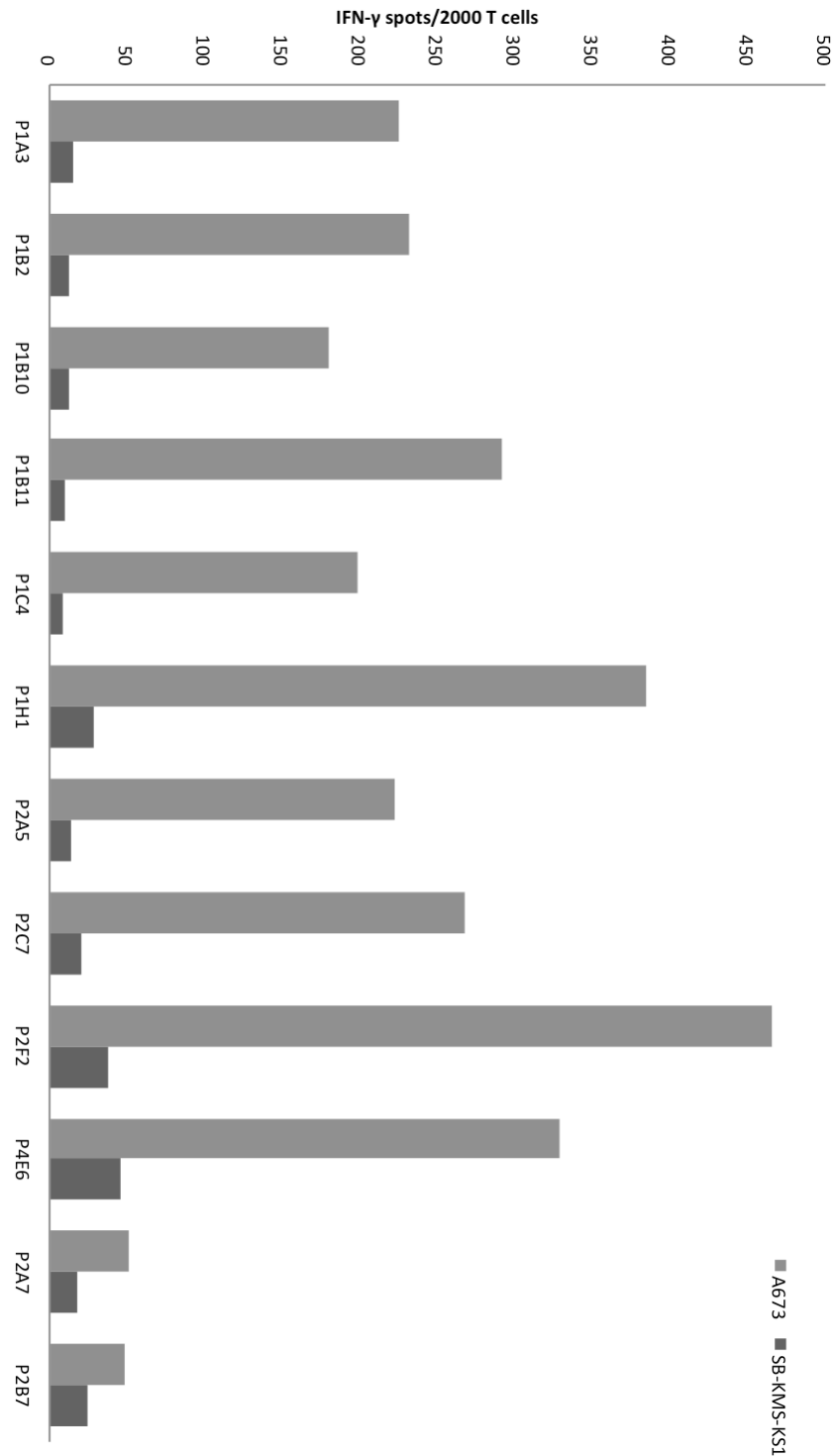


**Figure 28: Screening of FACS sorted T cell lines for HLA-A\*02:01 specific target recognition.** IFN $\gamma$  release of STEAP1<sup>130</sup>/HLA-A\*02:01 multimer<sup>+</sup> CD8<sup>+</sup> T cells upon co-culture with HLA-A\*02:01<sup>+</sup> ES cell line A673 or HLA-A\*02:01<sup>-</sup> ES cell line SB-KMS-KS1, analyzed via ELISpot assay.

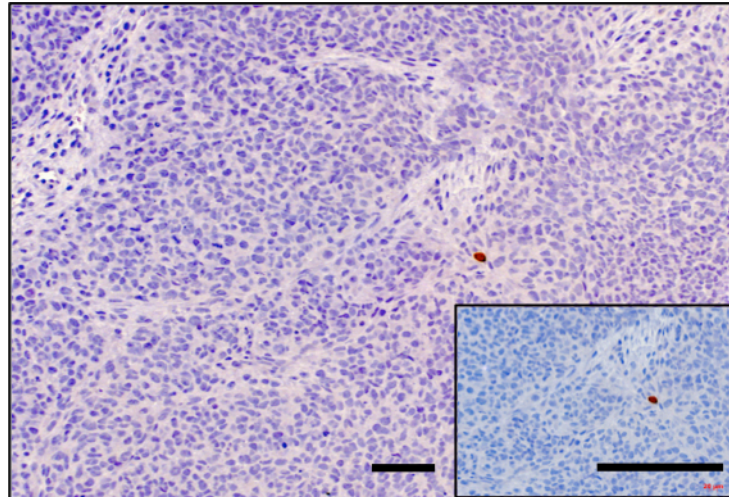


**Figure 29: Immunohistochemistry staining of CD8<sup>+</sup> cells within tumors from animals treated with tgSTEAP1hum T<sub>SCM</sub>.** Tumors were analyzed for immune cell infiltration 17 days after initial inoculation of animals with  $2 \times 10^6$  A673 cells and ip. infusion of  $3 \times 10^6$  tgSTEAP1hum T<sub>SCM</sub> cells 4 days later.

## 9.2 Supplemental Table

Table 2: Nucleotide sequence of STEAP1<sup>P2A5</sup> TCR humm and STEAP1<sup>P2A5</sup> TCR wt.

humm STEAP1 <sup>130</sup> TCR construct (β- chain, P2A, α-chain)	ATGGGCACCAGCCTCCTCTGCTGGATGGCCCTGTGTCTCCTGGGGG CAGATCACGCAGATACTGGAGTCTCCAGAACCCAGACACAAGAT CACAAAGAGGGGACAGAATGTAAC TTTCAGGTGTGATCCAATTTCT GAACACAACCGCCTTTATTGGTACCGACAGACCCTGGGGCAGGGCC CAGAGTTTCTGACTTACTTCCAGAATGAAGCTCAACTAGAAAAATC AAGGCTGCTCAGTGATCGGTTCTCTGCAGAGAGGCCTAAGGGATCT TTCTCCACCTTGGAGATCCAGCGCACAGAGCAGGGGGACTCGGCCA TGTATCTCTGTGCCAGCAGCTCGGACCGGGACAGTTACAAGAATGA GCAGTTCTTCGGGCCAGGGACACGGCTCACCGTGCTAGAGGACCTG AAAACGTGTTCCACCCGAGGTCGCTGTGTTTGAGCCATCAGAAGC AGAGATCTCCACACCCAAAAGGCCACACTGGTG <sup>5</sup> TGCCTGGCCAC AGGCTTCTACCCGACCACGTGGAGCTGAGCTGGTGGGTGAATGGG AAGGAGGTGCACAGTGGGGTCAGCACAGACCCGCAGCCCCCTCAAGG AGCAGCCCGCCCTCAATGACTCCAGATACTGCCTGAGCAGCCGCCT GAGGGTCTCGGCCACCTTCTGGCAGAACCCCGCAACCCTTCCGC TGTC AAGTCCAGTTCTACGGGCTCTCGGAGAATGACGAGTGGACCC AGGATAGGGCCAAACCTGTCACCCAGATCGTCAGCGCCGAGGCCTG GGGTAGAGCAGACTGTGGCTTACCTCCGAGTCTTACCAGCAAGGG GTCCTGTCTGCCACCATCCTCTATGAGATCTTGCTAGGGAAGGCCA CCTTGTATGCCGTGCTGGTCAGTGCCCTCGTGCTGATGGCCATGGT CAAGAGAAAGGATTCCAGAGGCGGAAGCGGCGCCACGAAC TTCTCT CTGTTAAAGCAAGCAGGAGACGTGGAAGAAAACCCCGTCCCATGG CATGCCCTGGCTTCCCTGTGGGCACTTGTGATCTCCACCTGTCTTGA ATTTAGCATGGCTCAGACAGTCACTCAGTCTCAACCAGAGATGTCT GTGCAGGAGGCAGAGACCGTGACCCTGAGCTGCACATATGACACCA GTGAGAGTGATTATTATTTATTCTGGTACAAGCAGCCTCCAGCAG GCAGATGATTCTCGTTATTCGCCAAGAAGCTTATAAGCAACAGAAT GCAACAGAGAATCGTTTCTCTGTGAACTTCCAGAAAGCAGCCAAAT CCTTCAGTCTCAAGATCTCAGACTCACAGCTGGGGGATGCCGCGAT GTATTTCTGTGCTTATGGATCTAACTTTGGAAATGAGAAATTAACC
---	--

Appendix

	<p>TTTGGGACTGGAACAAGACTCACCATCATACCCAATATCCAGAACC  CTGACCCTGCCGTGTACCAGCTGAGAGACTCTAAATCCAGTGACAA  GTCTGTCTGCCTATTCACCGATTTTGATTCTCAAACAAATGTGTCA  CAAAGTAAGGATTCTGATGTGTATATCACAGACAAAACCTGTGCTAG  ACATGAGGTCTATGGACTTCAAGAGCAACAGTGCTGTGGCCTGGAG  CAACAAATCTGACTTTGCATGTGCAAACGCCTTCAACAACAGCATT  ATTCCAGAAGACACCTTCTTCCCCAGCCCAGAAAGTTCCTGTGATG  TCAAGCTGGTCGAGAAAAGCTTTGAAACAGATACGAACCTAAACTT  TCAAACCTGTCAGTGATTGGGTTCCGAATCCTCCTCCTGAAAGTG  GCCGGGTTTAATCTGCTCATGACGCTGCGGCTGTGGTCCAGCTGA</p>
<p>wt STEAP1<sup>130</sup> TCR  construct (β-  chain, P2A, α-chain)</p>	<p>ATGGGAACATCTCTGCTGTGTTGGATGGCCCTGTGCCTGCTGGGAG  CCGATCATGCCGATACAGGCGTGTCCCAGAACCCCCGGCACAAGAT  CACCAAGCGGGGCCAGAACGTGACCTTCAGATGCGACCCCATCAGC  GAGCACAACCGGCTGTACTGGTACAGACAGACCCTGGGCCAGGGCC  CCGAGTTCCTGACCTACTTCCAGAACGAGGCCAGCTGGAAAAGAG  CCGGCTGCTGAGCGACAGATTCAGCGCCGAAAGACCCAAGGGCAGC  TTCAGCACCCCTGGAAATCCAGCGGACCGAGCAGGGCGACAGCGCCA  TGTATCTGTGTGCCAGCAGCAGCGACCGGGACAGCTACAAGAACGA  GCAGTTCCTCGGCCCTGGCACCCGGCTGACCGTGCTGGAAGATCTG  AAGAACGTGTTCCCCCAGAGGTGGCCGTGTTTCGAGCCTAGCAAGG  CCGAGATCGCCACACCCAGAAAGCCACCCCTCGTGTGTCTGGCCAC  CGGCTTCTACCCCGACCACGTGGAACGTCTTGGTGGGTCAACGGC  AAAGAGGTGCACAGCGGCGTGTCCACCGATCCCCAGCCTCTGAAAG  AACAGCCCGCCCTGAACGACAGCCGGTACTGCCTGAGCAGCAGACT  GAGAGTGTCCGCCACCTTCTGGCAGAACCCAGAAACCACTTCAGG  TGCCAGGTGCAGTTTACGGCCTGAGCGAGAACGACGAGTGGACCC  AGGACAGAGCCAAGCCCGTGACCCAGATCGTGTCTGCCGAAGCCTG  GGGCAGAGCCGATTGTGGCATCACCAGCGCCAGCTACCATCAGGGC  GTGCTGAGCGCCACCATCCTGTACGAGATCCTGCTGGGCAAGGCCA  CCCTGTACGCCGTGCTGGTGTCTGCCCTGGTGCTGATGGCCATGGT  CAAGCGGAAGGACAGCAGAGGCGGATCCGGCGCCACCAACTTCAGC  CTGCTGAAACAGGCCGGCGACGTGGAAGAGAACCCTGGCCCTATGG</p>

---

Appendix

---

CCTGCCCTGGATTTCTGTGGGCCCTCGTGATCAGCACCTGTCTGGA ATTTTCCATGGCCCAGACCGTGACACAGTCCCAGCCCGAGATGAGC GTGCAGGAAGCCGAGACAGTGACCCTGAGCTGCACCTACGACACCA GCGAGAGCGACTACTACCTGTTCTGGTACAAGCAGCCCCCAGCCG GCAGATGATCCTCGTGATTAGACAGGAAGCCTATAAGCAGCAGAAC GCCACCGAGAACAGGTTTCAGCGTGAAC TTTCAGAAGGCCGCAAGA GCTTTAGCCTGAAGATCAGCGACTCTCAGCTGGGCGACGCCGCTAT GTACTTCTGCGCCTACGGCAGCAACTTCGGCAACGAGAAGCTGACC TTCGGCACCGGCACCAGACTGACAATCATCCCCAACATCCAGAACC CTGACCCCGCCGTGTACCAGCTGAGGGACAGCAAGAGCAGCGACAA GAGCGTGTGCCTGTTCAACCGACTTCGACAGCCAGACCAATGTGTCC CAGTCCAAGGACAGCGACGTGTACATCACCGACAAGACAGTGCTGG ACATGCGGAGCATGGACTTCAAGAGCAACAGCGCCGTGGCCTGGTC CAACAAGAGCGATTTTCGCCTGCGCCAACGCCTTCAACAACAGCATT ATCCCCGAGGACACATTCTTCCCCAGCTCCGACGTGCCCTGCGACG TGAAGCTGGTGGAAAAGTCCTTCGAGACAGACACCAACCTGAATTT CCAGAACCTGAGCGTGATCGGCTTCAGAATCCTGCTGCTGAAGGTG GCCGGCTTCAATCTGCTGATGACCCTGCGGCTGTGGTCCAGCTGA
---

### 9.3 List of figures

Figure 1: Scheme of STEAP1 protein localization within the membrane. ....	9
Figure 2: Scheme of transgenic T cell development.....	16
Figure 3: Vector map of the retroviral pMP-71 vector containing the codon optimized and minimal murinized STEAP1 <sup>P2A5</sup> TCR.....	34
Figure 4: Vector map of the retroviral pMP-71 vector containing the wildtype STEAP1 <sup>P2A5</sup> TCR.....	34
Figure 5: Vector map of the STEAP1 expression vector .....	35
Figure 6: Vector map of the HLA-A*02:01 expression vector. ....	36
Figure 7: Transduction scheme for TCR $\alpha$ - and $\beta$ -chains into various target cells.....	44
Figure 8: Experimental set-up for <i>in vivo</i> experiments.....	53
Figure 9: STEAP1 expression profile.....	56
Figure 10: HLA-A*02:01 specific binding of STEAP1 peptides.....	58
Figure 11: Maturation status of moDCs. ....	59
Figure 12: Staining of <i>in vitro</i> primed CD8 <sup>+</sup> T cells for FACS sorting. ....	59
Figure 13: Target recognition of STEAP1 <sup>130</sup> specific T cell lines.....	60
Figure 14: ES specificity of STEAP1 <sup>130</sup> specific T cell line P2A5. ....	62
Figure 15: Anti-tumor reactivity of STEAP1 <sup>130</sup> specific T cell clone P2A5. ....	63
Figure 16: Identification of the STEAP1 <sup>130</sup> P2A5 TCR $\alpha$ - and $\beta$ -chains. ....	64
Figure 17: Generation of STEAP1 <sup>130</sup> TCR transgenic T <sub>SCM</sub> .....	65
Figure 18: Generation of STEAP1 <sup>P2A5</sup> transgenic cytotoxic T <sub>SCM</sub> . ....	66
Figure 19: Transduction efficacy of virus supernatant obtained from different packaging cell lines. ....	67
Figure 20: Transduction efficacy of humm and wt TCRs into human CD8 <sup>+</sup> T cells. ....	68
Figure 21: Antigen specific target cell recognition of STEAP1 <sup>P2A5</sup> TCR transgenic CD8 <sup>+</sup> T cells. ....	69
Figure 22: Cross-reactivity screen for STEAP1 <sup>P2A5</sup> TCR transgenic T cells.....	70
Figure 23: Verification of the T <sub>SCM</sub> phenotype of STEAP1 <sup>130</sup> TCR transgenic T cells prior to injection into animals. ....	71
Figure 24: <i>In vivo</i> activity and tumor infiltration of STEAP1 <sup>P2A5</sup> TCR transgenic T <sub>SCM</sub> . ..	73
Figure 25: <i>In vivo</i> anti ES reactivity of STEAP1 <sup>130</sup> TCR transgenic T <sub>SCM</sub> cells. ....	74

Figure 26: Relative binding affinity of various ES associated antigen peptides..... 102

Figure 27: Screening of FACS sorted T cell lines for specific peptide recognition. .... 103

Figure 28: Screening of FACS sorted T cell lines for HLA-A\*02:01 specific target recognition. .... 104

Figure 29: Immunohistochemistry staining of CD8<sup>+</sup> cells within tumors from animals treated with tgSTEAP1hum T<sub>SCM</sub>..... 105

#### 9.4 List of tables

Table 1: *In silico* binding scores of various STEAP1 peptides, predicted by NetCTL1.2, Bimas and SYFPEITHY web algorithms..... 57

Table 2: Nucleotide sequence of STEAP1<sup>P2A5</sup> TCR humm and STEAP1<sup>P2A5</sup> TCR wt. 106

## 9.5 List of abbreviations

Ab	Antibody
ADIPOR1	Adiponectin receptor 1
ACT	Adoptive cell therapy
ALL	Acute lymphoid leukemia
Allo-HSCT	Allogeneic hematopoietic stem cell transplantation
Alo-SCT	Allogeneic stem cell transplantation
APC	Allophycocyanin
BSA	Bovine serum albumin
CAR	Chimeric antigen receptor
CEA	Carcinoembryonal antigen
CD	Cluster of differentiation
cDNA	Complementary desoxyribonucleic acid
CDR3	Complementarity determining region 3
CLL	Chronic lymphoid leukemia
CMV	Cytomegalovirus
CR	Complete remission
CRS	Cytokine release syndrome
CTLA-4	Cytotoxic T-lymphocyte-associated Protein 4
DC	Dendritic cell
DMSO	Dimethylsulfoxide
dNTP	Desoxyribonucleosidtriphosphate
DTX3L	Deltex 3 like, E3 ubiquitin ligase
EBV	Epstein-Barr-Virus
EGFR	Epithelial growth factor receptor
ES	Ewing Sarcoma
ESFT	Ewing Sarcoma family tumors
ET	Ewing Tumor
EtBr	Ethidiumbromide
ETS	E-twenty-six

---

## Appendix

---

EWS	Ewing Sarcoma breakpoint region 1
EZH2	Enhancer of zeste homolog 2
FCS	Fetal calf serum
FITC	Fluorescein isothiocyanate
FLI1	Friend leukemia virus integration 1
FNO	F <sub>420</sub> H <sub>2</sub> :NADP <sup>+</sup> oxidoreductase (FNO)
GB	Granzyme B
GM-CSF	Granulocyte-macrophage colony-stimulating factor
GPR64	G protein-coupled receptor 64
GvHD	Graft versus host disease
Gy	Gray
HBSS	Hank's buffered salt solution
HCl	Hydrochloric acid
HLA	Human leukocyte antigen
Ig	Immunoglobulin
IGF1	Insuline like growth factor 1
IFN	Interferon
i.p.	Intra peritoneal
LAG3	Lymphocyte-activation gene 3
Luc	Luciferase
mAB	Monoclonal antibody
MART-1	Melanoma antigen recognized by T cells 1
MgCl <sub>2</sub>	Magnesium chloride
MHC-I	Major histocompatibility complex class 1
MMP-1	Matrix-metallopeptidase 1
MSC	Mesenchymal stem cell
NaN <sub>3</sub>	Sodium azide
NaOH	Sodium hydroxide
NCI	National cancer institute
NEAA	Non-essential amino acids

OS	Overall survival
PBMC	Peripheral blood mononuclear cell
PBS	Phosphate buffered saline
PCR	Polymerase chain reaction
PD1	Programmed cell death protein 1
PD-L1	Programmed death-ligand 1
PE	Phycoerythrin
PFA	Paraformaldehyde
PGE <sub>2</sub>	Prostaglandin E <sub>2</sub>
PNET	Peripheral primitive neuroectodermal tumors
qRT-PCR	Quantitative reverse transcriptase polymerase chain reaction
RNA	Ribonucleic acid
RNAi	RNA interference
ROS	Reactive oxygen species
s.c.	Subcutaneous
scFv	Single chain variable fragment
SEM	Standard error of the mean
siRNA	Small interfering RNA
STAMP1	Six transmembrane protein of the prostate 1
STAMP2	Six transmembrane protein of the prostate 2
STEAP1	Six transmembrane epithelial antigen of prostate 1
SV40	Simian Virus 40
TAA	Tumor associated antigen
TCM	T cell medium
TCR	T cell receptor
TIL	Tumor infiltrating lymphocytes
TIM3	T-cell immunoglobulin domain and mucin domain 3
TNF	Tumor necrosis factor
TSAP6	Tumor-suppressor activated pathway 6
T <sub>CM</sub>	Central memory T cell

T <sub>EFF</sub>	Effector T cell
T <sub>EM</sub>	Effector memory T cell
T <sub>N</sub>	Naïve T cell
T <sub>REG</sub>	Regulatory T cell
T <sub>SCM</sub>	Stem cell memory T cell
VDC-IE	Vincristine, ifosfamide, doxorubicin, cyclophosphamide, etoposide
VIDE	Vincristine, ifosfamide, doxorubicin, etoposide

## 9.6 Publications derived from this Ph.D thesis

### Peer-reviewed articles

**David Schirmer**, Thomas GP Grünewald, Richard Klar, Oxana Schmidt, Dirk Wohlleber, Rebeca Alba Rubío, Wolfgang Uckert, Uwe Thiel, Felix Bohne, Dirk H Busch, Angela M Krackhardt, Stefan Burdach, Günther HS Richter

**“Transgenic antigen-specific, HLA-A\*02:01-allo-restricted cytotoxic T cells recognize tumor-associated target antigen STEAP1 with high specificity”**

*submitted in Oncoimmunology*

Alexandra Sipol, Thomas T. G. Grunewald, Juliane Schmaeh, **David Schirmer**, Rebeca Alba Rubío, Michaela Baldauf, Caroline M. Wernicke, Hansjochem Kolb, Gunnar Cario, Günther Richter and Stefan Burdach

**“MondoA Mediates *In Vivo* Aggressiveness Of Common ALL and May Serve As A T Cell Immunotherapy Target”**

*in preparation*

Kristina von Heyking, Julia Calzada-Wack, Stefanie Göllner, Frauke Neff, Oxana Schmidt, **David Schirmer**, Annette Fasan, Irene Esposito, Carsten Müller-Tidow, Stefan Burdach, Günther H. S. Richter

**„The endochondral bone protein CHM1 maintains an undifferentiated, invasive phenotype in Ewing Sarcoma”**

*in preparation*

## Congress contribution

**David Schirmer**, Angela Krackhardt, Richard Klar, Dirk H Busch, Wolfgang Uckert, Stefan Burdach, Günther HS Richter

**Poster „Generation of transgenic antigen-specific, allogeneic HLA-A\*0201-restricted cytotoxic T cells directed against Ewing Sarcoma specific target antigen STEAP1“**

*Cancer immunotherapy meeting (2014), Mainz, Germany*

**David Schirmer**, Angela Krackhardt, Richard Klar, Dirk H Busch, Wolfgang Uckert, Stefan Burdach, Günther HS Richter

**Poster „Transgenic antigen-specific, allogeneic HLA-A\*0201-restricted cytotoxic T cells recognize tumor-associated target antigen STEAP1 with high specificity“**

*32. Deutscher Krebskongress (2016), Berlin, Germany*

## **Acknowledgements**

First of all I want to thank Prof. Dr. Stefan Burdach and PD Dr. Günther Richter for giving me the chance to accomplish my work at the Laboratory of Functional Genomics and Transplantation Biology.

PD Dr. Günther Richter, Prof. Dr. Stefan Burdach and Prof. Dr. Angela Krackhardt for supervising my project over the last years. There was always excellent input and constructive discussions promoting the development of the thesis.

PD Dr. Günther Richter for supervision of my thesis and all the help concerning technical and administrative problems.

My colleagues namely Andreas Kirschner, Tim Hensel, Oxana Schmidt, Kristina von Heyking, Henrieke Gerdes and Isabel Storz for support in technical and emotional issues.

My collaboration partners Dirk Wohleber and Thomas Grünewald for straightforward partnership.

Desislava Zlatanova for all the help regarding the requirements for the Ph.D program “Medical Life Science and Technology”. You really took a lot of burden from my shoulders.

Kristina von Heyking for reading my thesis very carefully and finding all the small mistakes that I missed.

And last but not least, thanks to the better part of me: Julia! You helped me in every way that I needed. No matter if it was reading my thesis critically, giving input for new methods or if it was just listening to my problems!!!